



# Experiments on RF Heating and Current Drive

---

**Ryuhei Kumazawa**

***National Institute for Fusion Science, Toki,  
509-5292 Japan***

**IISS 2012**

**Dec. 2-6 2012**

**Ahmedabad, India**



# Experiments on RF Heating and Current Drive

---

## Abstract

**After a brief introduction of the waves in plasmas, physics of the ion cyclotron range of frequency (ICRF) and the electron cyclotron resonance heating (ECRH) are discussed. Recent experimental results from major plasma magnetic confinement machines (LHD, DIII-D, Alcator C-Mod, JET, ASDEX, Tore Supra etc.) are reviewed. In a similar way, a brief introduction to the physics and the recent experimental results of RF current drive (CD) are given. Finally, RF heating and CD scenarios on ITER are also discussed.**



# Outlines

---

- 1. Waves in plasma**
- 2. Physics of ICRF heating**
- 3. Experiments of ICRF heating**
- 4. ICRF heating technologies**
- 5. Discussion of RFH and RFCD on ITER**
- 6. Summary**



# Outlines

---

- 1. Waves in plasma: CMA diagram**
- 2. Physics on ICRF heating**
- 3. Experiments on ICRF heating**
- 4. ICRF heating technologies**
- 5. Discussion of RFH and RFCD on ITER**
- 6. Summary**

# Waves in Plasma

Dispersion equation of plasma wave is obtained from the momentum equations of charged particles and Maxwell equation as follows:

$$\vec{E}, \vec{B} + B_0 \Rightarrow \text{momentum equations of charged particles} \Rightarrow \vec{v}_e, \vec{v}_i \Rightarrow \vec{j} \Rightarrow \text{Maxwell eq.} \Rightarrow \vec{E}', \vec{B}'$$

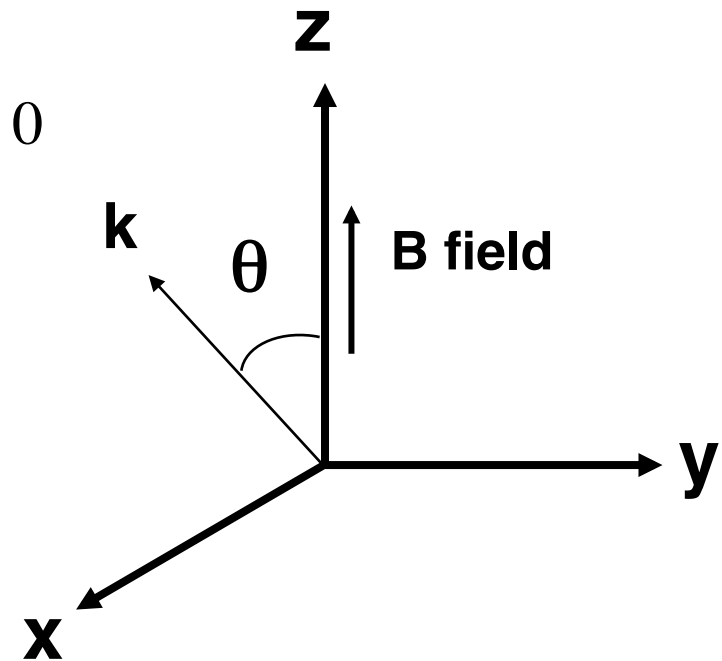
Then self-consistent solution  $\Rightarrow$  Dispersion equation:

$$\begin{bmatrix} K_{\perp} - N^2 \cos^2 \theta & -iK_x & N^2 \sin \theta \cos \theta \\ iK_x & K_{\perp} - N^2 & 0 \\ N^2 \sin \theta \cos \theta & 0 & K_{\parallel} - N^2 \sin^2 \theta \end{bmatrix} \begin{bmatrix} E_x \\ E_y \\ E_z \end{bmatrix} = 0$$

$$K_{\perp} = 1 - \sum_k \frac{\Pi_k^2}{\omega^2 - \Omega_k^2}, K_x = - \sum_k \frac{\Pi_k^2}{\omega^2 - \Omega_k^2} \frac{\Omega_k}{\omega}$$

$$K_{\parallel} = 1 - \sum_k \frac{\Pi_k^2}{\omega^2}, \Pi_k^2 = \frac{n_k q_k^2}{\epsilon_0 m_k}, \Omega_k = - \frac{q_k B_0}{m_k}$$

$$\vec{N} = \frac{\vec{k}c}{\omega} : \text{ratio of wave phase velocity to light}$$



**Coordinate**

**Dispersion (D.) eq. 1.**  
for  $N$  of solution of  
quadratic equation

$$\text{Then } N^2 = \frac{B \pm (B^2 - 4AC)^{1/2}}{2A}$$

$$= \frac{(K_{\perp}^2 - K_{\times}^2) \sin^2 \theta + K_{//} K_{\perp} (1 + \cos^2 \theta) \pm \left\{ (K_{\perp}^2 - K_{\times}^2 - K_{//} K_{\perp})^2 \sin^4 \theta + 4K_{//}^2 K_{\times}^2 \cos^2 \theta \right\}^{1/2}}{2(K_{\perp} \sin^2 \theta + K_{//} \cos^2 \theta)}$$

**D. eq. 2.**  
for  $N_{\perp}$

$$aN_{\perp}^4 + bN_{\perp}^2 + c = 0$$

$$a = K_{\perp}$$

$$b = -K_{\perp}^2 + K_{\times}^2 - K_{\perp} K_{//} + (K_{\perp} + K_{//}) N_{//}^2$$

$$c = K_{//} \{ (K_{\perp} - N_{//}^2)^2 - K_{\times}^2 \}$$

**D. eq. 3.**  
for  $N_{//}$

$$\alpha N_{//}^4 + \beta N_{//}^2 + \gamma = 0$$

$$\alpha = K_{//}$$

$$\beta = (K_{\perp} + K_{//}) N_{\perp}^2 - 2K_{//} K_{\perp}$$

$$\gamma = \{ K_{\perp} N_{\perp}^2 - (K_{\perp}^2 - K_{\times}^2) \} (N_{\perp}^2 - K_{//})$$

# Characteristics of Waves

## Propagating along B

$$\theta = 0, \text{ i.e., } N_{\perp} = 0 \text{ at D.eq.3} \Rightarrow K_{//} \{ N_{//}^4 - 2K_{\perp} N_{//}^2 + (K_{\perp}^2 - K_{\times}^2) \} = 0$$

$$\Rightarrow K_{//} = 0, \quad N_{//}^2 = K_{\perp} + K_{\times} = R, \quad N_{//}^2 = K_{\perp} - K_{\times} = L$$

**R: right hand circularly polarized**

**L: left hand circularly polarized**

## Propagating perpendicular to B

$$\theta = \frac{\pi}{2}, \text{ i.e., } N_{//} = 0 \text{ at D.eq.2} \Rightarrow K_{\perp} N_{\perp}^4 - (K_{\perp}^2 - K_{\times}^2 + K_{//} K_{\perp}) N_{\perp}^2 + K_{//} (K_{\perp}^2 - K_{\times}^2) = 0$$

$$\Rightarrow \{ K_{\perp} N_{\perp}^2 - (K_{\perp}^2 - K_{\times}^2) \} (N_{\perp}^2 - K_{//}) = 0$$

$$\text{then } N_{\perp}^2 = \frac{K_{\perp}^2 - K_{\times}^2}{K_{\perp}} (X), \quad N_{\perp}^2 = K_{//} (O)$$

**O: ordinary wave**

**X: extraordinary wave**

# Waves in Simple Plasma

In two-component plasma, i.e., electrons and ions

$$K_{\perp} = 1 - \frac{\Pi_i^2}{\omega^2 - \Omega_i^2} - \frac{\Pi_e^2}{\omega^2 - \Omega_e^2}$$

$$K_{\times} = -\frac{\Pi_i^2}{\omega^2 - \Omega_i^2} \frac{\Omega_i}{\omega} - \frac{\Pi_e^2}{\omega^2 - \Omega_e^2} \frac{\Omega_e}{\omega}, \text{ here } \Omega_i < 0$$

$$K_{\parallel} = 1 - \frac{\Pi_i^2 + \Pi_e^2}{\omega^2}$$

$$R = 1 - \frac{\Pi_e^2 + \Pi_i^2}{(\omega - \Omega_i)(\omega - \Omega_e)} \approx \frac{\omega^2 - (\Omega_i + \Omega_e)\omega + \Omega_i\Omega_e - \Pi_e^2}{(\omega - \Omega_i)(\omega - \Omega_e)}$$

$$L = 1 - \frac{\Pi_e^2 + \Pi_i^2}{(\omega + \Omega_i)(\omega + \Omega_e)} \approx \frac{\omega^2 + (\Omega_i + \Omega_e)\omega + \Omega_i\Omega_e - \Pi_e^2}{(\omega + \Omega_i)(\omega + \Omega_e)}$$

## Propagating along B

**Electron plasma wave:**  $K_{\parallel} = 0 \rightarrow \omega^2 = \Pi_e^2$

**R wave:**  $\frac{1}{N_{\parallel}^2} = \frac{\omega^2}{k_{\parallel}^2 c^2} = \frac{1}{R} \leftarrow R = \frac{\omega^2 - (\Omega_i + \Omega_e)\omega + \Omega_i \Omega_e - \Pi_e^2}{(\omega - \Omega_i)(\omega - \Omega_e)}$

from previous view graph  $\frac{\omega^2}{k_{\parallel}^2 c^2} = \frac{(\omega - \Omega_i)(\omega - \Omega_e)}{\omega^2 - (\Omega_i + \Omega_e)\omega + \Omega_i \Omega_e - \Pi_e^2} = \frac{(\omega + |\Omega_i|)(\omega - \Omega_e)}{(\omega - \omega_R)(\omega + \omega_L)}$

**L wave:**  $\frac{1}{N_{\parallel}^2} = \frac{\omega^2}{k_{\parallel}^2 c^2} = \frac{1}{L} \leftarrow L = \frac{\omega^2 + (\Omega_i + \Omega_e)\omega + \Omega_i \Omega_e - \Pi_e^2}{(\omega + \Omega_i)(\omega + \Omega_e)}$

from previous view graph  $= \frac{(\omega + \Omega_i)(\omega + \Omega_e)}{\omega^2 + (\Omega_i + \Omega_e)\omega + \Omega_i \Omega_e - \Pi_e^2} = \frac{(\omega - |\Omega_i|)(\omega + \Omega_e)}{(\omega + \omega_R)(\omega - \omega_L)}$

**Here**

$$\omega_R = \frac{\Omega_e + \Omega_i}{2} + \left\{ \left( \frac{\Omega_e + \Omega_i}{2} \right)^2 + \Pi_e^2 + |\Omega_i| \Omega_e \right\}^{1/2} > \Omega_e$$

$$\omega_L = -\frac{\Omega_e + \Omega_i}{2} + \left\{ \left( \frac{\Omega_e + \Omega_i}{2} \right)^2 + \Pi_e^2 + |\Omega_i| \Omega_e \right\}^{1/2} \approx \omega_R - \Omega_e$$



# Waves along B

## Propagating along B

In the case of  $n_e = 10^{20} m^{-3}$ ,  $B = 3T$ :

$$\Omega_e = 5.28 \times 10^{11} \text{ rad/s}, |\Omega_i| = 2.87 \times 10^8 \text{ rad/s}$$

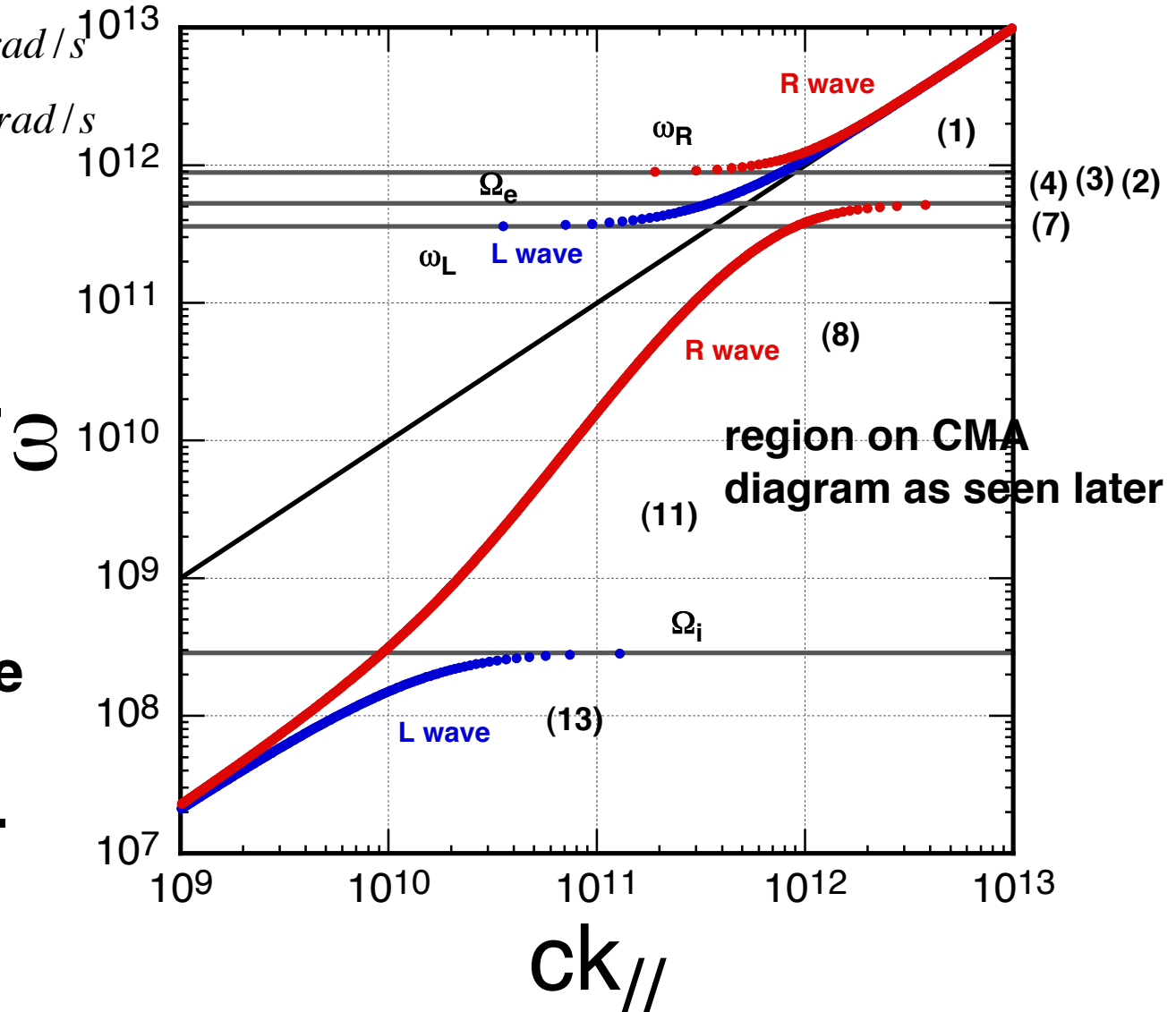
$$\omega_R = 8.87 \times 10^{11} \text{ rad/s}, \omega_L = 3.59 \times 10^{11} \text{ rad/s}$$

$$|\Omega_i| < \omega_L < \Omega_e < \omega_R$$

**L wave** can propagate at  $\omega < |\Omega_{ci}|$  with  $v_\phi < c$  and again at  $\omega > \omega_L$  with  $v_\phi > c$ . It becomes cut-off at  $|\Omega_{ci}| < \omega < \omega_L$ .

**R wave** can propagate at  $\omega < \Omega_{ce}$  with  $v_\phi < c$  and again at  $\omega > \omega_R$  with  $v_\phi > c$ . It becomes cut-off at  $\Omega_{ce} < \omega < \omega_R$ .

Numbers show regions as shown in CMA diagram as seen later.





# Waves Perpendicular to B

## Propagating in the direction perpendicular to B

**O wave** 
$$\frac{1}{N_{\perp}^2} = \frac{\omega^2}{k_{\perp}^2 c^2} = \frac{1}{K_{//}} = \left(1 - \frac{\Pi_e^2}{\omega^2}\right)^{-1} = 1 + \frac{\Pi_e^2}{k_{\perp}^2 c^2}$$

**X wave** 
$$\frac{1}{N_{\perp}^2} = \frac{\omega^2}{k_{\perp}^2 c^2} = \frac{K_{\perp}}{K_{\perp}^2 - K_{\times}^2} = \frac{K_{\perp}}{RL}$$

$$\rightarrow \frac{\omega^2}{k_{\perp}^2 c^2} = \frac{\omega^4 - (\Omega_i^2 + \Omega_e^2 + \Pi_e^2)\omega^2 + \Omega_i^2 \Omega_e^2 + \Pi_i^2 \Omega_e^2 + \Pi_e^2 \Omega_i^2}{(\omega^2 - \omega_R^2)(\omega^2 - \omega_L^2)}$$

**Using**  $\omega_{UH}^2 = \Omega_e^2 + \Pi_e^2, \quad \frac{1}{\omega_{LH}^2} = \frac{1}{\Omega_i^2 + \Pi_i^2} + \frac{1}{|\Omega_i| \Omega_e}$

**Then X waves:** 
$$\frac{\omega^2}{k_{\perp}^2 c^2} = \frac{(\omega^2 - \omega_{UH}^2)(\omega^2 - \omega_{LH}^2)}{(\omega^2 - \omega_R^2)(\omega^2 - \omega_L^2)}$$



# Waves Perpendicular to B

## Propagating in the direction perpendicular to B

In the case of  $n_e = 10^{20} m^{-3}$ ,  $B = 3T$ :

$$\Pi_e^2 = 3.18 \times 10^{23} rad^2 / s^2, \omega_R = 8.87 \times 10^{11} rad / s$$

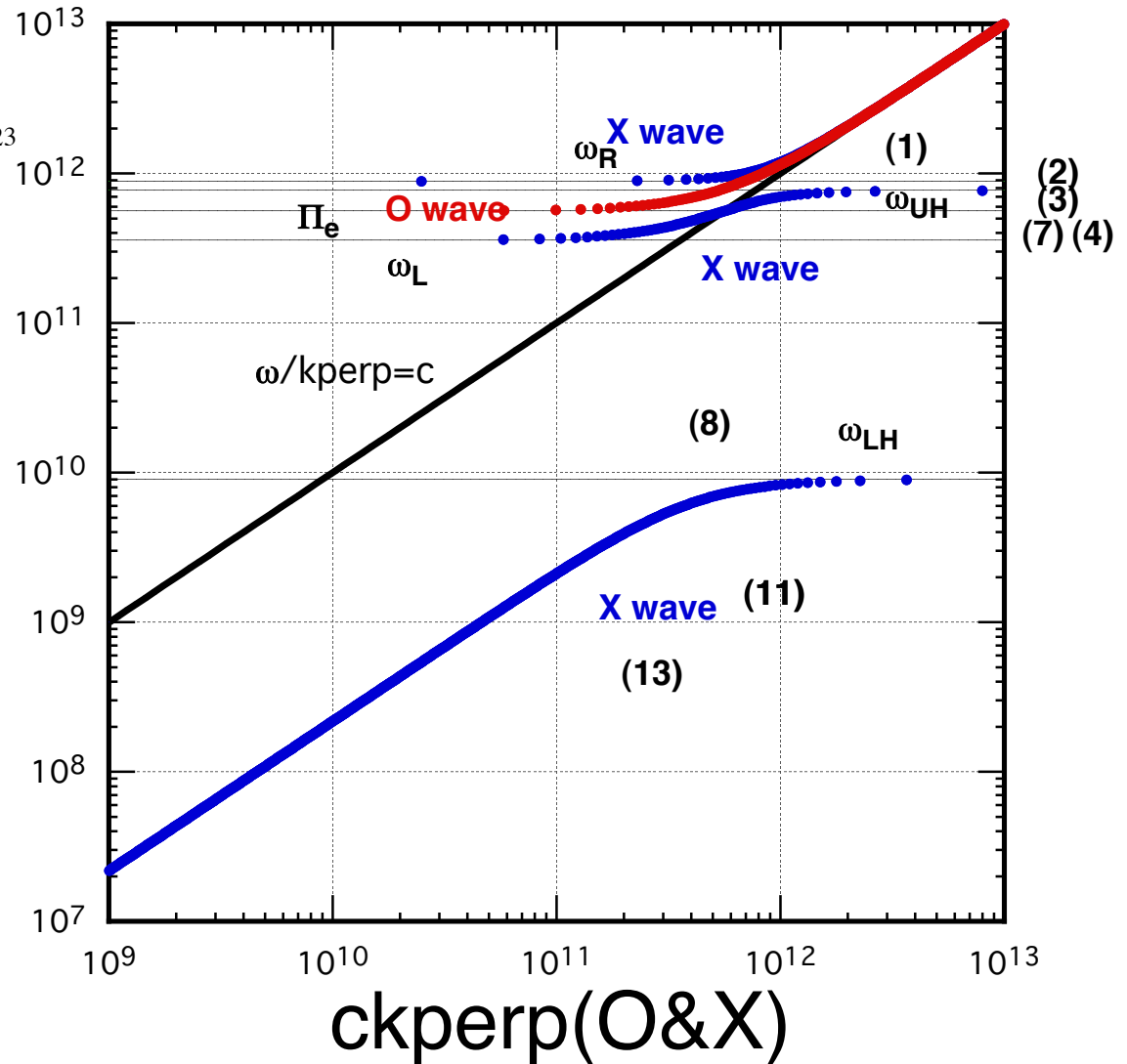
$$\omega_L = 3.59 \times 10^{11} rad / s, \omega_{UH}^2 = \Omega_e^2 + \Pi_e^2 = 5.97 \times 10^{23}$$

$$\frac{1}{\omega_{LH}^2} = \frac{1}{\Omega_i^2 + \Pi_i^2} + \frac{1}{\Omega_e |\Omega_i|} \rightarrow \omega_{LH}^2 = 8.1 \times 10^{19}$$

$$\omega_{LH} < \omega_L < \Pi_e < \omega_R$$

**X wave** can propagate at  $\omega < \omega_{LH}$  with  $v_\phi < c$ ,  
 at  $\omega_L < \omega < \omega_{UH}$  with  $v_\phi \sim c$  and  
 $\omega_R < \omega$  with  $v_\phi > c$ .  
 It becomes cut-off at  
 $\omega_{LH} < \omega < \omega_L$  and  $\omega_{UH} < \omega < \omega_R$ .

**O wave** can propagate only at  
 $\omega < \Pi_e$  with  $v_\phi > c$ .





# CMA Diagram-1

In CMA(Clemmow, Mullaly and Allis) diagram  $\omega_R$ ,  $\omega_L$ ,  $\omega_{UH}$  and  $\omega_{LH}$  are expressed using  $x$  and  $y$ .

For example:

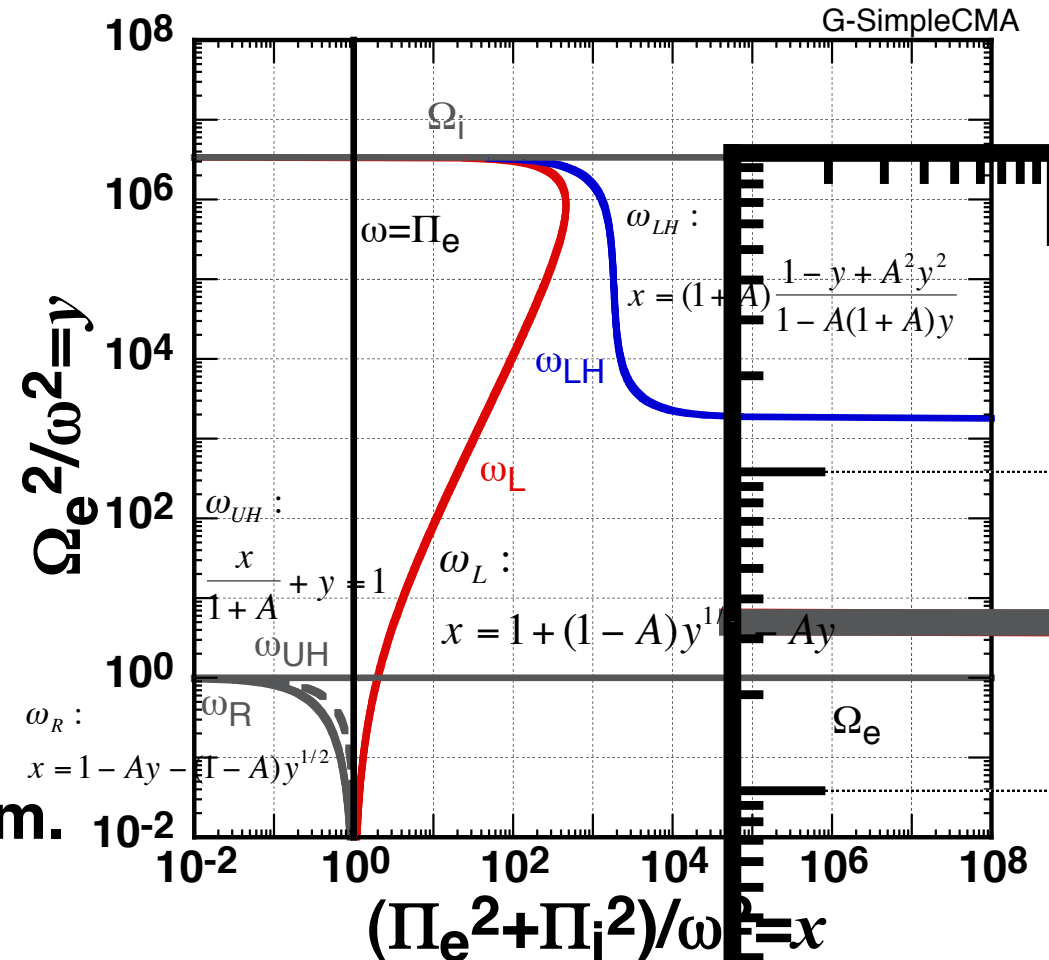
$$\omega_R = \frac{\Omega_e + \Omega_i}{2} + \left\{ \left( \frac{\Omega_e + \Omega_i}{2} \right)^2 + \Pi_e^2 + \Pi_i^2 + |\Omega_e \Omega_i| \right\}^{1/2} = \omega$$

$$\leftarrow \frac{\Omega_e + \Omega_i}{\omega} = (1 - A)y^{1/2} \leftarrow \leftarrow y = \frac{\Omega_i^2}{\omega^2} \text{ and } \Omega_i < 0$$

$$x = 1 - Ay - (1 - A)y^{1/2} \leftarrow A = \frac{|\Omega_i|}{\Omega_e}$$

$$x = 1, \quad y = 0 \text{ and } x = 0, \quad y = 1$$

In the similar ways  $\omega_L$ ,  $\omega_{UH}$  and  $\omega_{LH}$  are formulated using  $x$  and  $y$  as shown in the right CMA diagram.



## CMA(Clemmow, Mullaly and Allis) diagram

in the case of  $n_e = 10^{20} m^{-3}$ ,  $B = 3T$  :

$$\Omega_e = 5.28 \times 10^{11} rad/s, |\Omega_i| = 2.87 \times 10^8 rad/s$$

$$\Pi_e^2 = 3.18 \times 10^{23} rad^2/s^2 \quad \omega_R = 8.87 \times 10^{11} rad/s$$

$$\omega_L = 3.59 \times 10^{11} rad/s, \omega_{UH}^2 = \Omega_e^2 + \Pi_e^2 = 5.97 \times 10^{23}$$

$$\Pi_i^2 = \Pi_e^2 m_e / A m_i = 1.74 \times 10^{20}$$

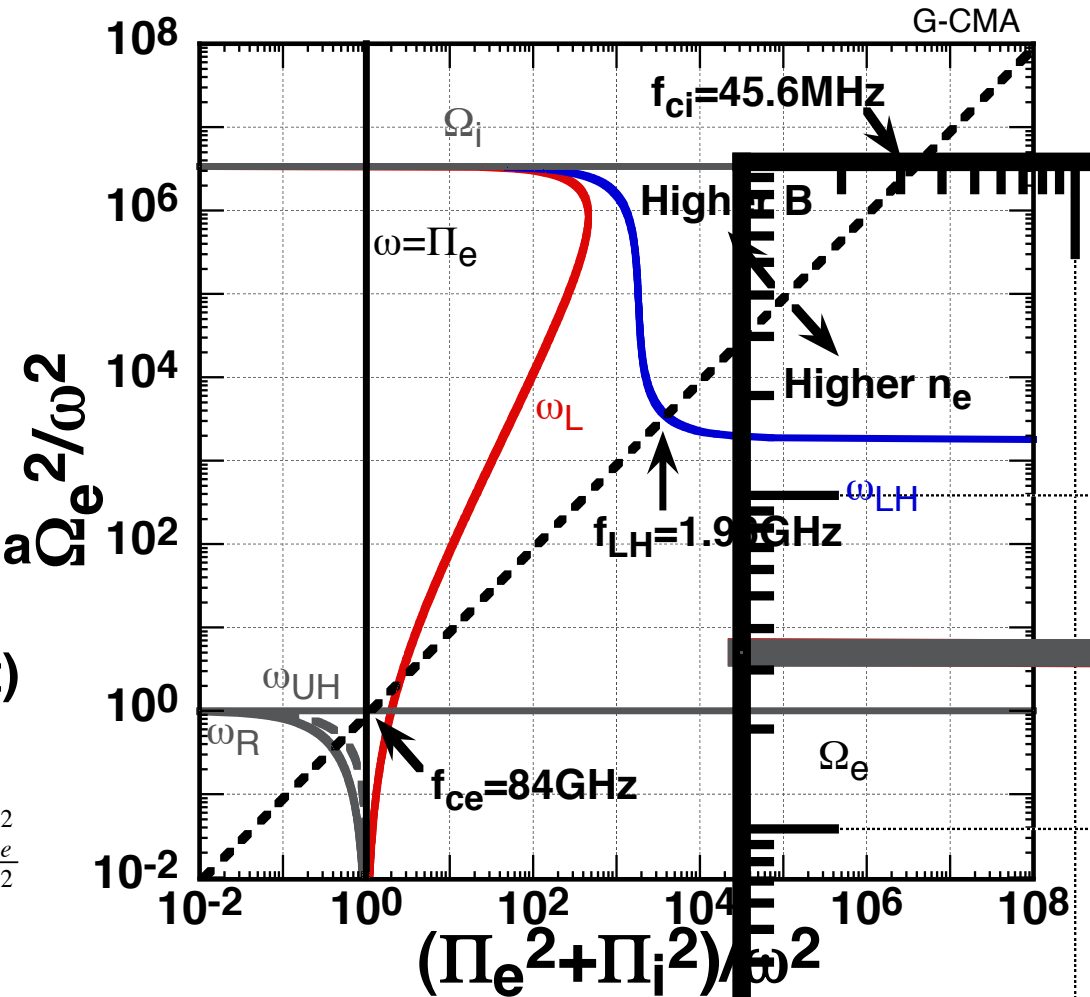
$$\frac{1}{\omega_{LH}^2} = \frac{1}{\Omega_i^2 + \Pi_i^2} + \frac{1}{\Omega_e |\Omega_i|} \rightarrow \omega_{LH}^2 = 8.1 \times 10^{19}$$

In addition a dotted straight line shows a plasma waves from high frequency (bottom-left) to low frequency (top-right) at  $n_e = 10^{20} m^{-3}$  and  $B=3T$ .

$$x = \frac{\Pi_e^2 + \Pi_i^2}{\omega^2} \rightarrow x = (1+A) \frac{\Pi_e^2}{\omega^2} \rightarrow \omega^2 = (1+A) \frac{\Pi_e^2}{x}, \quad y = \frac{\Omega_e^2}{\omega^2}$$

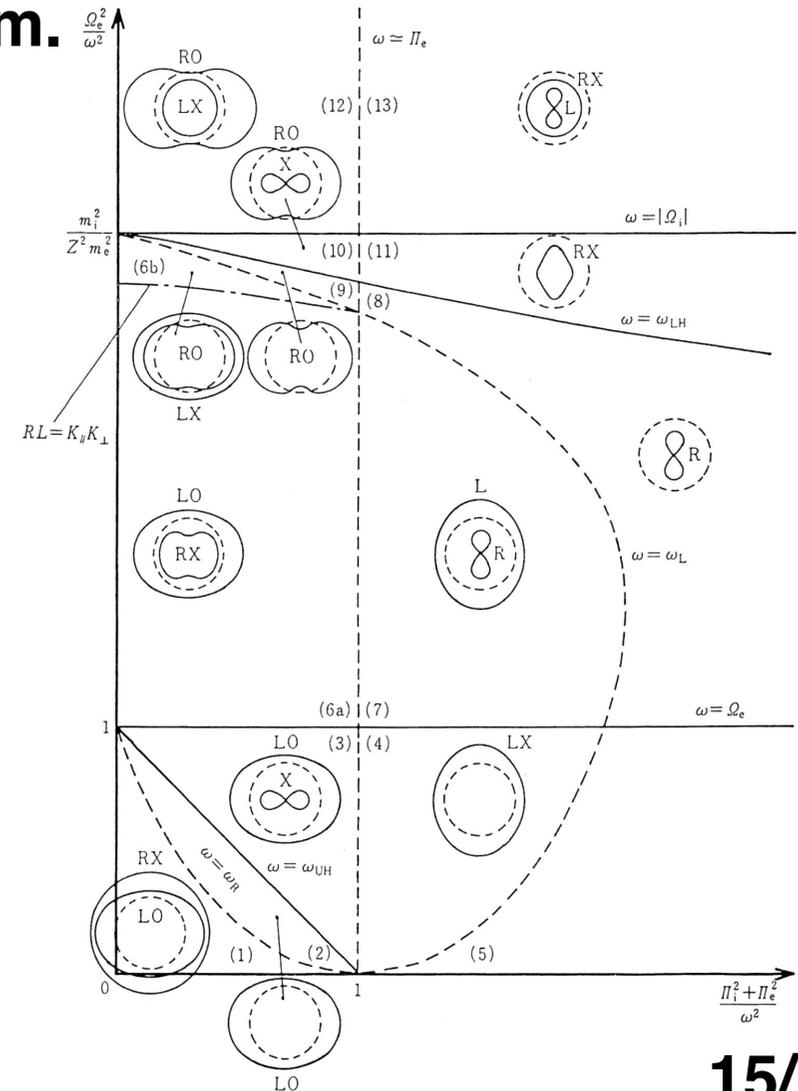
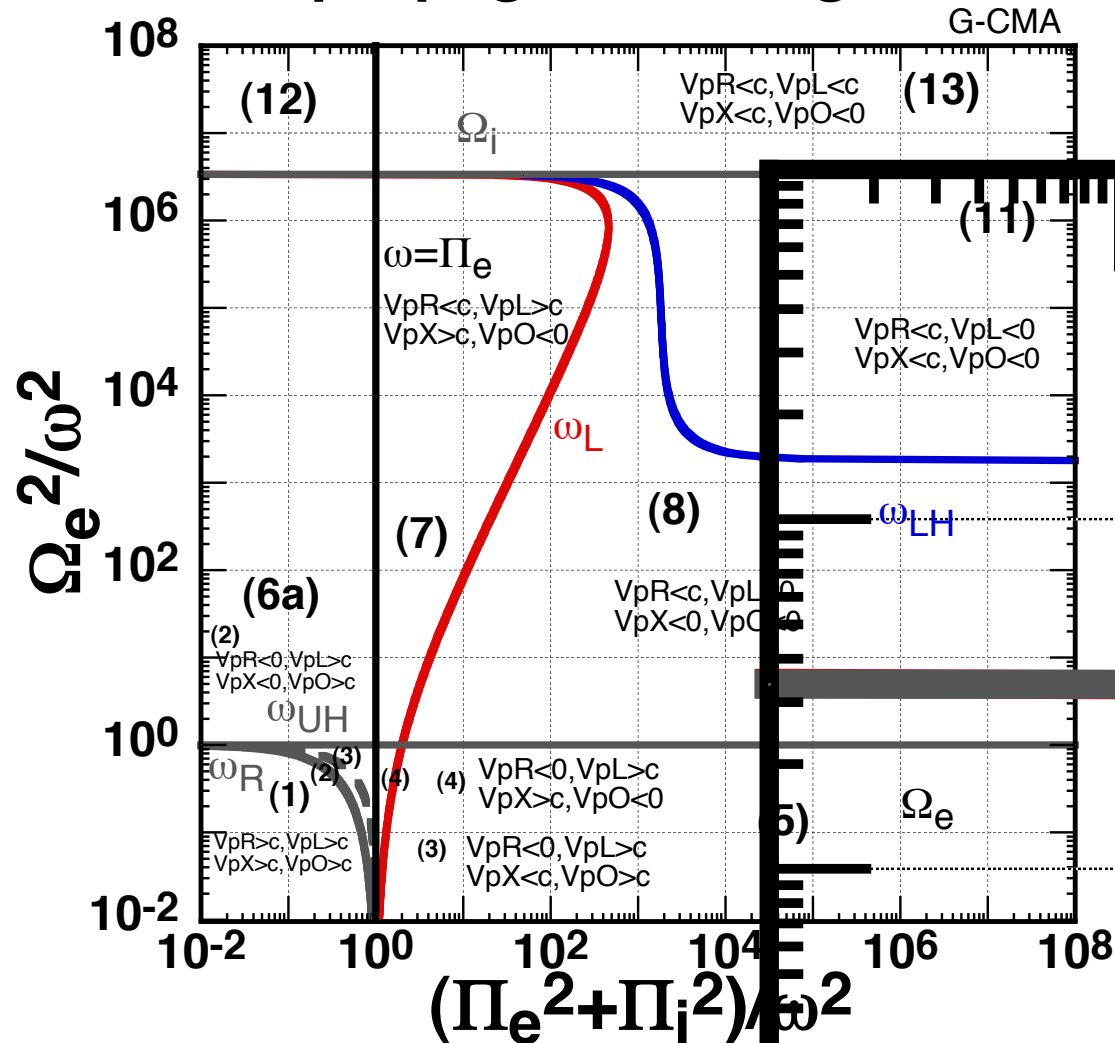
$$y = \frac{\Omega_e^2}{\omega^2} = \frac{\Omega_e^2}{\Pi_e^2} \frac{\Pi_e^2}{\omega^2} = \frac{\Omega_e^2}{\Pi_e^2} \frac{x}{1+A} = \frac{0.88}{1+A} x \approx 0.88x$$

$$\therefore y = 0.88x$$



## CMA diagram: log plot and log and linear plot:

Figures show wave propagation, dotted circles show wave propagation of light in vacuum.





# Outlines

---

1. Waves in plasma
2. **Physics of ICRF heating**
3. Experiments of ICRF heating
4. ICRF heating technologies
5. Discussion of RFH and RFCD on ITER
6. Summary



# Landau and Cyclotron Damping

Wave energy is transferred to charged particles in the plasma via. Landau damping.

$$m \frac{dv}{dt} = eE \cos(kz - \omega t) \leftarrow E(z,t) = E \cos(kz - \omega t)$$

Then,

$$\frac{d}{dt} \left( \frac{mv^2}{2} \right) \approx mv_1 \frac{dv_1}{dt} + mv_0 \frac{dv_2}{dt} = \frac{e^2 E^2}{m} \frac{\sin(kz_0 + \alpha t) - \sin(kz_0)}{\alpha} \cos(kz_0 + \alpha t) - \frac{kv_0 e^2 E^2}{m} \sin(kz_0 + \alpha t) \left( \frac{-\cos(kz_0 + \alpha t) + \cos(kz_0)}{\alpha^2} - \frac{t \sin(kz_0)}{\alpha} \right) \text{ here } \alpha = kv_0 - \omega$$

averaging for  $z_0$

$$\left\langle \frac{d}{dt} \left( \frac{mv^2}{2} \right) \right\rangle_{z_0} = \frac{e^2 E^2}{2m} \frac{\omega}{k} \frac{d}{dv} \left( \frac{\sin(kv - \omega)t}{kv - \omega} \right) \leftarrow \alpha = kv - \omega$$

$$\text{absorbed power} : \int dv f(v) \left\langle \frac{d}{dt} \left( \frac{mv^2}{2} \right) \right\rangle_{z_0} = - \frac{e^2 E_{||}^2}{2m} \frac{\pi \omega}{k^2} \frac{df(v)}{dv} \Big|_{(v=\omega/k)}$$



# Cyclotron Damping

**Wave energy is transferred to charged particles in the plasma via. cyclotron damping.**

$$E_x = E_1 \cos \varepsilon(kz - \omega t), \quad E_y = E_1 \sin \varepsilon(kz - \omega t)$$

$$\text{with } \frac{\partial B}{\partial t} = -\nabla \times E \rightarrow B_{1x} = \frac{k_z E_1}{\omega} \sin \varepsilon(kz - \omega t), \quad B_{1y} = \frac{k_z E_1}{\omega} \cos \varepsilon(kz - \omega t)$$

$$m \frac{dv}{dt} = -e(E_1 + v_{\perp} \times B_0 + v_{z0} \times B_1 + v_{\perp} \times B_1)$$

$$\rightarrow \frac{d}{dt} \left( \frac{mv_{\perp}^2}{2} \right) = -e \left( 1 - \frac{kv_{z0}}{\omega} \right) E \cdot v_{\perp} \quad \text{and} \quad \frac{d}{dt} \left( \frac{mv_z^2}{2} \right) = -\frac{ekv_{z0}}{\omega} E \cdot v_{\perp}$$

$$\frac{d}{dt} \left( \frac{mv_{\perp}^2}{2} \right) + \frac{d}{dt} \left( \frac{mv_z^2}{2} \right) = \frac{d}{dt} \left( \frac{mv^2}{2} \right) = -eE \cdot v_{\perp} = \frac{e^2 E_1^2}{m} \frac{1 - \frac{kv_{z0}}{\omega}}{\varepsilon(kv_{z0} - \omega) - \Omega} \times \sin\{\varepsilon(kv_{z0} - \omega) - \Omega\}t$$

$$\text{then, } \int_{-\infty}^{\infty} dv_{z0} f(v_{z0}) \frac{d}{dt} \left( \frac{mv^2}{2} \right) = \frac{\pi e^2 E_1^2}{mk} \left( -\frac{\Omega}{\varepsilon \omega} \right) f \left( \frac{\omega + \Omega/\varepsilon}{k} \right)$$

here,  $\varepsilon$  is a sign of charged particle

# Cyclotron Damping

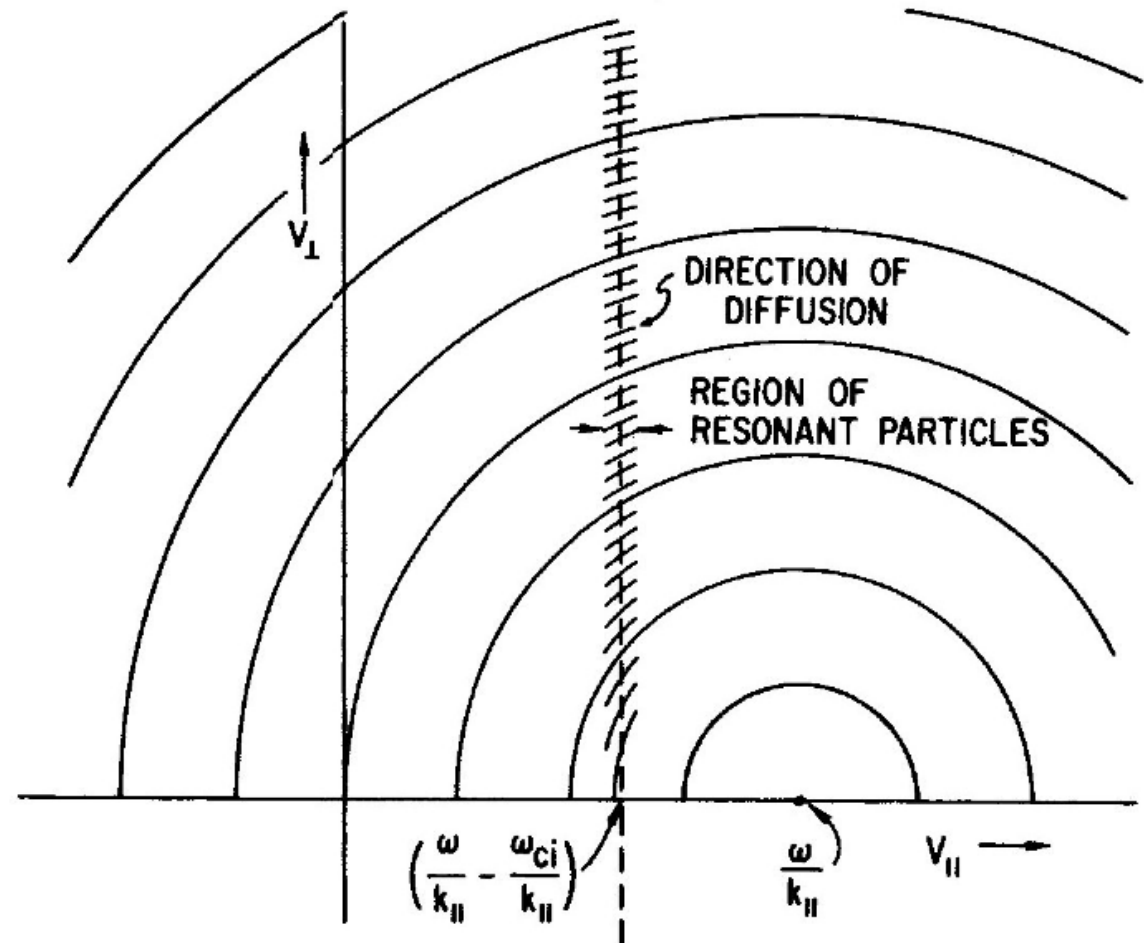
## Conservation law in cyclotron damping:

$$\text{during analysis } mv_z \frac{dv_z}{dt} + mv_{\perp} \frac{dv_{\perp}}{dt} = m \frac{\omega}{k} \frac{dv_z}{dt}$$

$$\text{then } \frac{mv_{\perp}^2}{2} + \frac{m(v_{\parallel} - \omega/k)^2}{2} = C$$

In velocity space of charged particles, i.e.,  $(v_{\parallel}, v_{\perp})$ , accelerated particle moves along the above conservation law.

⇒ When  $v_{\parallel} \ll v_{\phi} = \omega/k$ , particle is accelerated perpendicularly to B.  
 When  $v_{\parallel} \sim v_{\phi} = \omega/k$ , particle is accelerated parallelly to B.





# ICRF Heating

## -Polarization of RF electric field-

In the range  $\omega \sim |\Omega_{ci}|$ :

$$\begin{pmatrix} R + L - 2N_{//}^2 & -i(R - L) \\ i(R - L) & R + L - 2N_{//}^2 - 2N_{\perp}^2 \end{pmatrix} \begin{pmatrix} E_x \\ E_y \end{pmatrix} = 0$$

## Polarization of RF electric field, $\mathbf{E}$

$$(R + L - 2N_{//}^2)E_x - i(R - L)E_y = 0 \rightarrow (R + L - 2N_{//}^2)E_x = i(R - L)E_y$$

$$\frac{iE_y}{E_x} = \frac{R + L - 2N_{//}^2}{R - L} = \frac{S - N_{//}^2}{D} \leftarrow S = K_{\perp}, \quad D = K_x$$

$$\text{slow wave: } \frac{iE_y}{E_x} = \frac{S - N_{//}^2}{D} = -\frac{\Omega_i}{\omega} \frac{k_{//}^2}{k_{//}^2 + k_{\perp}^2} \leftarrow \omega \approx -\Omega_i$$

$$\frac{iE_y}{E_x} \approx \frac{k_{//}^2}{k_{//}^2 + k_{\perp}^2} : \text{left hand polarized}$$

$$\text{fast wave: } \frac{S - N_{//}^2}{D} = \frac{\Omega_i^2(1 + \omega^2 / \Omega_i^2 \cos^2 \theta)}{\omega \Omega_i(1 + \cos^2 \theta)} \leftarrow \omega \approx -\Omega_i$$

$$\frac{iE_y}{E_x} \approx -1 : \text{left hand polarized}$$

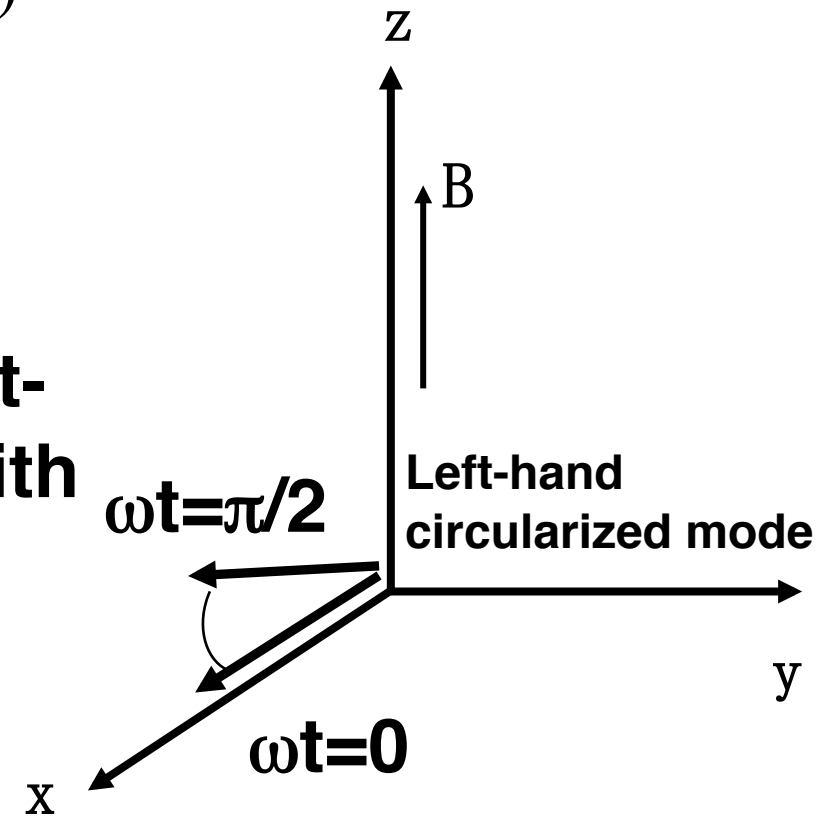


# Polarization of RF Electric Field

## Defining $E_+$ and $E_-$ ;

$$E_+ = \frac{1}{2}(E_x + iE_y), E_- = \frac{1}{2}(E_x - iE_y)$$

In Cartesian coordinate (x, y, z),  $E_+$  and  $E_-$  are a left-handed polarized wave coupling with ions and a right-handed polarized wave coupling with electrons, respectively.



in case of  $iE_y/E_x=1$



# Polarization of RF Electric Field

## -depending $iE_y/E_x$ -

When defining,  $i \frac{E_y}{E_x} = a + bi$

$$E_+ = \frac{1}{2} E_x \left(1 + i \frac{E_y}{E_x}\right) = \frac{1}{2} E_x (1 + a + bi) \leftarrow i \frac{E_y}{E_x} = a + bi$$

$$E_- = \frac{1}{2} E_x (1 - a - bi)$$

$$\frac{|E_+|^2}{|E_+|^2 + |E_-|^2} = \frac{1}{2} \frac{(1+a)^2 + b^2}{1+a^2+b^2}$$

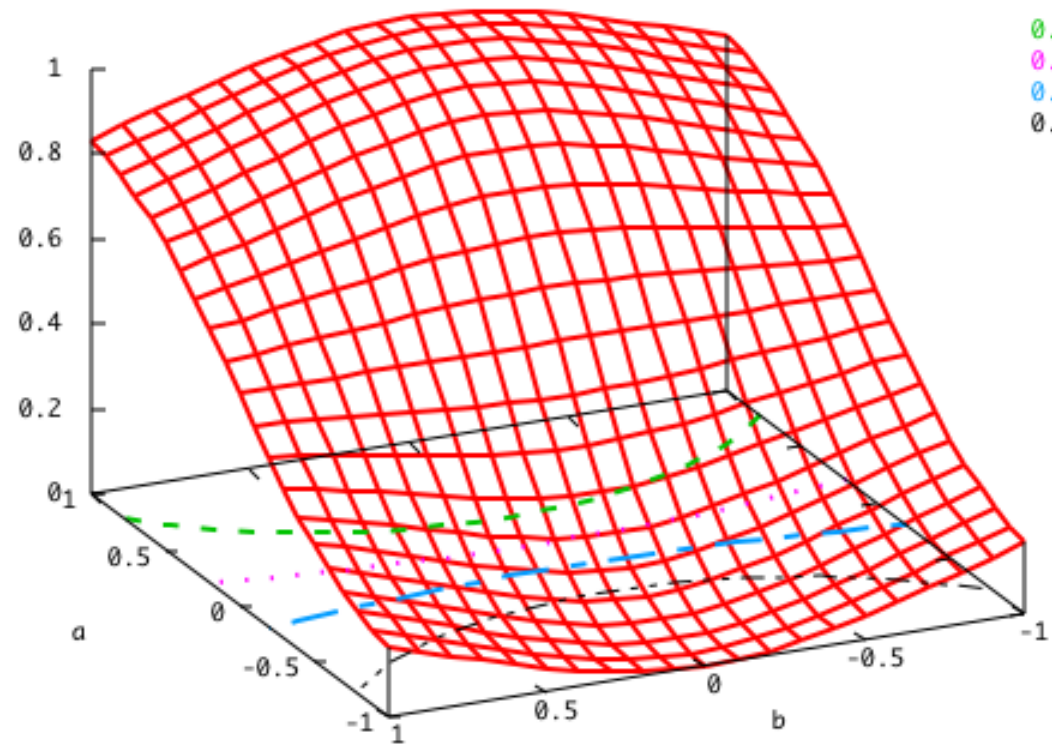
$$a = 1, b = 0 \rightarrow \frac{|E_+|^2}{|E_+|^2 + |E_-|^2} = 1$$

$$a = -1, b = 0 \rightarrow \frac{|E_+|^2}{|E_+|^2 + |E_-|^2} = 0$$

$$a = 0, -1 \leq b \leq 1 \rightarrow \frac{|E_+|^2}{|E_+|^2 + |E_-|^2} = \frac{1}{2}$$

$E+2/(E+2+E-2)$

Maximized  $E_+$



Maximized  $E_-$



# ICRF Heating Methods

---

**Slow wave (L wave) has a left-handed polarized field in the range  $\omega < |\Omega_{ci}|$  and a powerful tool to heat ions. But as seen in the plot of  $k_{//}$  vs.  $\omega$ , i.e., the previous view graph it becomes cut-off at  $\omega > |\Omega_{ci}|$ . In torus devices RF waves are launched from the outer region, where the magnetic field strength is lower than that at axis. Therefore the slow wave can not propagate in the plasma.**

**On the other hand again seen in the plot of  $k_{//}$  vs.  $\omega$ , fast wave (R wave) can propagate in the plasma. But it has a right-handed polarized field in the range  $\omega \sim |\Omega_{ci}|$ . Therefore the wave energy does not damp to ions.**



# ICRF Heating Methods

## -minority heating method-

Minority heating method: **finding  $E_+$  in plasma with two ions**

**Two ions: minority ions and majority ions**

minority ions: weight ( $m_m$ ), charge ( $Z_m$ ), density ( $n_m$ )

majority ions: weight ( $m_M$ ), charge ( $Z_M$ ), density ( $n_M$ )

Defining 
$$\eta_M = \frac{Z_M^2 n_M}{n_e}, \eta_m = \frac{Z_m^2 n_m}{n_e}$$

**From charge neutrality**

$$n_e = Z_M n_M + Z_m n_m \rightarrow \frac{\eta_M}{Z_M} + \frac{\eta_m}{Z_m} = 1$$

**Dispersion relation of ICRF wave**

$$\begin{vmatrix} K_{\perp} - N_{//}^2 & K_{\times} \\ -K_{\times} & K_{\perp} - N_{//}^2 - N_{\perp}^2 \end{vmatrix} = \begin{vmatrix} R + L - 2N_{//}^2 & -i(R - L) \\ i(R - L) & R + L - 2N_{//}^2 - 2N_{\perp}^2 \end{vmatrix} = 0$$



# Fast Wave can Propagate

## -minority heating method-

### Solution of $N_{\perp}^2$

$$N_{\perp}^2 = \frac{(R - N_{\parallel}^2)(L - N_{\parallel}^2)}{S - N_{\parallel}^2}$$

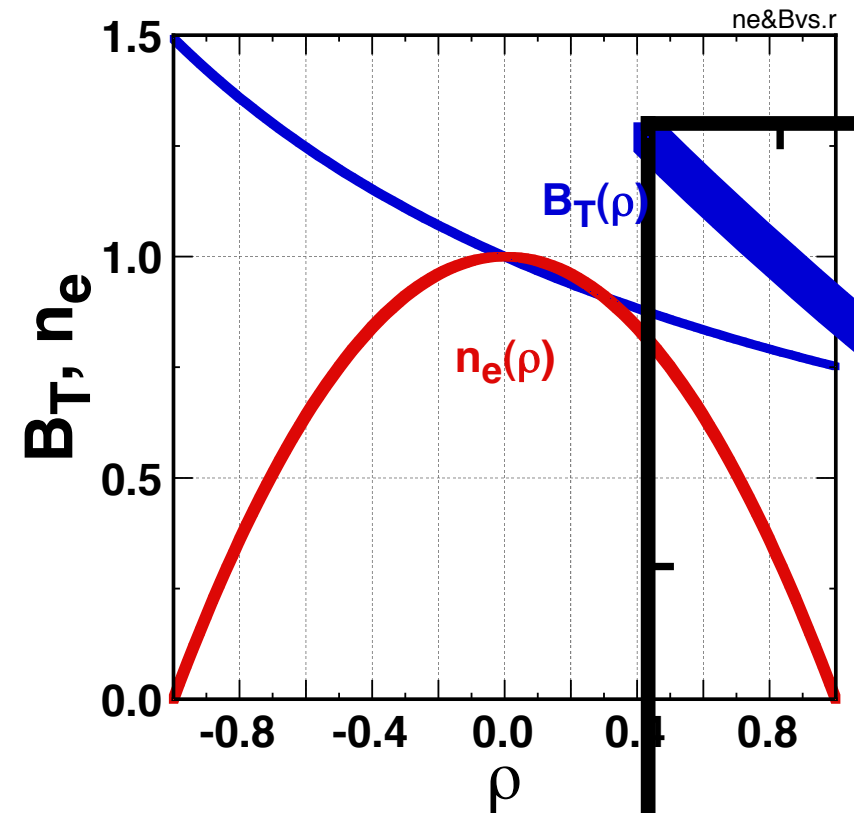
**R, L, S are**

$$R = -\frac{\Pi_i^2}{\omega^2} \left( \frac{m_M}{m_m} \frac{\eta_m \omega}{\omega + \Omega_m} + \frac{\eta_M \omega}{\omega + \Omega_M} - \frac{\Omega_M}{Z_M} \omega \right)$$

$$L = -\frac{\Pi_i^2}{\omega^2} \left( \frac{m_M}{m_m} \frac{\eta_m \omega}{\omega - \Omega_m} + \frac{\eta_M \omega}{\omega - \Omega_M} + \frac{\Omega_M}{Z_M} \omega \right)$$

$$S = -\frac{\Pi_i^2}{\omega^2} \left( \frac{m_M}{m_m} \frac{\eta_m \omega^2}{\omega^2 - \Omega_m^2} + \frac{\eta_M \omega^2}{\omega^2 - \Omega_M^2} \right)$$

**$B_T(\rho)$  and  $n_e(\rho)$**



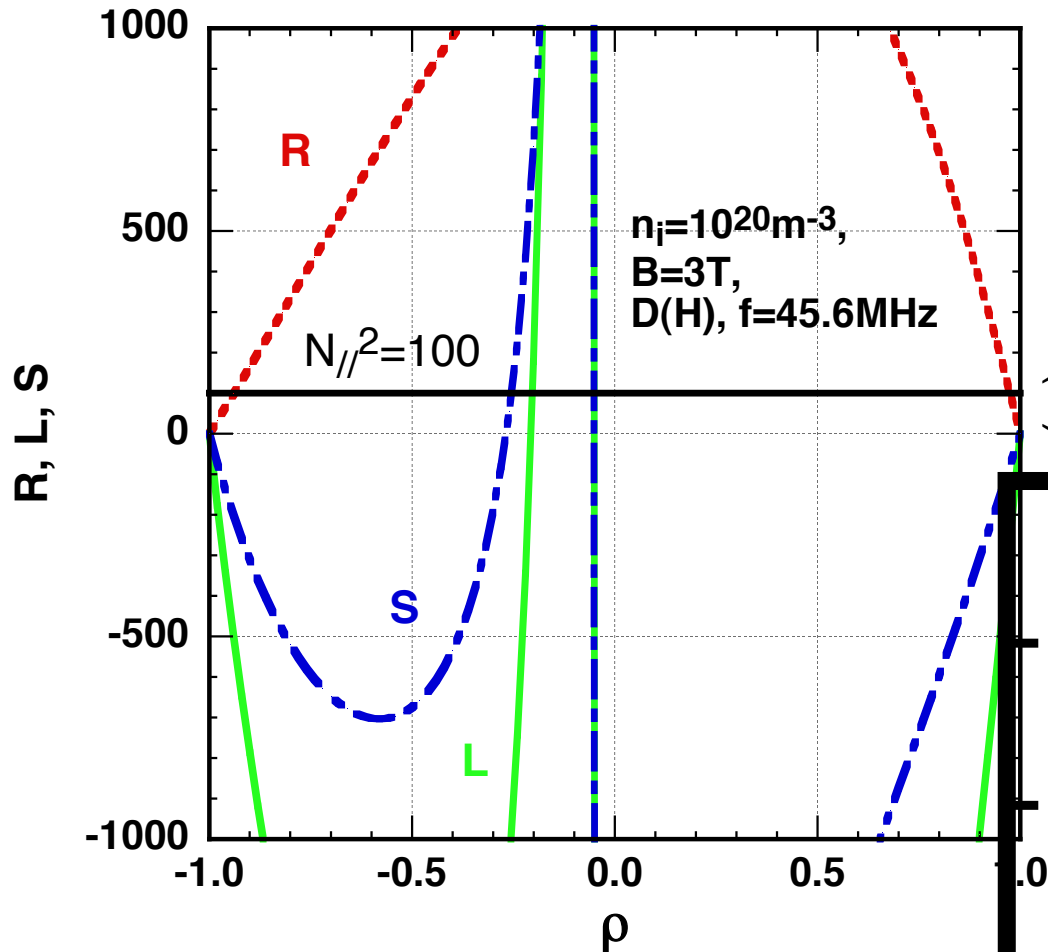


# Fast Wave Propagating Region

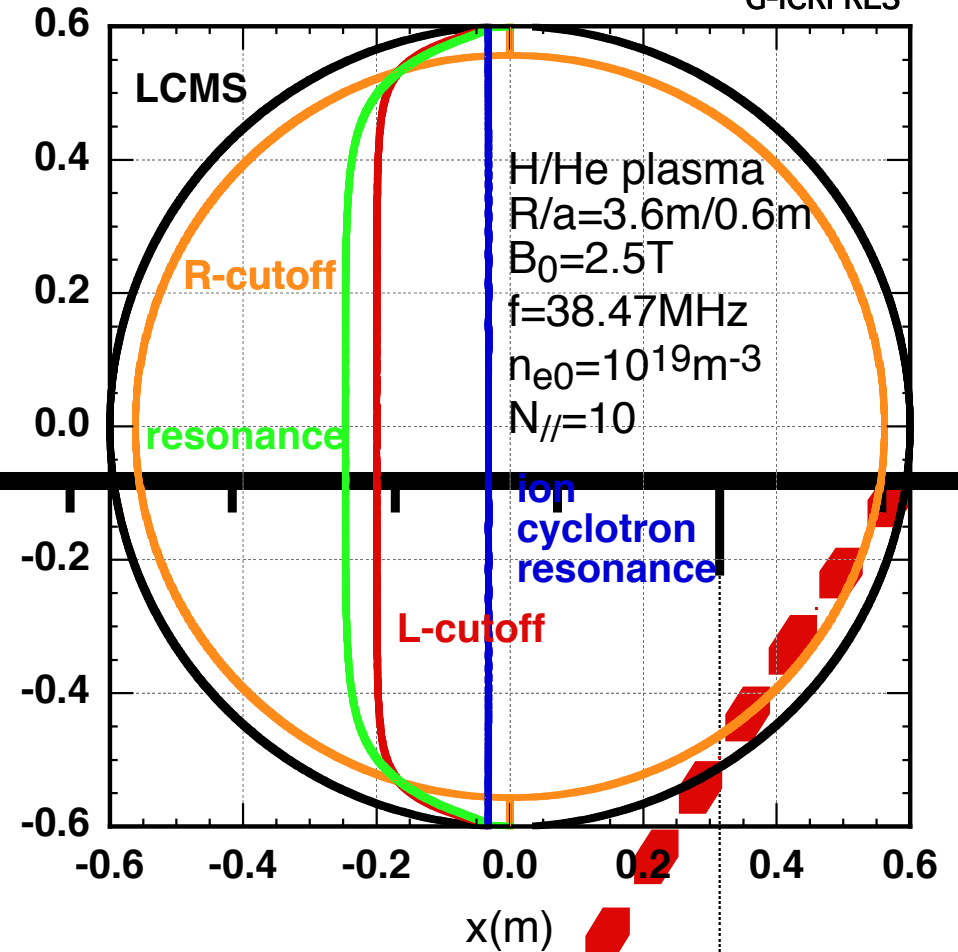
R, L and are plotted on  $\rho$  for  $n_{e0}=10^{19}\text{m}^{-3}$ ,  $B_0=3\text{T}$ ,  $f=39\text{MHz}$ ,  $N_{//}=10$ ,  $R/a=3.6\text{m}/0.6\text{m}$ .

Fast wave is cut-off at the outside of R layer and between L-cutoff and hybrid resonance layers.

G-RLS



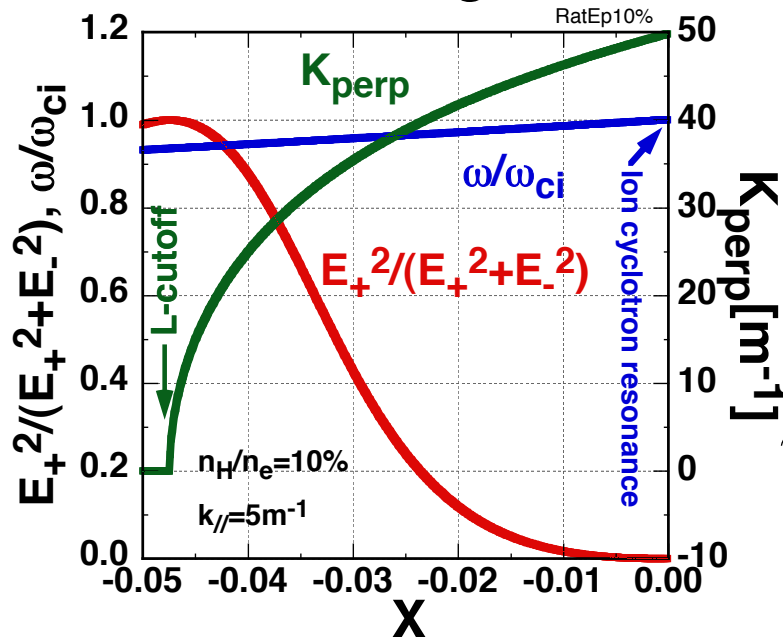
G-ICRFRLS



In minority heating,  $E_+$  coexists with  $E_-$  in the plasma. The ratio of  $E_+/E_-$  depends on the minority density ratio and  $\omega/\omega_{ci}$  etc;

$$\frac{|E_+|^2}{|E_+|^2 + |E_-|^2} = \frac{1}{2} \frac{(1+a)^2 + b^2}{1+a^2 + b^2} = f\left(\frac{\omega}{\omega_{ci}}\right) \Leftarrow i \frac{E_y}{E_x} = a + bi$$

$E_+/E_-$  has its maximum L-cutoff layer and decreases as reaching to  $\omega/\omega_{ci} = 1$  as in the bottom view figure.



RF electric field energy is absorbed with resonant ions,  $v_{thi} = (\omega - \omega_{ci})/k_{//}$  via. cyclotron damping and they are accelerated to high energy ions. The smaller the minority ratio is, the shorter the distance between L-cutoff and ion cyclotron layers becomes. Then ions with relatively low energy becomes a resonant ion for an cyclotron damping. But total number of resonant ions becomes smaller.

**Heating efficiency:**

$$\eta = \int (\text{antenna spectram}) \times (\text{wave coupling}) \times (\text{absorption}) dk_{//}$$



# ICRF Higher Harmonic Heating

When this heating method is employed in fusion reactors, several % of minority ions such as H ions is required in the majority plasma consisting of Deuterium and Tritium ions.

Q value. i.e., ratio of fusion output to plasma heating power depends on density of Deuterium and Tritium ions in the limited  $\beta$  value.

$$P_N = 100(\beta_{DT} B_t^2)^2 R a^2 (MW)$$

$$P_{Fusion} \propto \beta_{DT}^2 \propto n_{DT}^2$$

When  $n_H/n_e=10\%$ ,  $n_D/n_e=n_T/n_e=45\%$ .  $P_{Fusion}$  is reduced to 80% of  $P_{fusion}$  without H ions.

**No minority ions are required in ICRF 2<sup>nd</sup> harmonic Heating.**



# ICRF $n^{\text{th}}$ Harmonic Heating



Heating power of ICRF  $n^{\text{th}}$  harmonic heating can be deduced using a hot dispersion equation and a plasma dispersion function.

$$P_{in} = \frac{\omega \epsilon_0}{2} |E_x + iE_y|^2 \left( \frac{\Pi_i}{\omega} \right)^2 \left( \frac{n^2}{2n!} \right) \left( \frac{b}{2} \right)^{n-1} \frac{\omega}{2^{1/2} k_z v_{Ti}} \pi^{1/2} \exp \left( -\frac{(\omega - n|\Omega_i|)^2}{2(k_z v_{Ti})^2} \right)$$

$$\text{Here, } b = \left( \frac{k_{\perp} v_{Ti}}{\Omega_i} \right)^2 : \text{finite Larmor radius effect}$$

$$\text{for } n = 2 \text{ then } P_{in} \propto \omega \left( \frac{\Pi_i}{\omega} \right)^2 \left( \frac{\Pi_i}{\Omega_i} \right)^2 \frac{T_i}{\Omega_i^2} \omega \leftarrow N_{\perp}^2 \propto k_{\perp}^2 \propto \left( \frac{\Pi_i}{\omega_{ci}} \right)^2$$

$$\propto \frac{nT_i}{B^2} \propto \beta$$

For example in the 2<sup>nd</sup> harmonic heating, ions are accelerated and decelerated during one period cyclotron motion with the polarized RF electric field. Ions eventually gain no energy. Intuitively we noticed that when the RF wave field length ( $\pi/k_{\perp}$ ) is the same order of an ion Larmor radius  $\rho_i$ , ions are accelerated with the RF electric field. => **Finite Larmor radius effect.**

The high energy ions are accelerated more than the lower energy ions.



# ICRF n<sup>th</sup> Harmonic Heating

## -fraction of E<sub>+</sub>-

**Polarization RF electric field:**

$$i \frac{E_y}{E_x} = \frac{(1 - N_{||}^2)(n+1)(n-1)}{n^2} \frac{\Omega_i^2}{\Pi_i^2} - \frac{1}{n} = a + bi$$

$$\frac{\Omega_i^2}{\Pi_i^2} \ll 1 (\text{High density}) \Rightarrow a = -\frac{1}{n}, \frac{\Omega_i^2}{\Pi_i^2} \gg 1 (\text{Low density}) \Rightarrow a = -\infty \because 1 - N_{||}^2 < 0$$

**In the high density region, i.e.,**

$$\frac{|E_+|^2}{|E_+|^2 + |E_-|^2} = \frac{1}{2} \frac{(1+a)^2 + b^2}{1+a^2 + b^2} = \frac{1}{2} \frac{(1-1/n)^2}{1+(1/n)^2}$$

$$n = 2 \rightarrow \frac{|E_+|^2}{|E_+|^2 + |E_-|^2} = \frac{1}{10}, n = 3 \rightarrow \frac{|E_+|^2}{|E_+|^2 + |E_-|^2} = \frac{2}{9}$$

$$n \gg 1 \rightarrow \frac{|E_+|^2}{|E_+|^2 + |E_-|^2} \approx \frac{1}{2}$$

**30/71**

**In higher (n<sup>th</sup>) harmonic heating, a fraction of E<sub>+</sub><sup>2</sup> is increased with n. But heating efficiency reduces with n due to finite Larmor radius effect, b<sup>n-1</sup>.**



# Outlines

---

1. Waves in plasma
2. Physics on ICRF heating
3. **Experiments of ICRF heating on LHD**
4. ICRF heating technologies
5. Discussion of RFH and RFCD on ITER
6. Summary



# Large Helical Device (LHD)



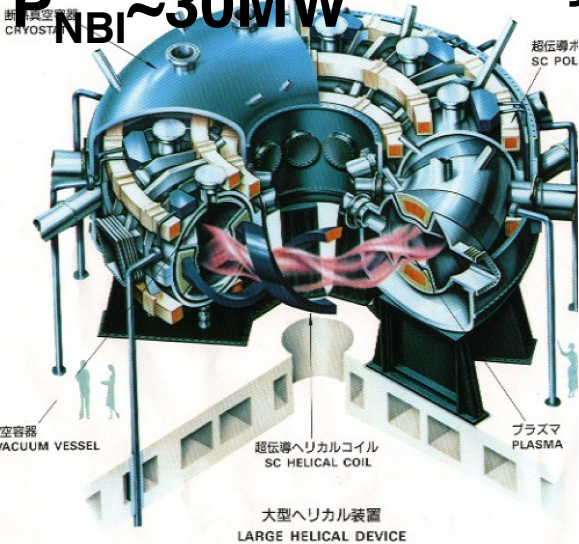
$R_{ax}: 3.6 \sim 3.75\text{m}$

$B: 2.75\text{T} \sim 2.64\text{T}$

$P_{ICH} \sim 2.5\text{MW}$

$P_{ECH} \sim 3\text{MW}$

$P_{NBI} \sim 30\text{MW}$



#1 NNBI

ECH System

#2 NNBI

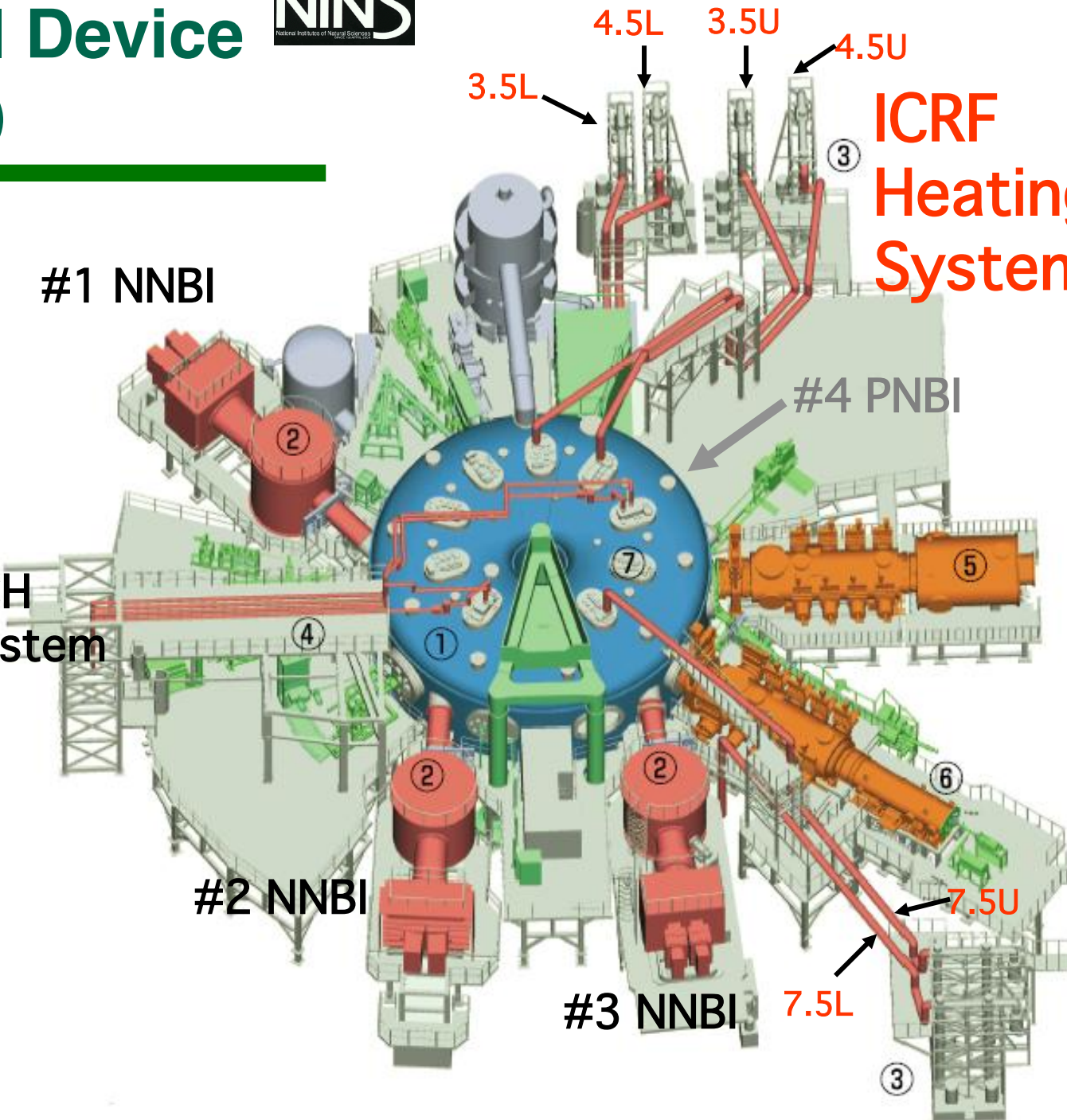
#3 NNBI

7.5L

3.5L 4.5L 3.5U 4.5U

ICRF Heating System

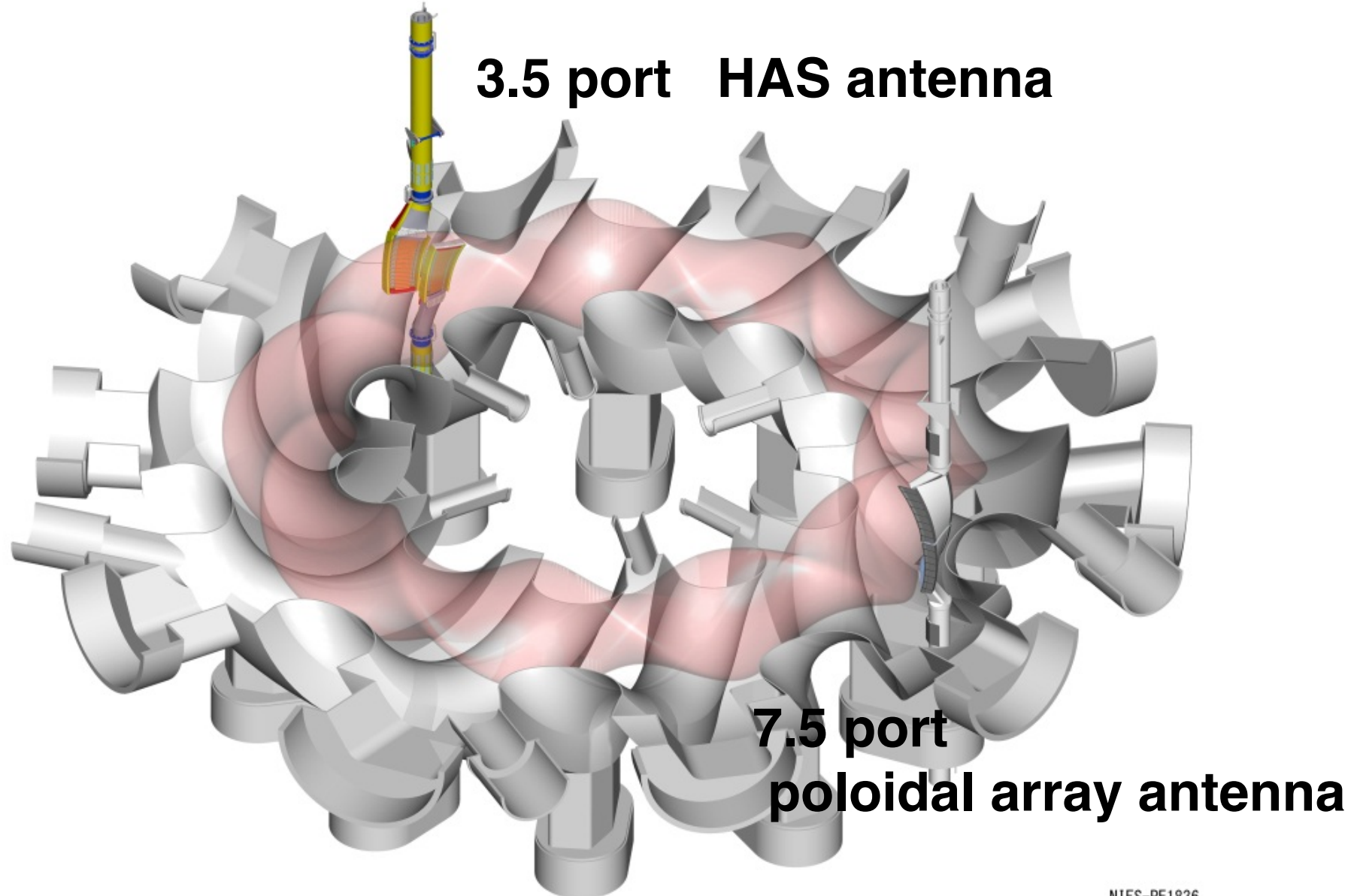
#4 PNBI



# ICRF Heating Antennas

-poloidal and toroidal array antennas-

---





# ICRF Heating Antenna

## -poloidal array antenna-

**U & L antenna: a pair of antennas are installed from upper & lower vacuum port.**

**Antenna shape fitting to last closed magnetic surface.**

**Antenna size:**

**Length: 60cm**

**width: 46cm**

**width of strap: 30cm**

**All components are water-cooled.**

**Antenna is movable in radial direction.**





# HAS ICRF Heating Antenna

**-hand shake antenna with toroidal array antenna-**



- strap width : 20cm
- strap length : 75cm
- antenna width : 54cm
- antenna gap : 10cm
- antenna thickness : 12cm
- water-cooled strap and backplate
- Faraday shield is made by Cu-SUS clad
- Side protector is made by CFC
- Movable in horizontal direction

## -minority heating-

### Dispersion eq. of fast wave

$$\begin{pmatrix} R+L-2N_{\parallel}^2 & -i(R-L) \\ i(R-L) & R+L-2N_{\parallel}^2-2N_{\perp}^2 \end{pmatrix} \begin{pmatrix} E_x \\ E_y \end{pmatrix} = 0$$

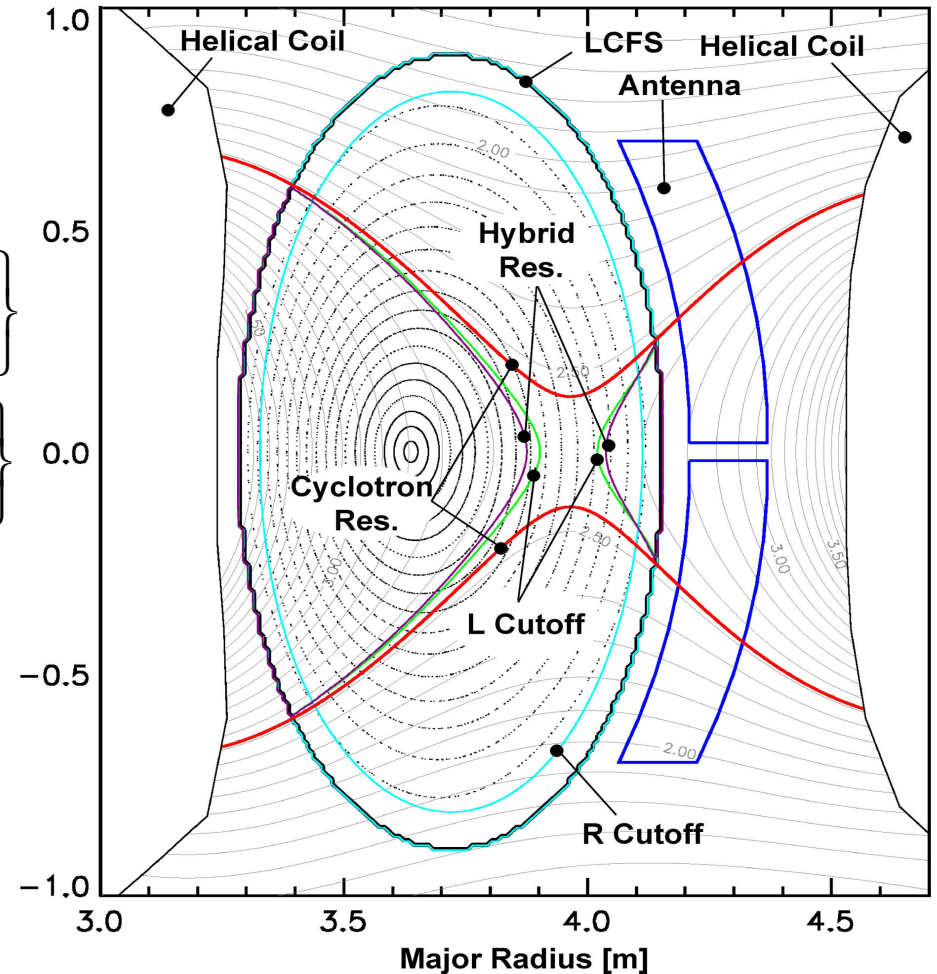
$$R = -\frac{\omega_{piHe}^2}{\omega^2} \left\{ \frac{4n_H}{n_e} \frac{\omega}{\omega - \omega_{ciH}} + \left(1 - \frac{n_H}{n_e}\right) \frac{\omega}{\omega - \omega_{ciHe}} - \frac{\omega}{\omega_{ciHe}^2} \right\}$$

$$L = -\frac{\omega_{piHe}^2}{\omega^2} \left\{ \frac{4n_H}{n_e} \frac{\omega}{\omega + \omega_{ciH}} + \left(1 - \frac{n_H}{n_e}\right) \frac{\omega}{\omega + \omega_{ciHe}} - \frac{\omega}{\omega_{ciHe}^2} \right\} \quad z \text{ [m]}$$

$$S = -\frac{\omega_{piHe}^2}{\omega^2} \left\{ \frac{4n_H}{n_e} \frac{\omega^2}{\omega^2 - \omega_{ciH}^2} + \left(1 - \frac{n_H}{n_e}\right) \frac{\omega^2}{\omega^2 - \omega_{ciHe}^2} \right\}$$



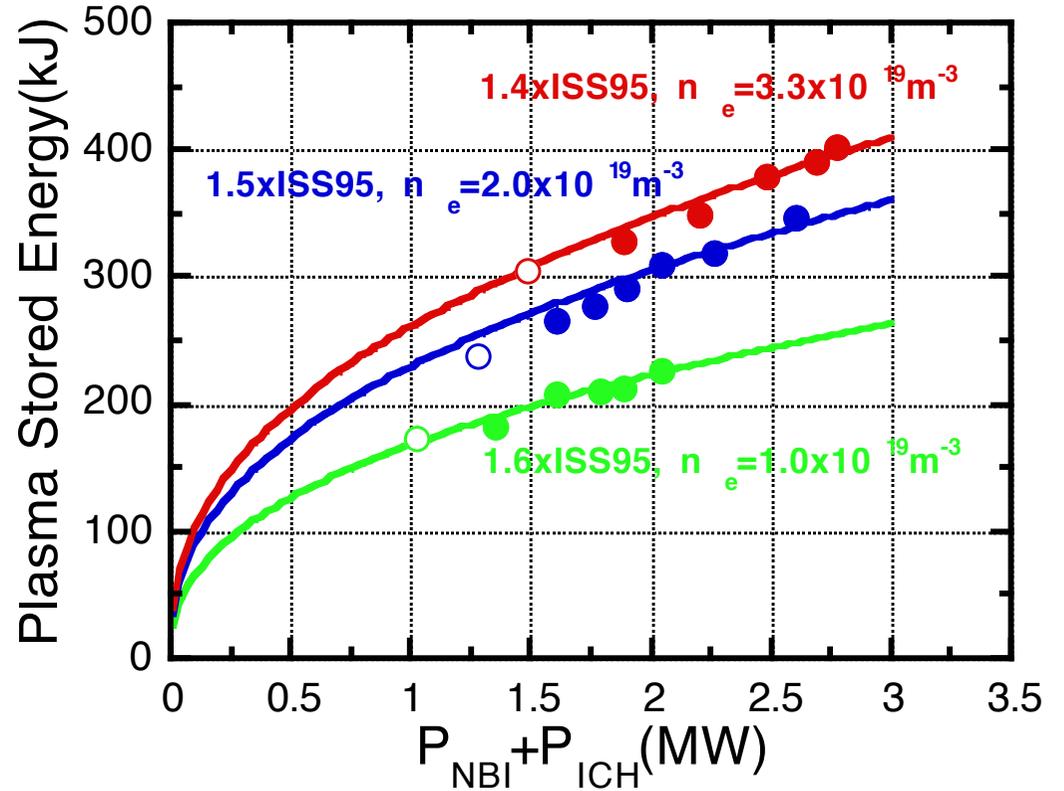
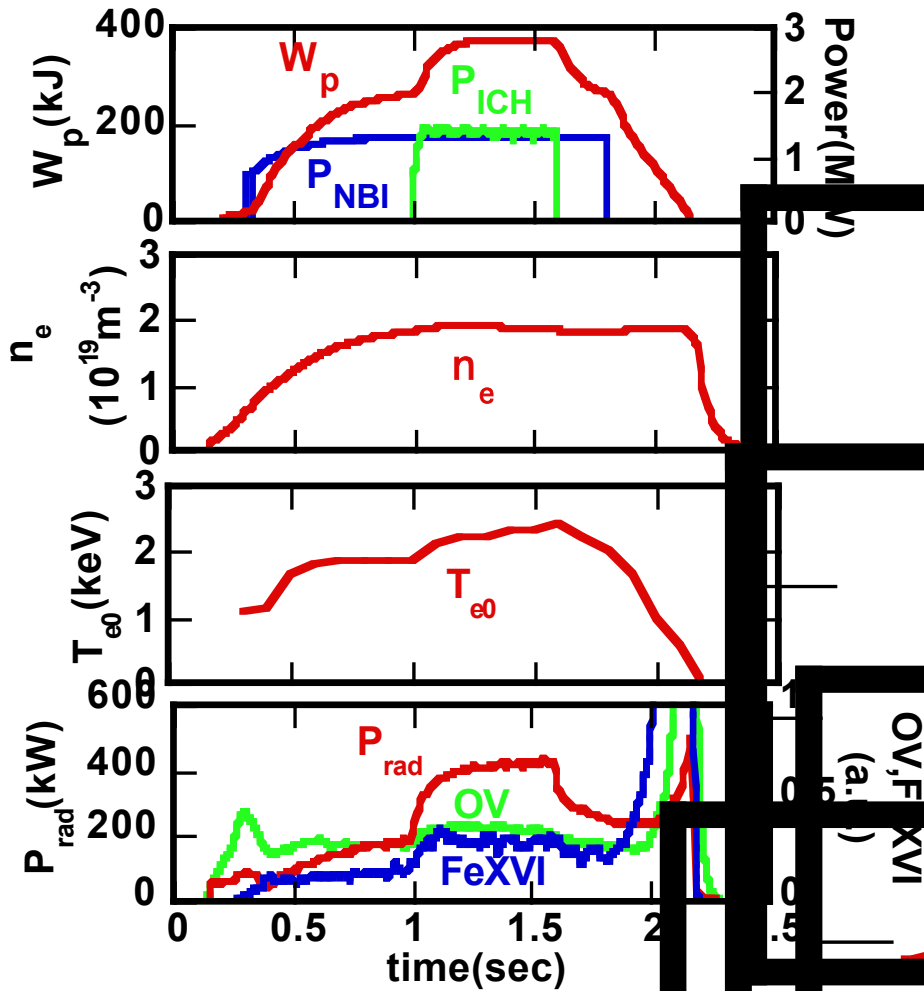
$$N_{\perp}^2 = \frac{(R - N_{\parallel}^2)(L - N_{\parallel}^2)}{S - N_{\parallel}^2}$$





# Additional ICRF Heating to NBI Plasma

#12988, He(H) plasma,  $R_{ax}=3.6m/B=2.75T$ ,  $f=38.47MHz$



**$W_p$  vs.  $P_{NBI} + P_{ICH}$   
on scaling of ISS95**



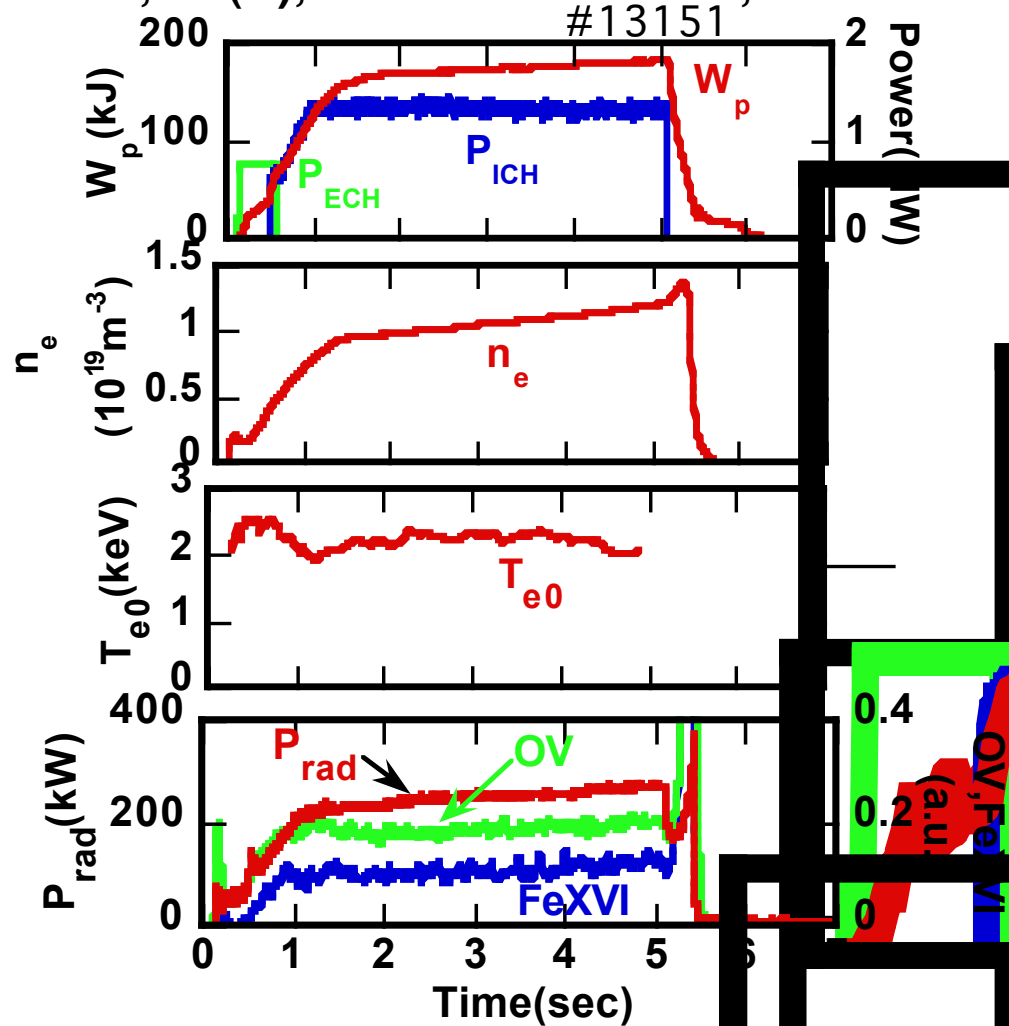
# Comparison of Plasma with ICRF Heating with that with NBI



-same plasma parameters with same heating power-

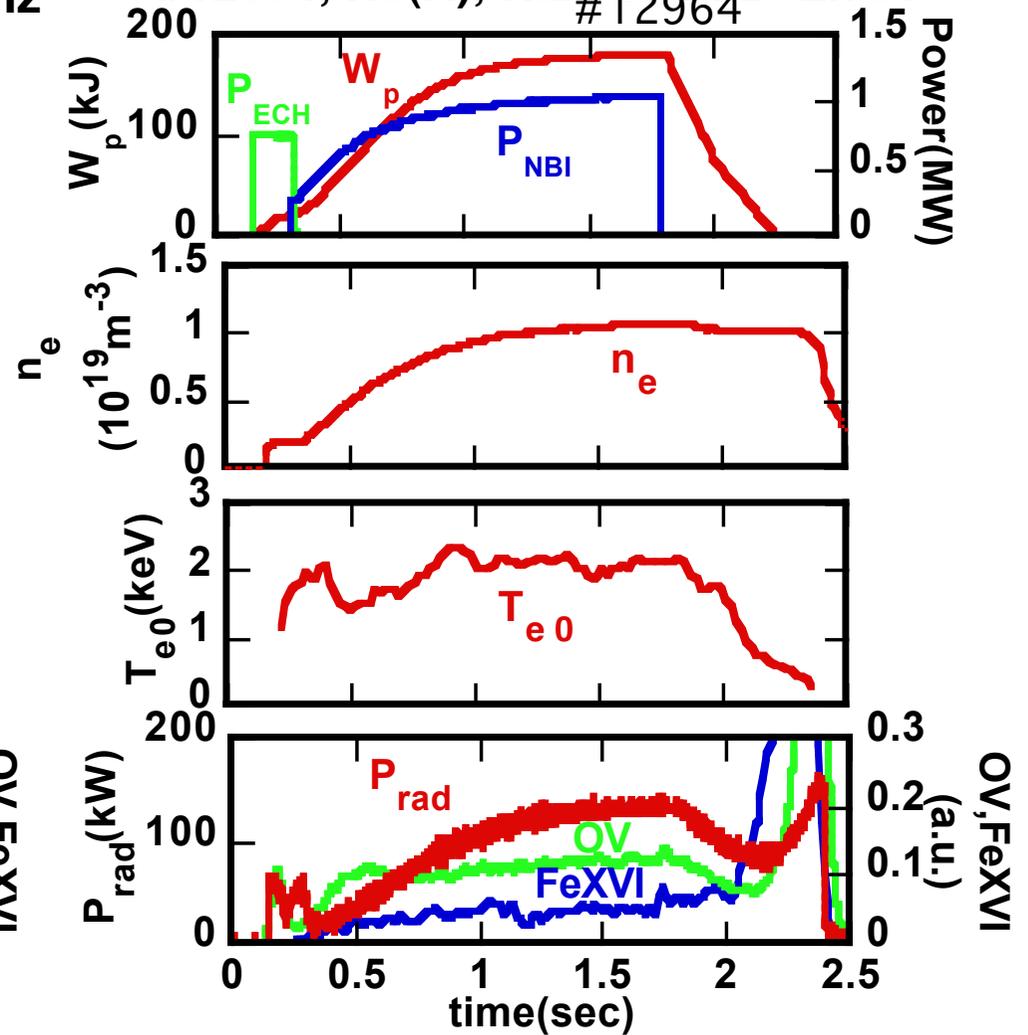
## ICH Plasma

#13151, He(H),  $R_{ax}=3.6m/B=2.75T, f=38.47MHz$



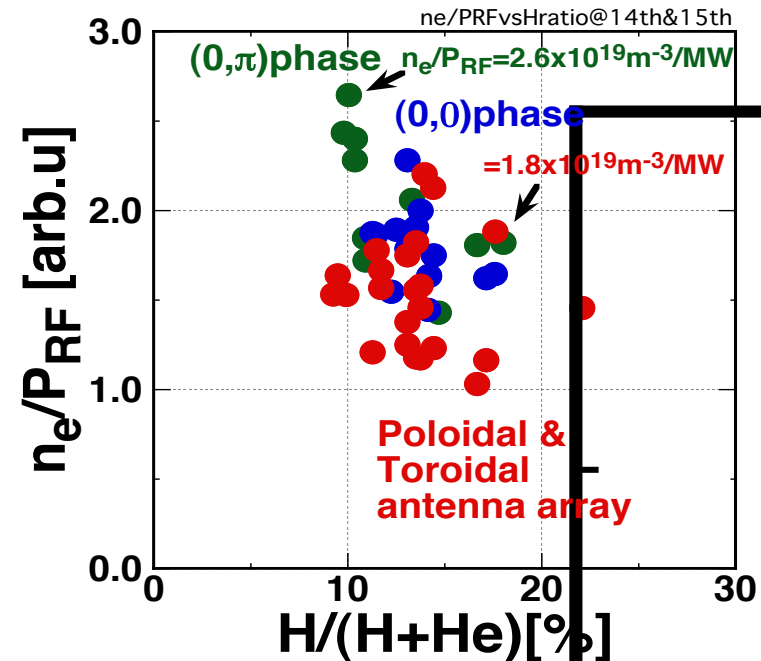
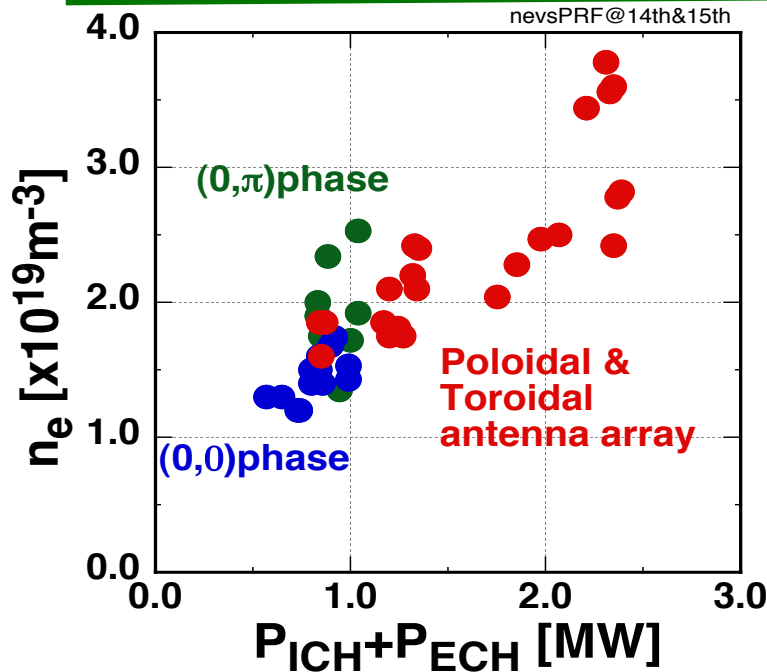
## NBI Plasma

#12964, He(H),  $R_{ax}=3.6m/B=2.75T$



# Relation of Density on $P_{RF}$ and Minority Ratio

-up to  $n_e=3.6 \times 10^{19} \text{m}^{-3}$ -

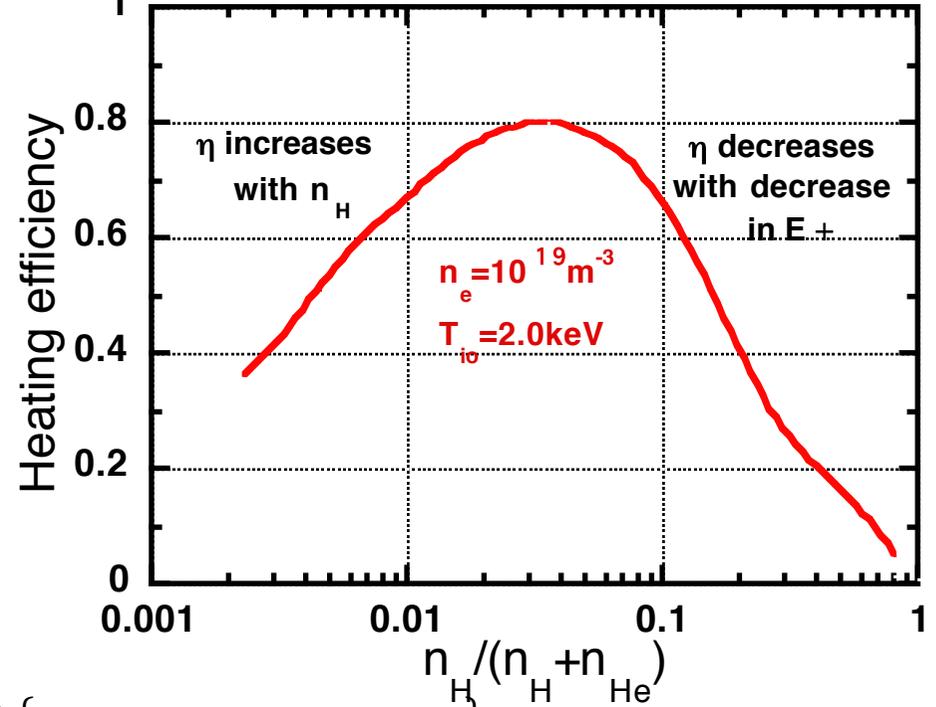
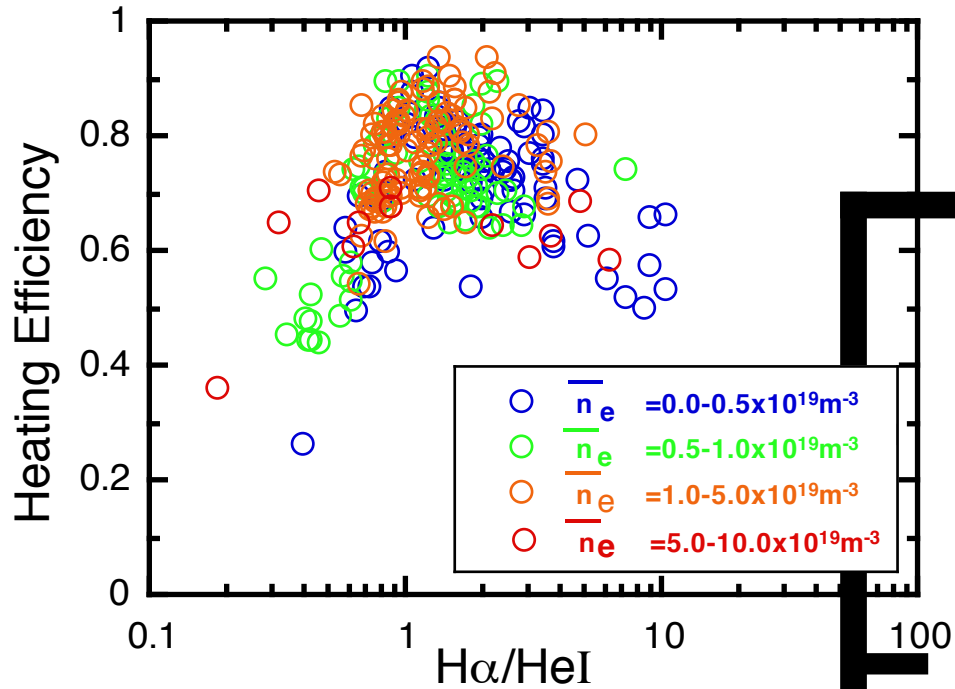


- High density plasma ( $n_e=3.6 \times 10^{19} \text{m}^{-3}$ ,  $T_e \sim T_i \sim 1 \text{keV}$ ,  $W_p=300 \text{kJ}$ ) was sustained with  $P_{ICH}=2 \text{MW}$  and  $P_{ECH}=0.37 \text{MW}$ .
- Density increases with RF power,  $P_{RF}(P_{ICH}+P_{ECH})$ .
- Ratio of  $H/(H+He)$  is a key parameter for high density operation. Highest density was achieved at  $H/(H+He) \sim 10\%$ .
- $n_e/P_{RF}$  is an index for achievement of high density. Higher  $n_e/P_{RF}$  is achieved with HAS antenna with  $(0, \pi)$ . Generally the lower  $H/(H+He)$  is, the higher density is achieved.

# Heating Efficiency

## -dependence of minority ratio-

$\omega/\omega_{ci}=0.92, B=2.75T, R_{ax}=3.6m, f=38.47MHz$



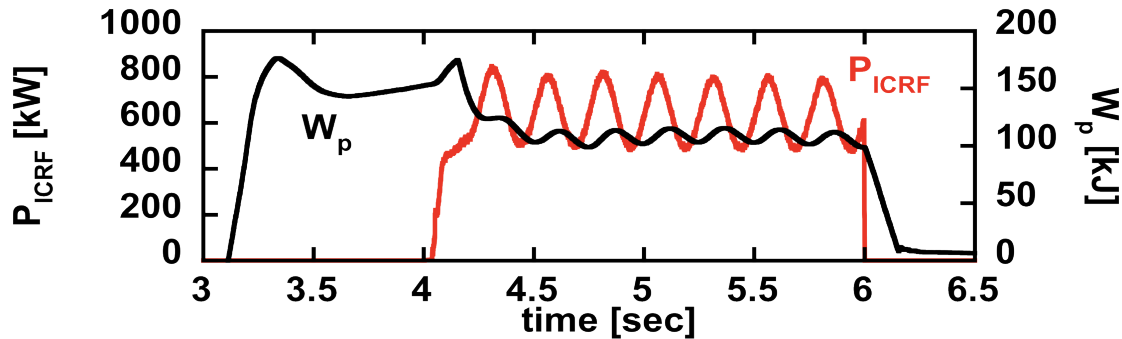
$$\frac{P_{abs}}{|E_0|^2} = \iint \frac{\epsilon_0}{2} \omega_{pi}^2 \frac{\pi^{1/2}}{|k_z|(2T_i/m_i)^{1/2}} \exp\left\{-\left(\frac{\omega - \omega_{ci}}{k_z(2T_i/m_i)^{1/2}}\right)^2\right\} \left\{\frac{1}{2} + \frac{\text{Im}(K_{xy}/(n_z^2 - K_{xx}))}{|K_{xy}/(n_z^2 - K_{xx})|^2 + 1}\right\} dk_z dV$$

$$K_{xx} = 1 + \sum_{\alpha} \frac{i\sqrt{\pi}\omega_{p\alpha}^2 z_0}{\omega^2 \mu_{\alpha}} \exp(-\mu_{\alpha}) \sum_{l=-\infty}^{\infty} l^2 I_l(\mu_{\alpha}) w(z_l), \quad K_{xy} = \sum_{\alpha} \frac{\sqrt{\pi}\omega_{p\alpha}^2 z_0}{\omega^2} \exp(-\mu_{\alpha}) \sum_{l=-\infty}^{\infty} l(I_l(\mu_{\alpha}) - I_l(\mu_{\alpha})) w(z_l)$$

$$\mu_{\alpha} = \frac{k_x^2 v_{t\alpha}^2}{2\omega_{c\alpha}^2}, \quad z_l = \frac{\omega - l\omega_{c\alpha}}{k_z v_{t\alpha}}$$



# Heating Efficiency Calculated with RF Power Modulation Method -dependence on phase difference-

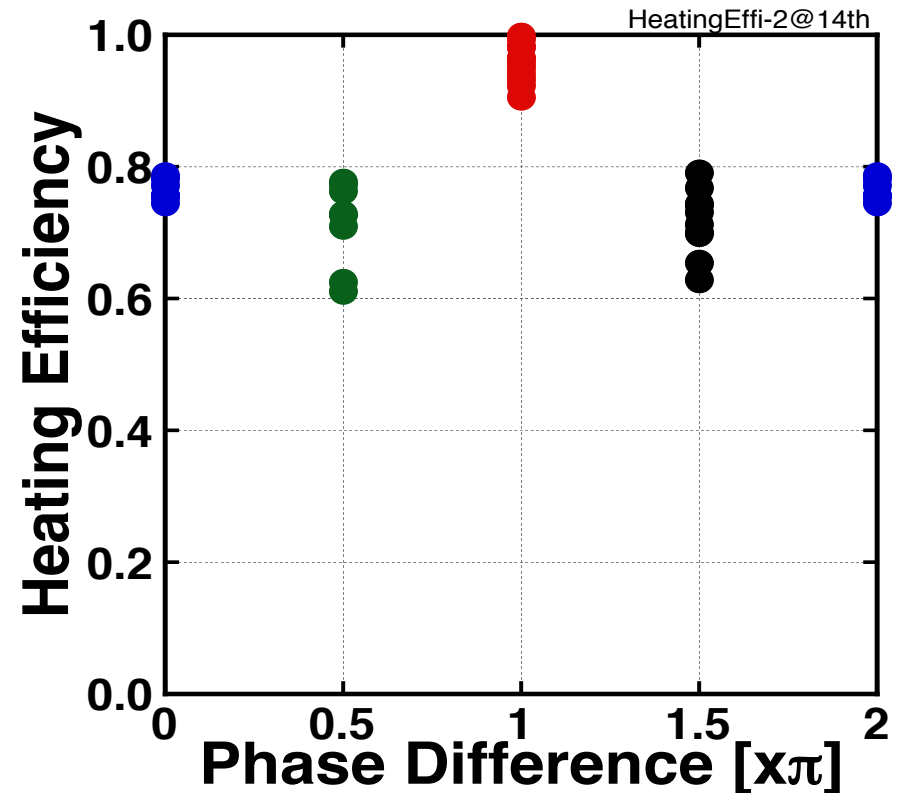


**modulation frequency**

$$\eta = \omega_{\text{mod}} \left\{ 1 + \frac{1}{(\omega_{\text{mod}} \tau_E)^2} \right\}^{1/2} \frac{\delta W_p}{\delta P_{ICH}},$$

$$\tau_E = \frac{\tan \delta}{\omega_{\text{mod}}}$$

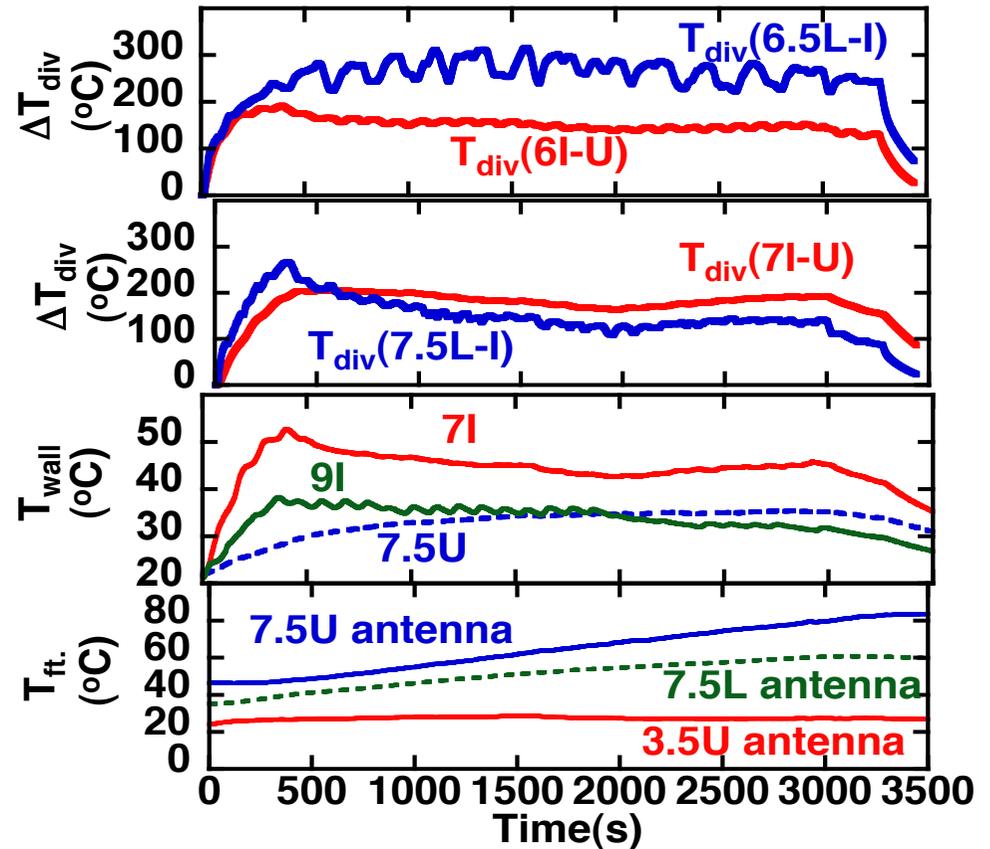
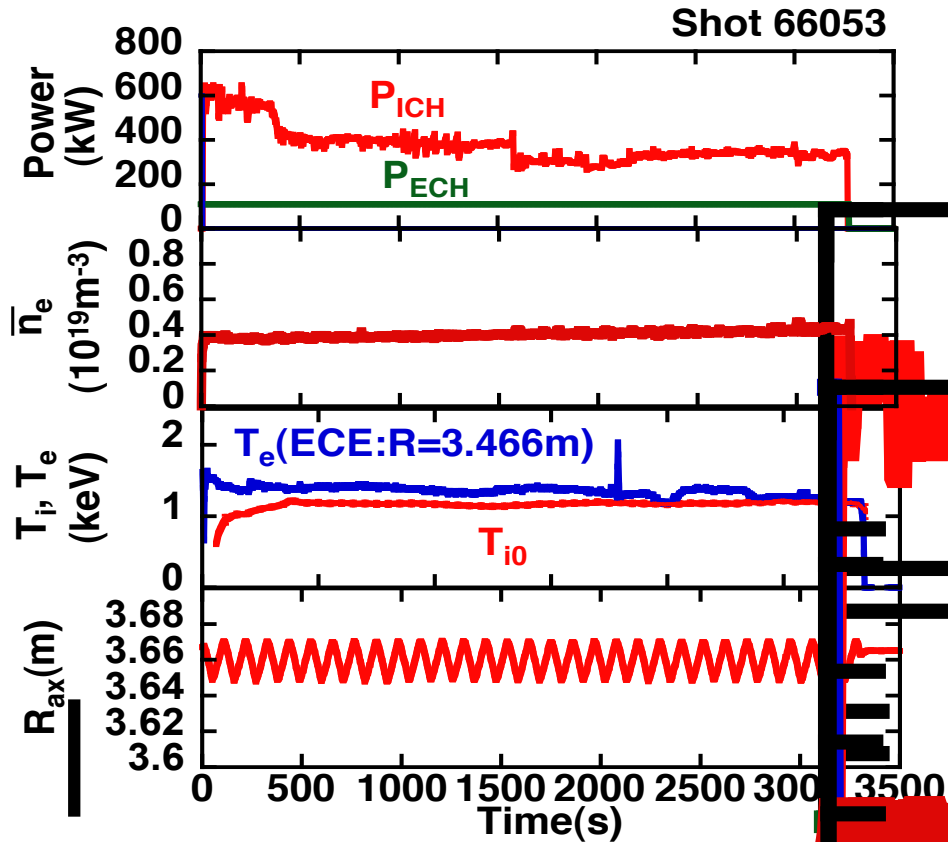
**phase difference  
between  $P_{ICH}$  and  $W_p$**





# Long Pulse Discharge

-54min. 28sec./0.5MW/1.6GJ-



Liquid stub tuner could reduce the reflected RF power, introduced later during the long pulse operation.



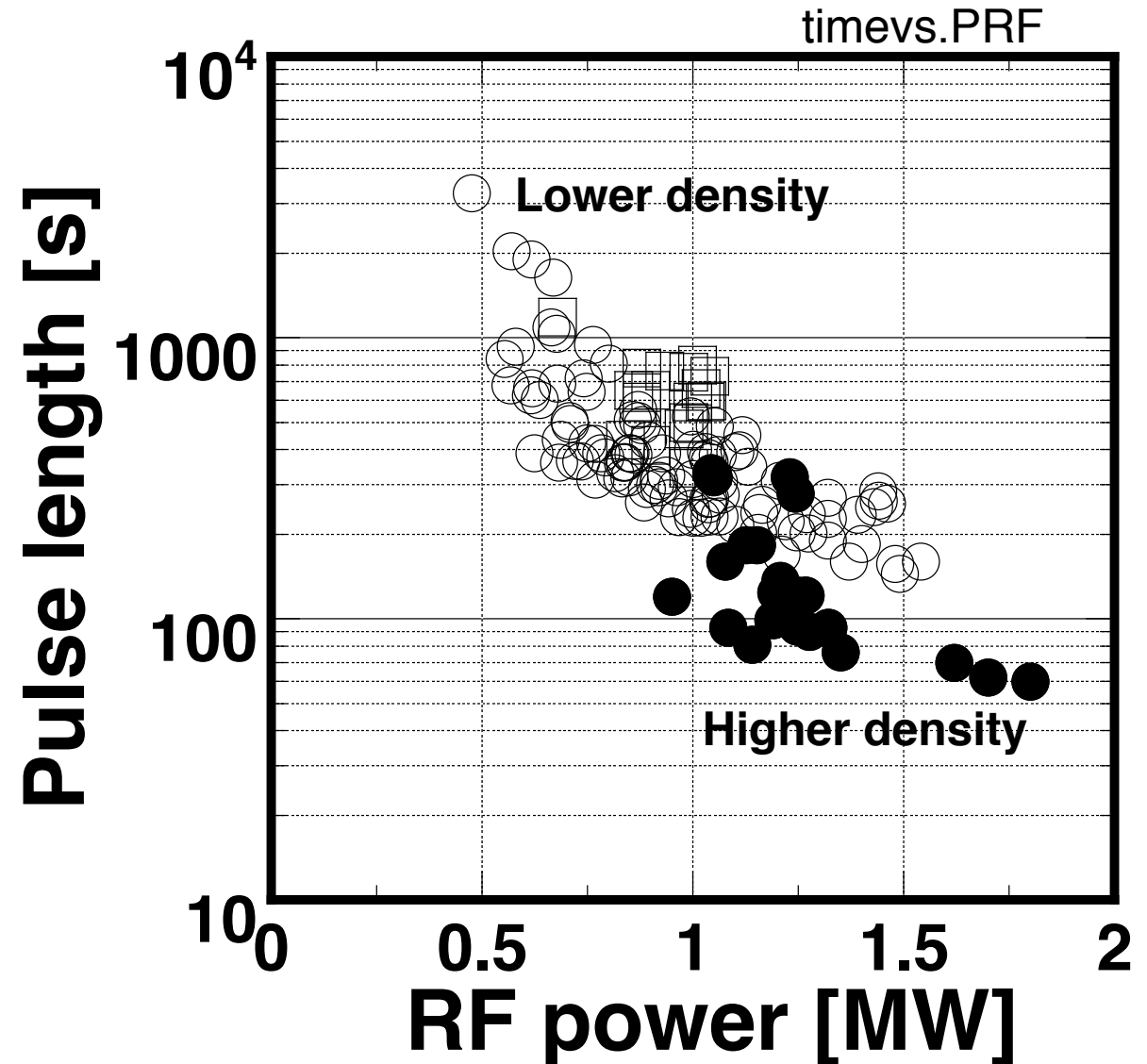
# Long Pulse operation

## -Duration time vs. RF heating power-

Plasma duration time is decreased with heating RF power.

This may be caused with increase in temperature of divertors.

In higher density plasma duration time may be shorter than that in lower density.





# Time Evolution of Plasma Collapse

t=1641.0s  
normal

t=1641.34s,  
arcing near 7-  
I, Fe injection

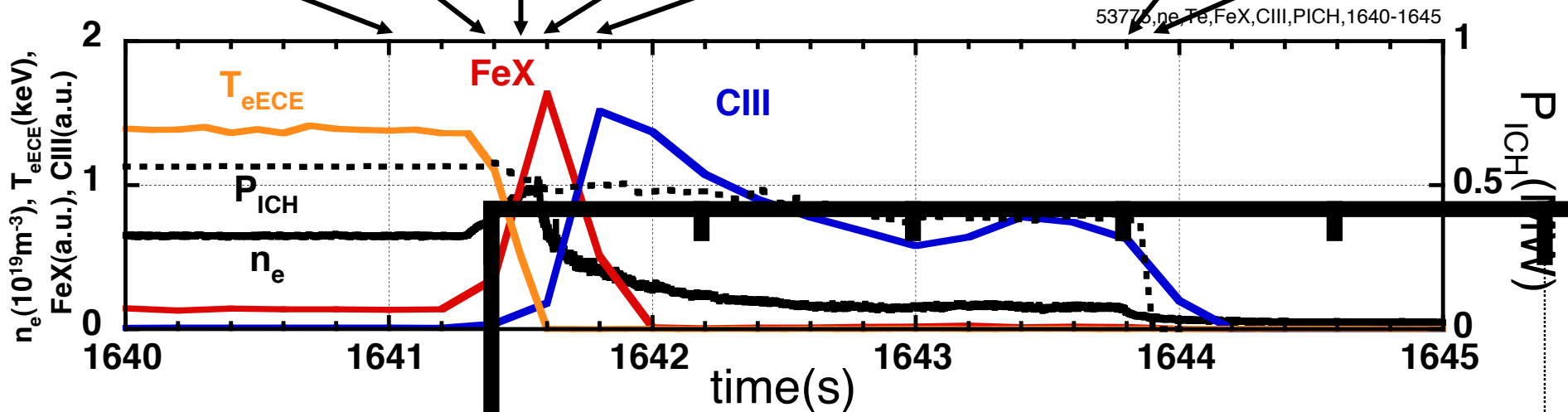
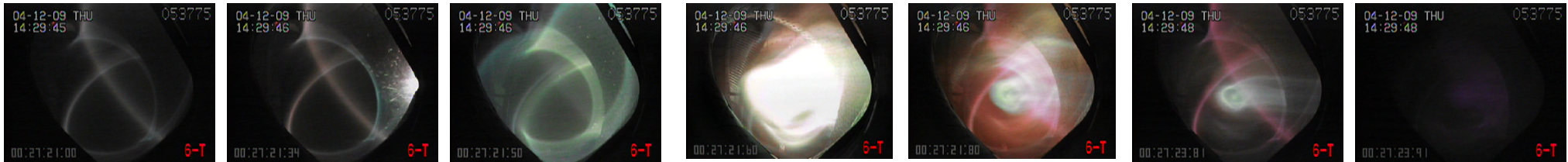
t=1641.5s  
Lower  
Te~0.5keV

t=1641.60s,  
Max. of FeX

t=1641.80s,  
Max. of CIII

t=1643.81s  
Just before  
ICH power-off

t=1643.91s  
Just after  
ICH-off



However at next discharge of 31m. 45s, no arcing was observed near 7-I just before the plasma collapse.

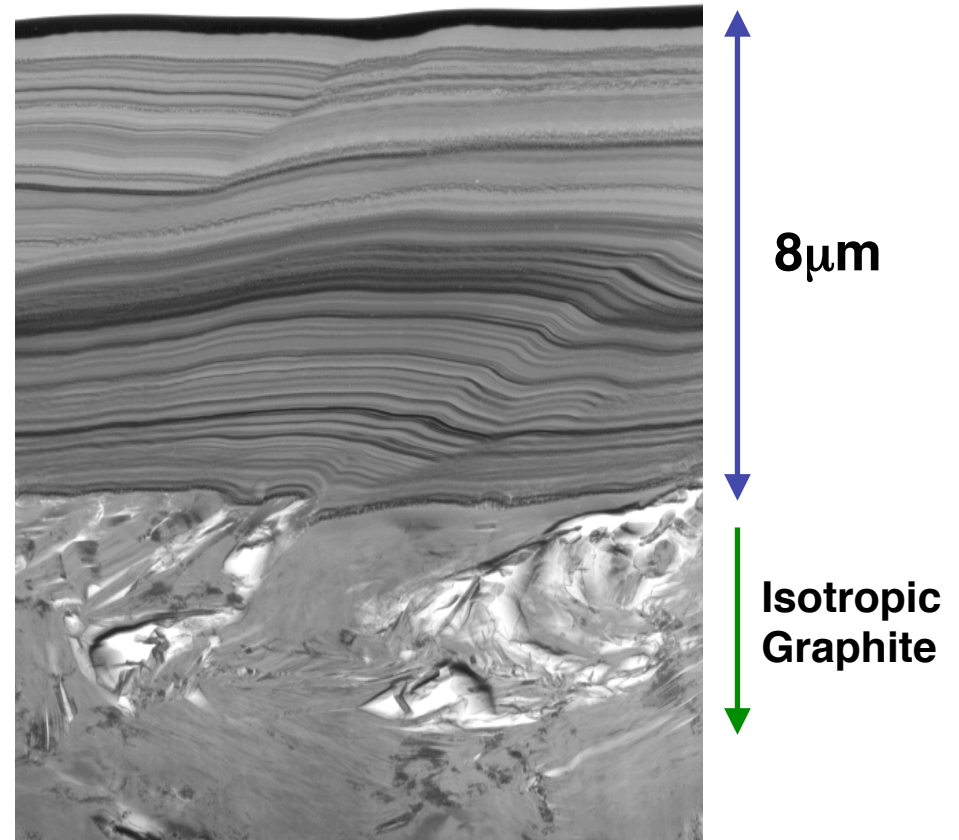
# Flakes with Fe/C on Divertor Plates

Many thin metal flakes were accumulated on the inner divertor plates.

Thickness:  $8\mu\text{m}$   
 with stratified structure  
 of high-Z (Fe etc.): **with He-glow discharge**  
 low-Z (C etc.) : **with main plasma discharge**  
 material layers.



Cross section of thin metal flakes



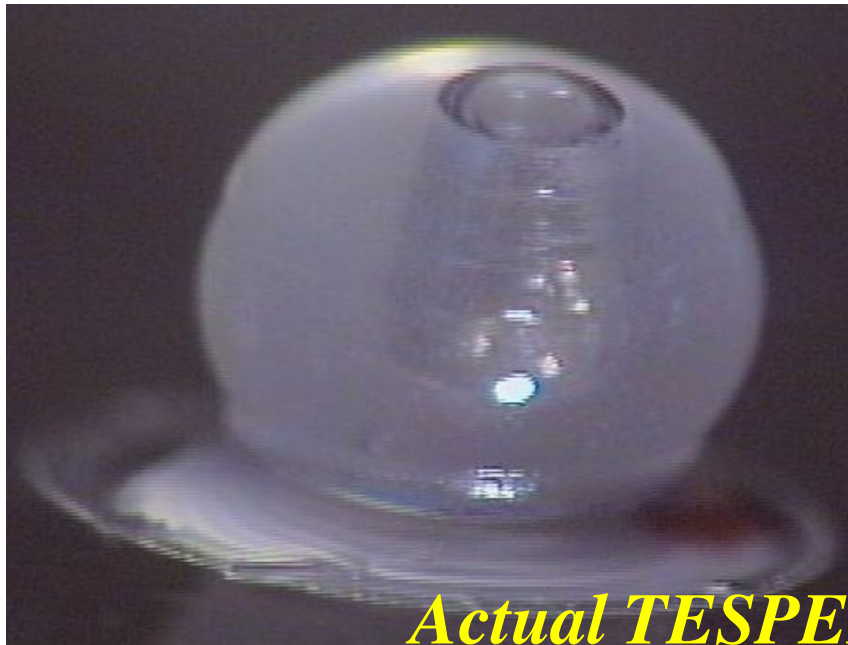
Deposition layers are amorphous.  
 Bright layers: graphite  
 Dark layers: metals  
 8 years-history of plasma discharges



# External Fe/C Pellet Injection

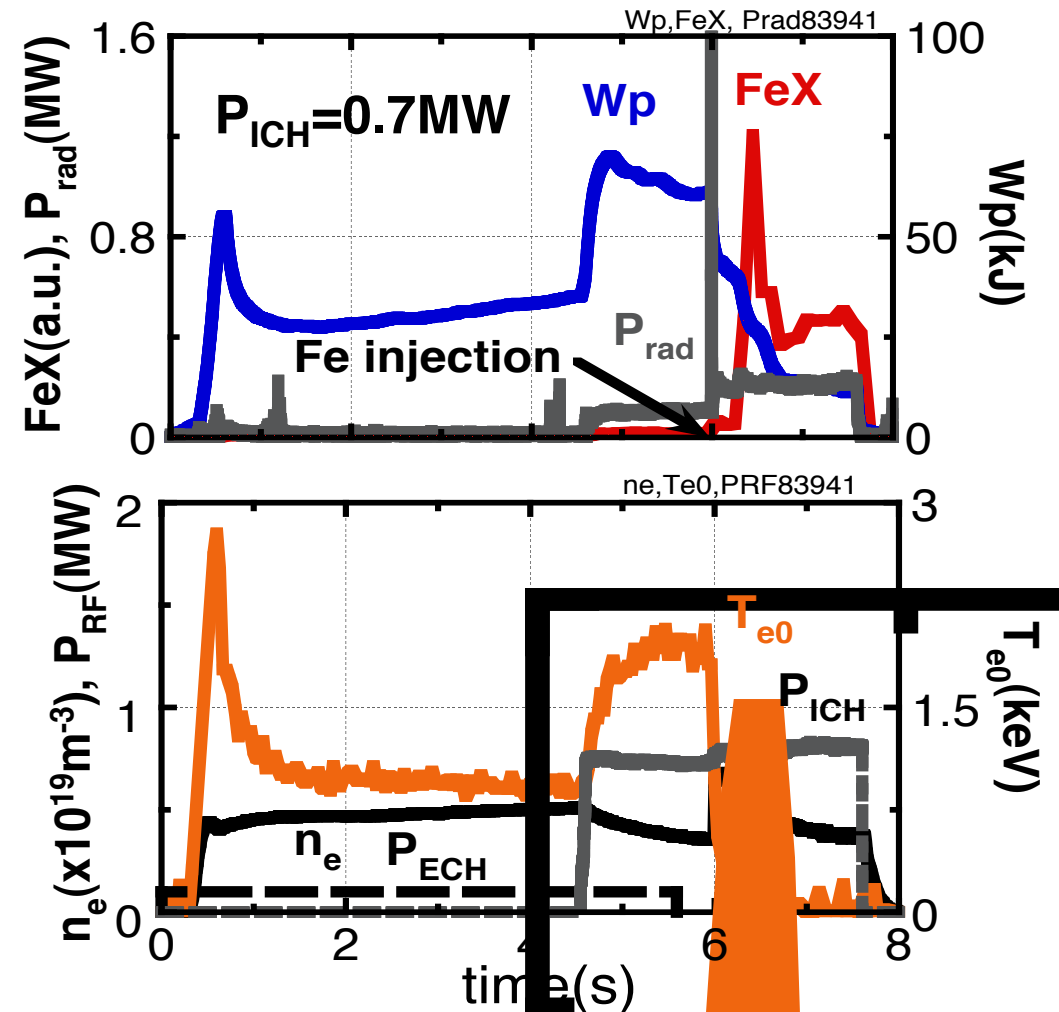
-to simulate plasma collapse by penetrating Fe impurities-

**TESPEL:**  
Tracer-Encapsulated Solid PELlet

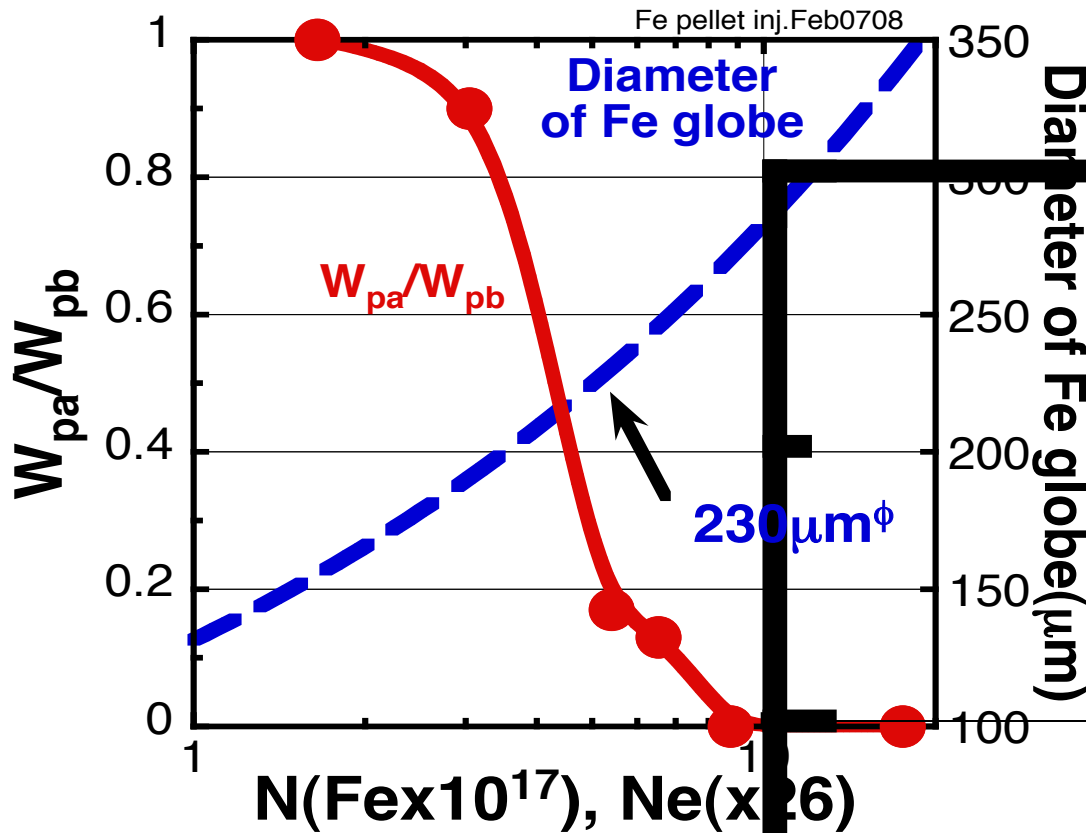


Diameter:0.1~0.35mm  
Outer shell:Polystyrene( $C_8H_8$ )<sub>n</sub>  
Velocity:200~500m/s  
Up to 59 TESPELs

## External injection Fe/C pellet



# Injection of Fe/C Pellet with Various Size



**Flakes:**  
**Thickness: 8 $\mu m$**   
**with stratified structure**  
**of high-Z (Fe etc.) and**  
**low-Z (C etc.) material layers**



**Penetration of thin flakes**  
**with area of several mm<sup>2</sup>**  
**will lead the plasma to**  
**collapse.**

Various atomic number of Fe  
 $W_{pa}$  &  $W_{pb}$ : plasma store energy  
 after and before Fe/C injection



# 2<sup>nd</sup> Harmonic ICRF Heating

#24615

Additional ICRF heating to  
NBI plasma

$B=1.30\text{T}/R_{ax}=3.6\text{m}$

$f=38.47\text{MHz}\& 40.47\text{MHz}$

$W_p=212\text{kJ}, \Delta W_p=40\text{kJ}$

$n_e=3.9\times 10^{19}\text{m}^{-3}$

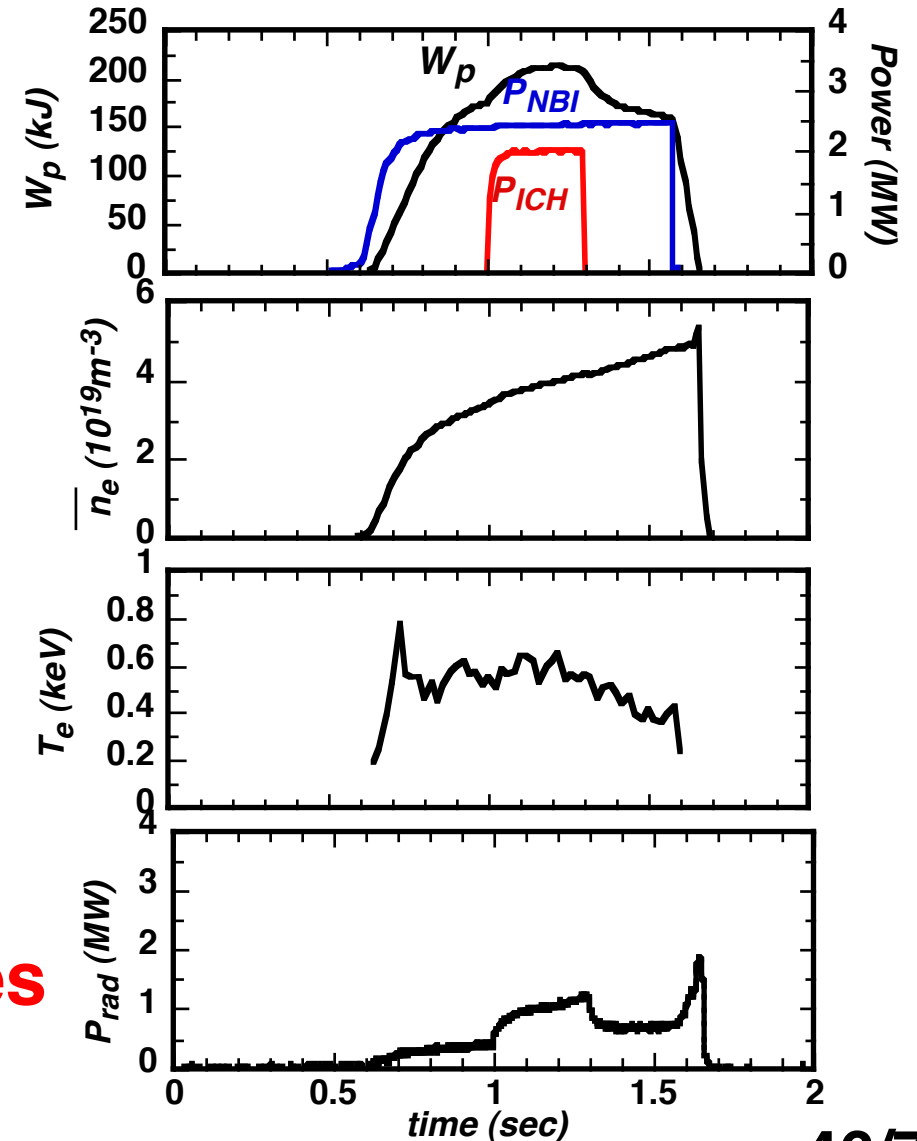
$\beta_t=0.84\%$

$P_{ICH}=2.0\text{MW}$

$P_{INBI}=2.5\text{MW}$

$\eta=P_{abs}/P_{ICH}=47\%$

Heating efficiency  $\eta$  increases  
with  $\beta_t$ .





# Outlines

---

1. Waves in plasma
2. Physics of ICRF heating
3. Experiments of ICRF heating
4. **ICRF heating technologies,**  
**RF generators**  
**Advanced impedance matching system**
5. Discussion of RFH and RFCD on ITER
6. Summary

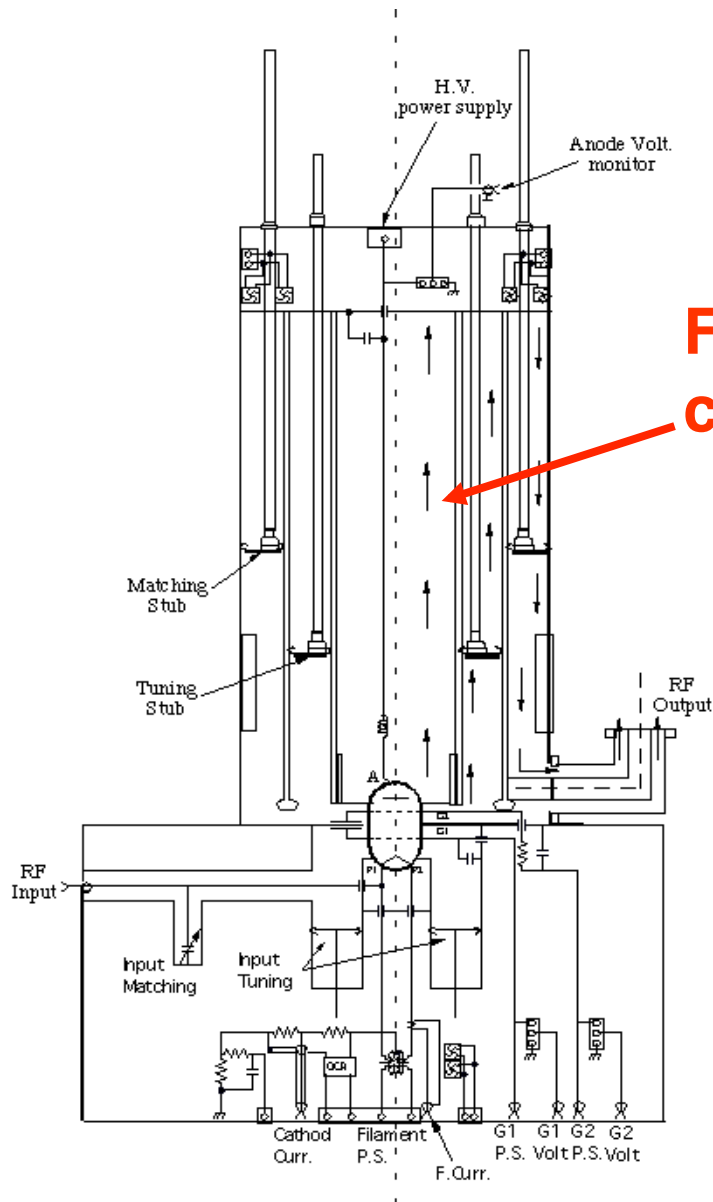


# Hardware for ICRF Heating

---

- **RF generator for high power with steady-state operation**
- **Impedance matching system for steady-state operation**
- **Quick response for a sudden change of plasma loading due to e.g., H-L mode transition**

# Steady-state High Power of RF Generator with Wide frequency Range



**Forced air to cool cavity**

**Double coaxial cavity  
4m in length**

**Outside:  
matching stub tuner**

**Inside:  
Tuning stub tuner**

**Frequency range:  
 $25\text{MHz} < f < 100\text{MHz}$**



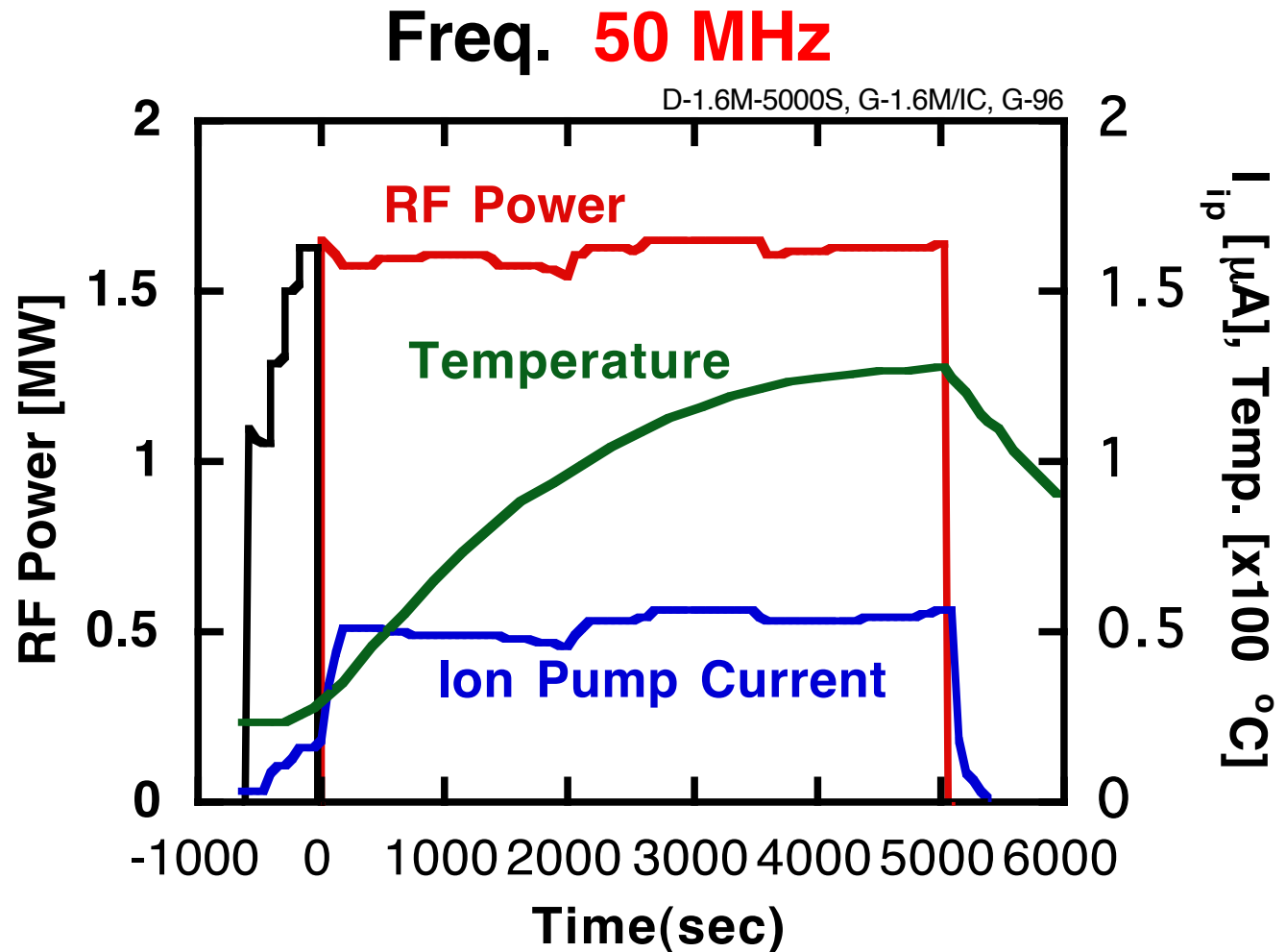
# Steady-state High Power of RF Generator

## -1.6 MW/5,000s-

Test of RF generator using dummy load:  
1.6MW/5,000s/f=50MHz

Ion pump current is a monitor in the vacuum tube: 0.6 $\mu$ A is low vacuum pressure for operation.

Increase in temperature of co-axial transmission line is up to 100 $^{\circ}$ C with air flow of 2m/s.



Kumazawa, 19<sup>th</sup> SOFT, vol.1(1996), 617  
Seki, Fusion Tech. Vol.40(2001), 253

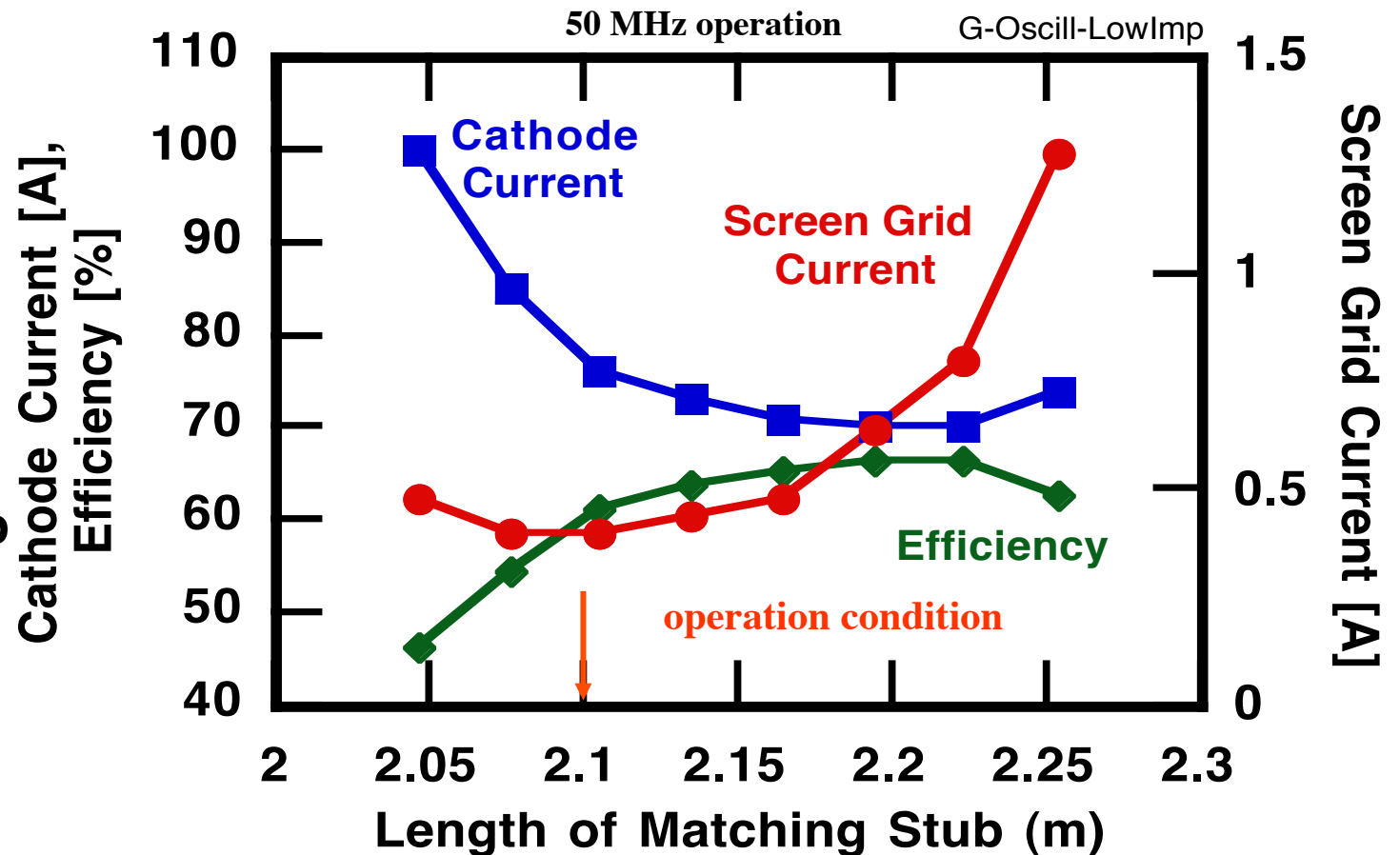
# Operation in Low-impedance Mode

Adjusting position of M & T stub tuner in output cavity provides a low-impedance mode, i.e., large cathode current.

Screen grid current can be suppressed to low level in the high power operation.  
=> Lowering ion pump

But RF converting efficiency is degraded in low-impedance mode.

## Keeping 1MW output



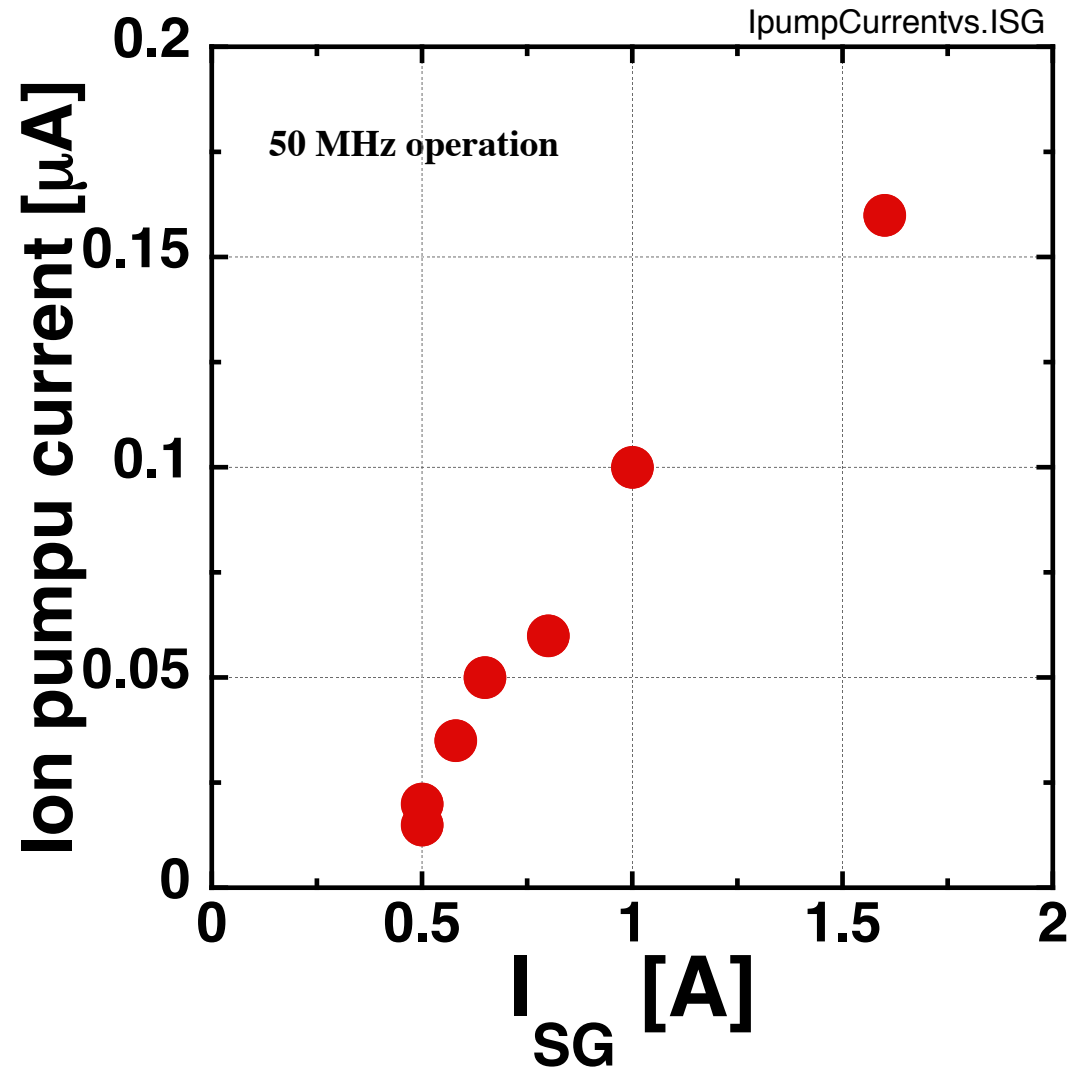


# Ion pump current vs. $I_{SG}$

Ion pump current is an important parameter to indicate the pressure in the vacuum tube.

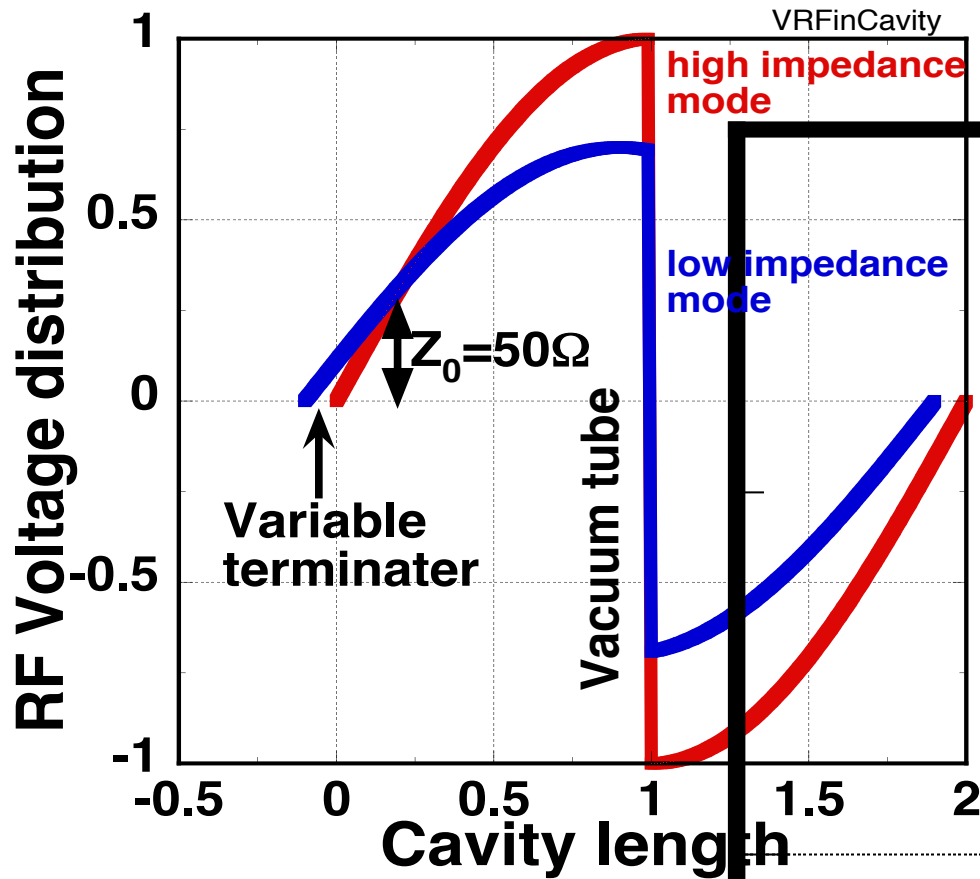
There is a close relation between screen grid current,  $I_{SG}$  and Ion pump current.

$I_{SG}$  is a key parameter for long-pulse operation of high RF power.

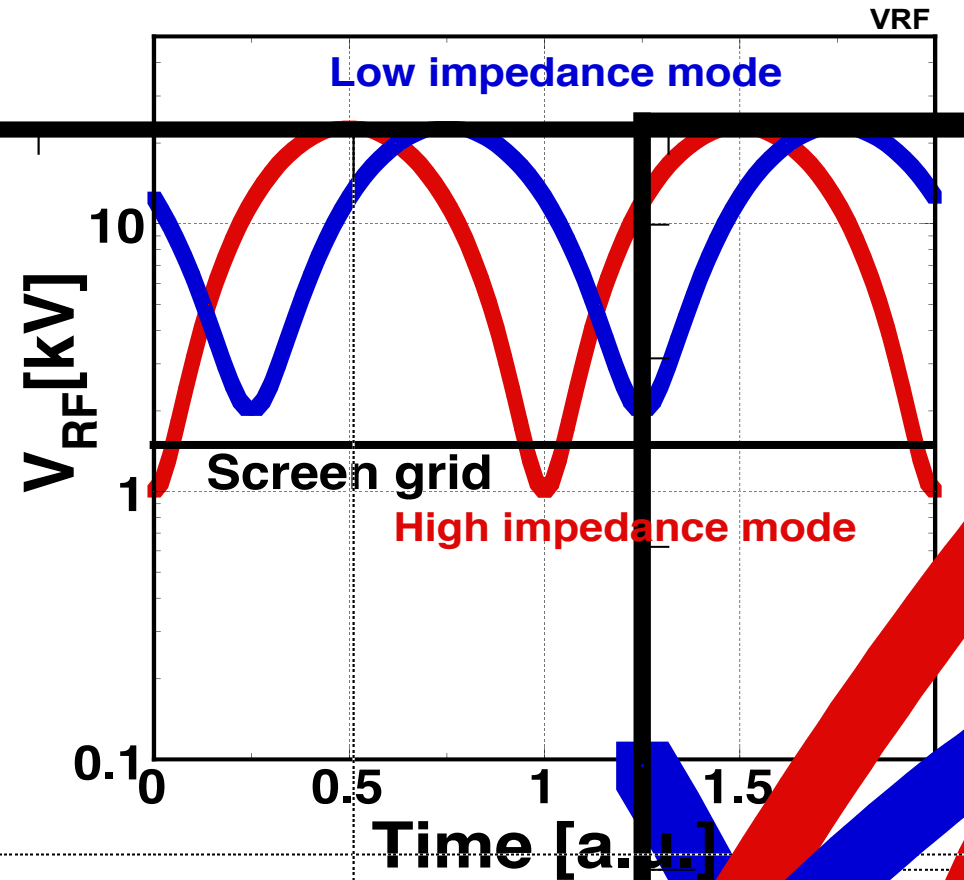


# Low-impedance Mode

## RF voltage distribution in cavity



## Time variation of RF voltage on anode





# Limited RF Power output due to large reflected power

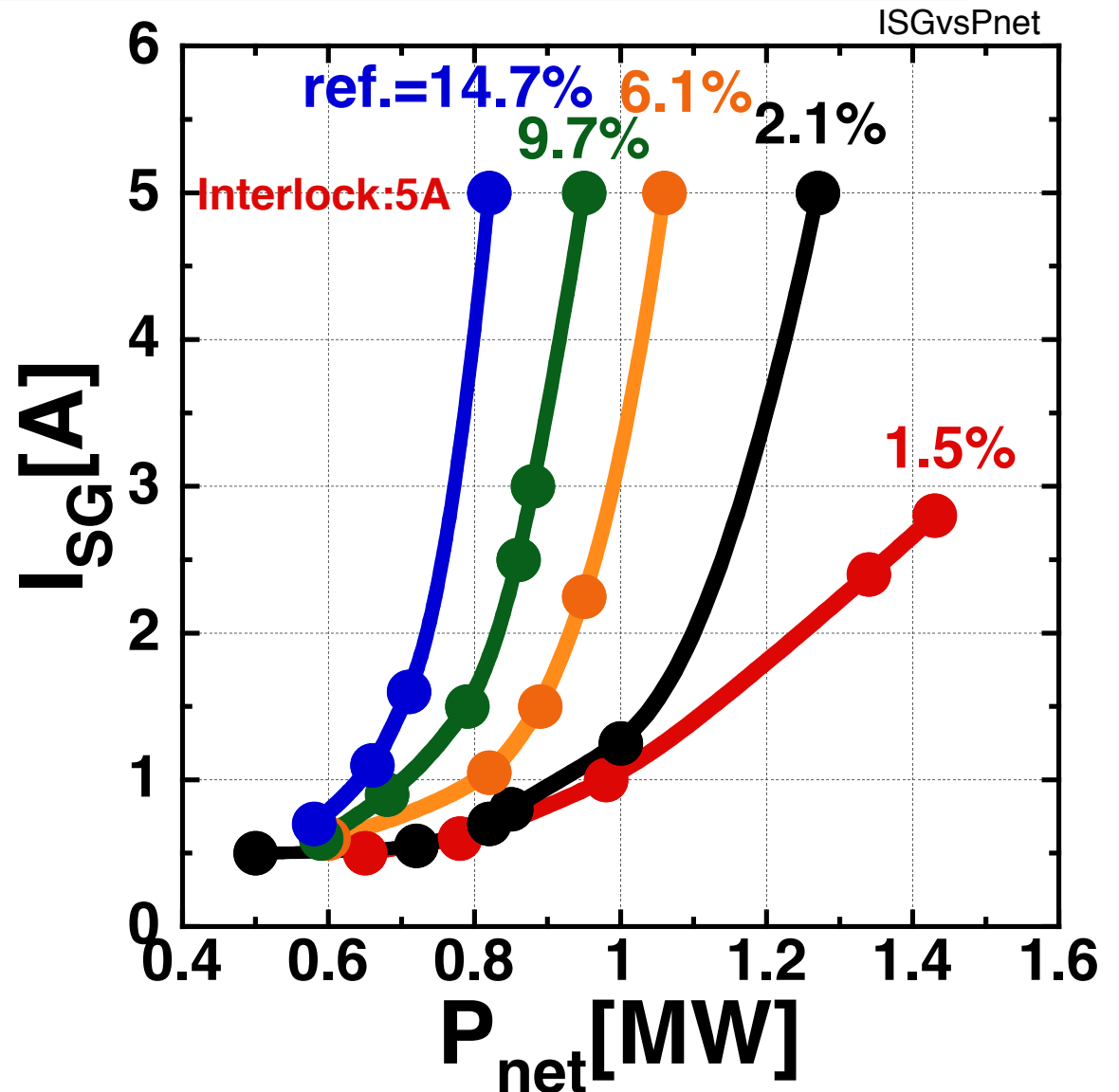
-operation limit with  $I_{SG}$ -

Dependence of Limitation  
of RF power output on  
fraction of reflected RF  
power (Ref.):

$1.5\% < \text{Ref.} < 14.7\%$   
( $1.3 < \text{VSWR} < 2.2$ )

$I_{SG}$  is increased with ref.  
 $\Rightarrow$  then RF output power is  
limited with Interlock  
( $I_{SG} < 5A$ ).

collaboration with ITER  
ICRF group





# Principle of Impedance Matching

In the right figure a standing RF wave is excited between antenna and a stub tuner:

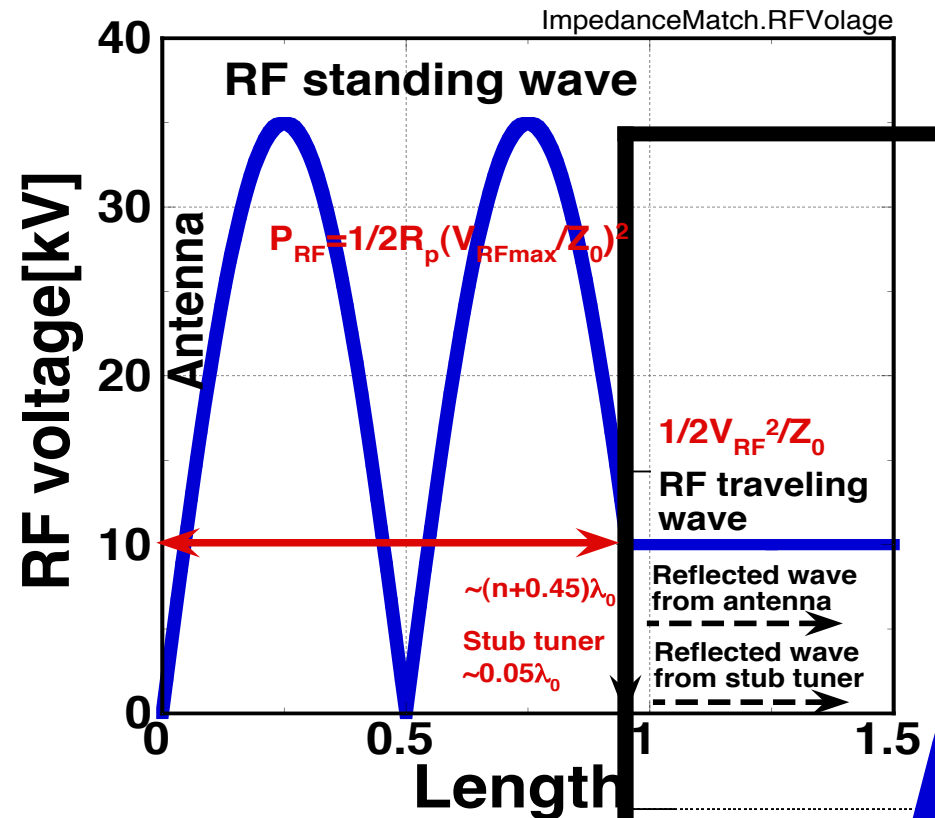
$P_{RFA}$ : RF power between antenna and a stub tuner

$$P_{RFA} = 1/2 R_p (V_{RFS}/Z_0)^2, R_p \ll Z_0$$

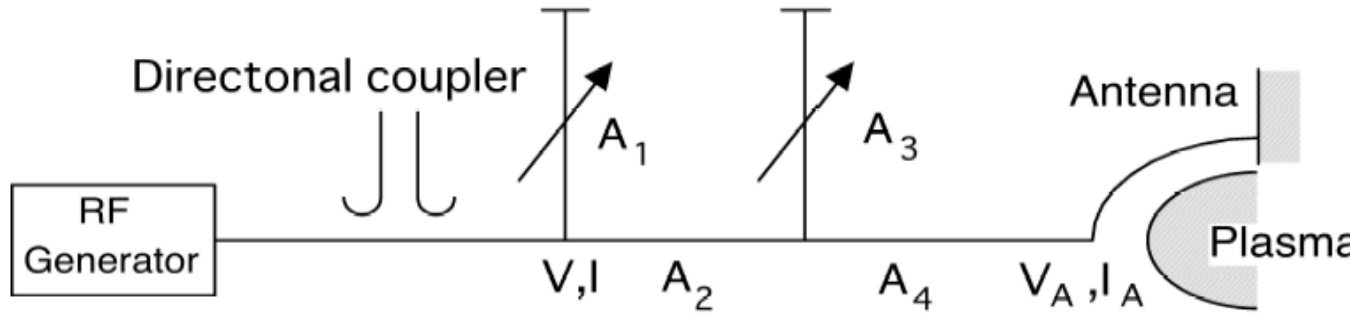
$P_{RFS}$ : RF power between stub tuner and RF generator

$$P_{RFS} = 1/2 V_{RF}^2 / Z_0^2$$

$P_{RFA} = P_{RFS}$ , Then the length of stub tuner is determined taking into account the phase of reflected RF wave at the stub tuner junction.

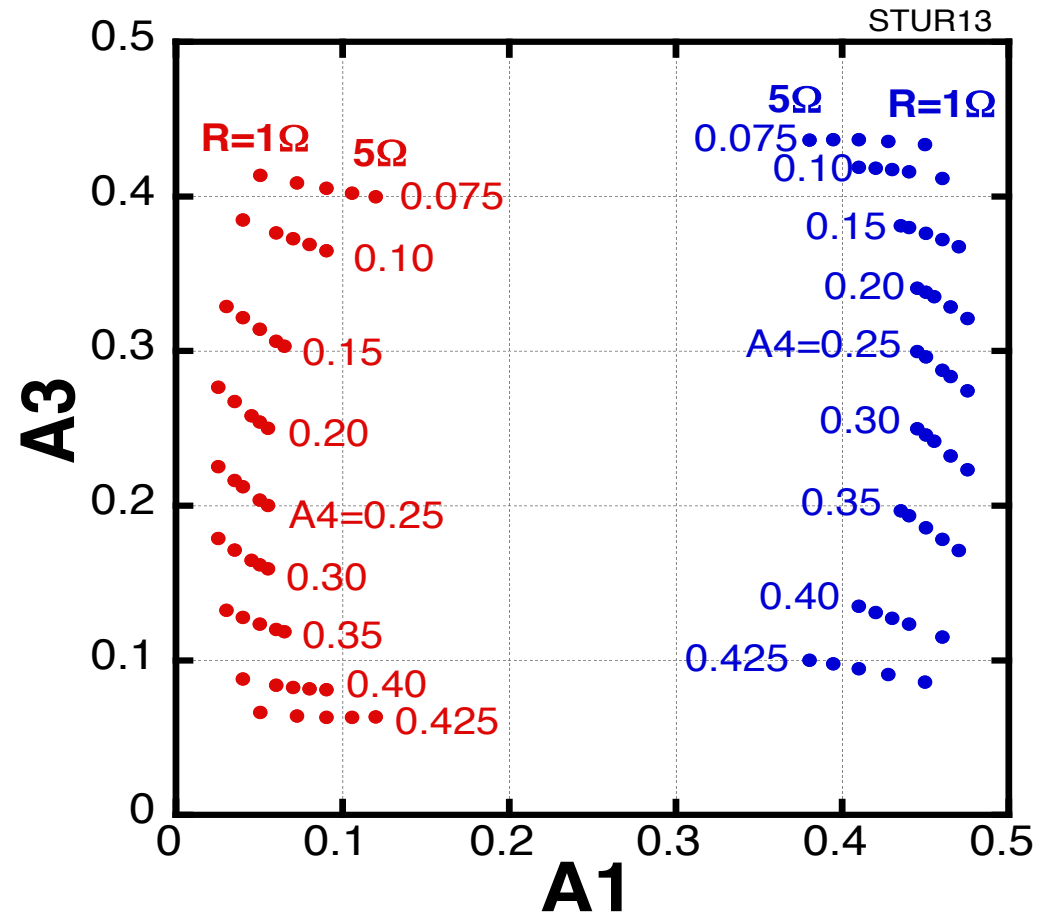


# Double Stub Tuner System



Map of impedance matching points for R with various  $A_4$  at  $A_2=0.25$

$$\begin{pmatrix} V \\ I \end{pmatrix} = \begin{pmatrix} 1 & 0 \\ -j/Z_0 \tan(2\pi A_1) & 1 \end{pmatrix} \times \begin{pmatrix} \cos(2\pi A_2) & jZ_0 \sin(2\pi A_2) \\ j/Z_0 \sin(2\pi A_2) & \cos(2\pi A_2) \end{pmatrix} \times \begin{pmatrix} 1 & 0 \\ -j/Z_0 \tan(2\pi A_3) & 1 \end{pmatrix} \times \begin{pmatrix} \cos(2\pi A_4) & jZ_0 \sin(2\pi A_4) \\ j/Z_0 \sin(2\pi A_4) & \cos(2\pi A_4) \end{pmatrix} \begin{pmatrix} V_A \\ I_A \end{pmatrix}$$



# Liquid Stub Tuner

## -for steady-state ICRF heating-

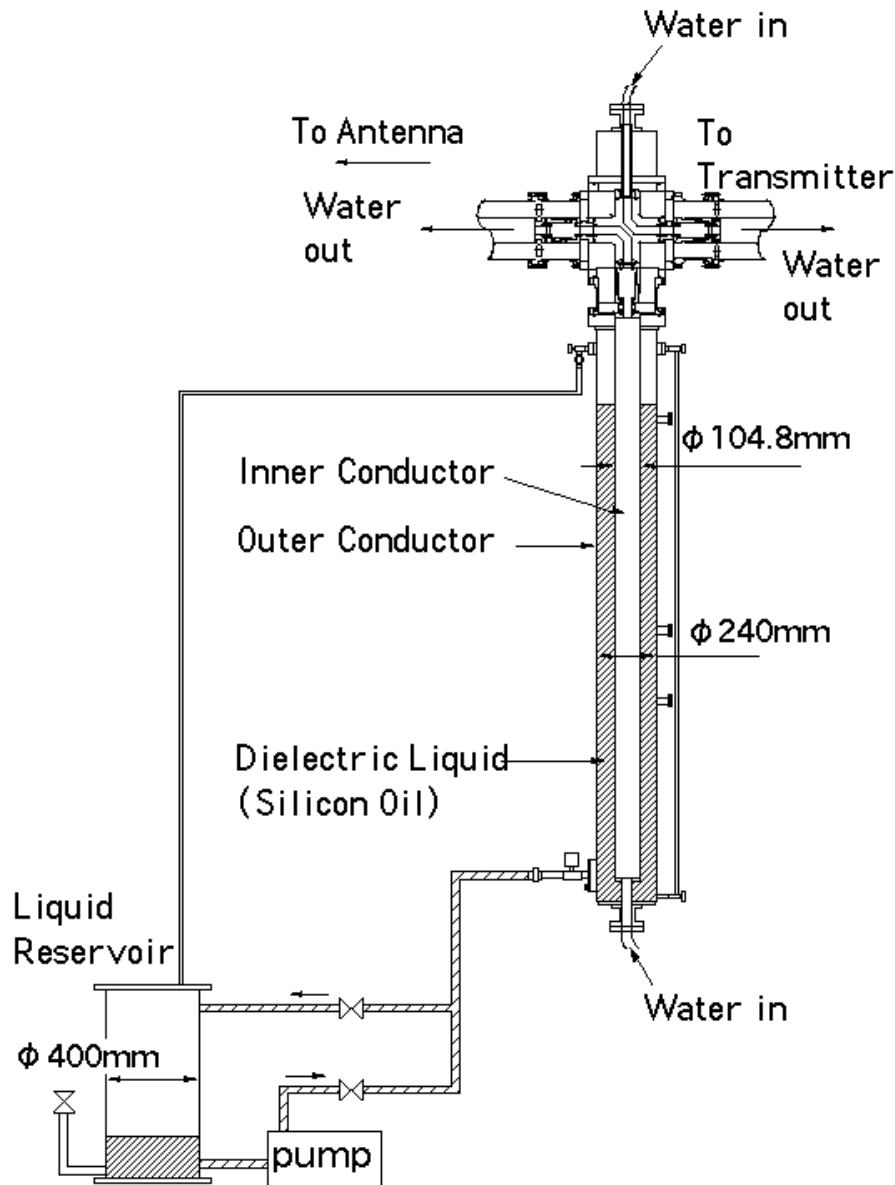
liquid: Dimethyl Polysiloxane

dielectric constant     $\tan\delta$     vapour pressure    specific heat

比誘電率	誘電正接	蒸気圧	比熱
2.72	$1 \times 10^{-4}$ at 10MHz	0.04torr at 240°C	0.36
	$3.3 \times 10^{-4}$ at 100MHz	2torr at 320°C	

**dielectric constant ;  $\epsilon=2.72$**   
**Shortening ratio of RF wave in liquid:  $\lambda/\lambda_0=\epsilon^{1/2}=0.606$**

RSI, vol.70(1999), 2665  
 Saito, RSI, vol.72(2001), 2015





# Characteristics of Liquid Stub Tuner

Effective normalized length of liquid stub tuner;

$$\frac{1}{\tan 2\pi A} = \frac{1 - Z_L / Z_0 \tan 2\pi A_{GS} \tan 2\pi A_{LS}}{\tan 2\pi A_{GS} + Z_L / Z_0 \tan 2\pi A_{LS}}$$

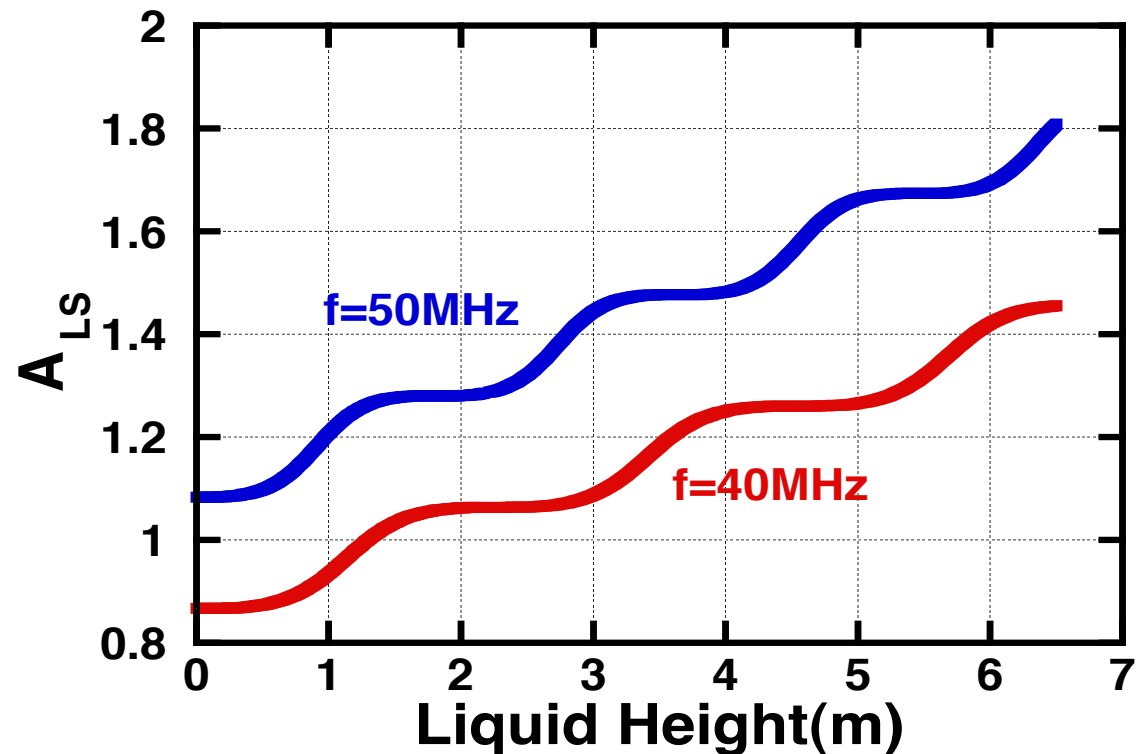
**A** : normalized length of liquid stub tuner

**A<sub>GS</sub>** : normalized length in gas region

**A<sub>LS</sub>** : normalized length in liquid region

**Z<sub>0</sub>** ; characteristic impedance in gas region

**Z<sub>L</sub>** ; characteristic impedance in liquid region





# Reduction in Reflected RF Power during Long Pulse Operation



#66053

(Plasma with 54min.45sec):

Plasma loading resistance:  
from  $4\Omega$  to  $3\Omega$

Co-axial transmission line ( $\sim 40\text{m}$ )  
Is extended by 12cm.

In accordance with that:

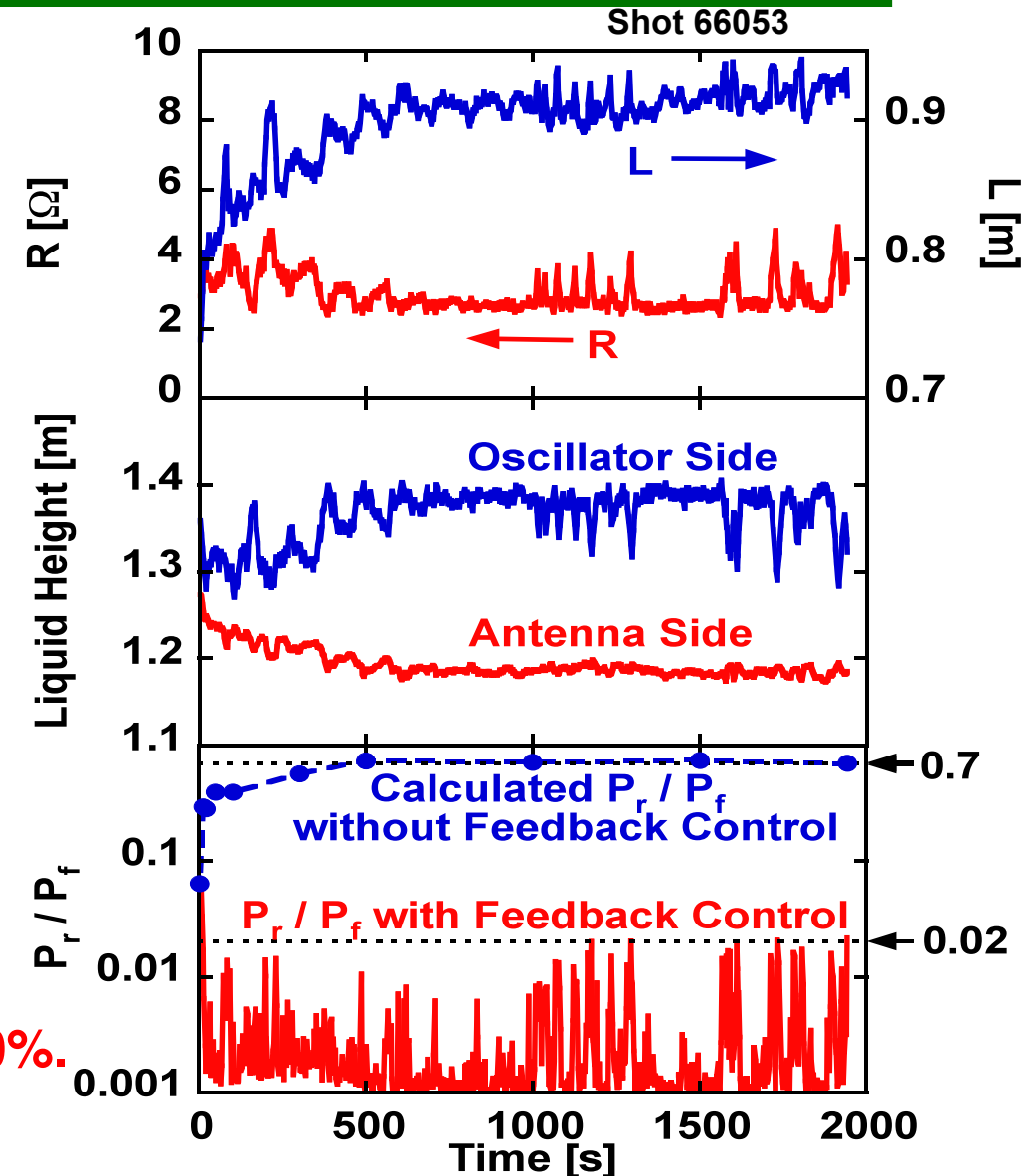
Liquid surface on oscillator side 10cm up  
Liquid surface on antenna side 5cm down

As result:

**Reflected RF power fraction is  
always less than 2%.**

**If no feedback control of liquid height,  
it would have increased to more than 70%.**

Saito, FED, vol.81(2006), 2834





# ICRF Heating Power Capability

## -Plasma Loading Resistance-

Injected RF power from ICRF heating antenna is calculated using the maximum RF voltage on the RF standing voltage:

$$P_{inj} = \frac{1}{2} (R_V + R_p) \left( \frac{V_{RF \max}}{Z_0} \right)^2$$

$R_V$  : vacuum resistance,  $R_p$  : plasma resistance

Therefore injection efficiency antenna is

$$\eta_{inj} = \frac{R_p}{R_V + R_p}$$

In the case of  $R_V + R_p = 5\Omega$  and  $Z_0 = 50\Omega$ ,  $V_{RF \max} \sim 45kV_{op}$  is required in the transmission line of unmatched section, i.e., between RF antenna and stub tuner system.



# Plasma Loading Resistance

When RF power is radiated from from ICRF heating antenna with  $N_{//}$ , this wave is evanescent up to R-cutoff layer :

$$R \text{ cutoff layer} : N_{//}^2 \approx \frac{\Pi_i^2}{\omega^2}$$

$$N_{//}^2 + N_{\perp}^2 = 1 \rightarrow N_{\perp}^2 < 0 \because N_{//} \gg 1$$

Therefore RF wave decreases exponentially,

$$P_{RF} \propto \exp(-k_{\perp} x)$$

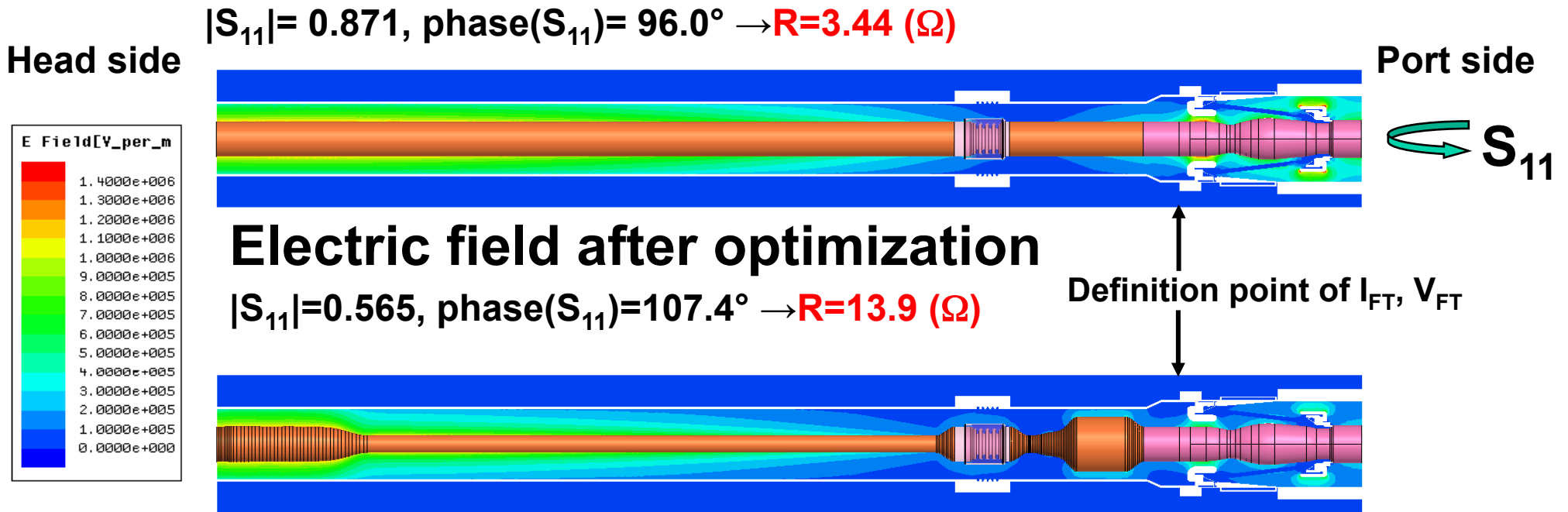
*x* : distance between RF antenna and R – cutoff layer

Therefore only small fraction of RF power can penetrate in large  $k_{//}$  (with large  $k_{\perp}$ ) and large  $x$ , i.e., large separation between RF antenna and R-cutoff. In addition the distance between antenna and L-cutoff layer will be increased because of the plasma heat load and neutron damage, then the plasma loading may be much reduced.

# Increase in Plasma Loading Resistance

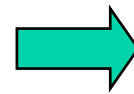
-Optimization of characteristic impedance-

With varied characteristic impedance,  $Z_c$  along co-axial transmission line from antenna to ceramic feed-through, the plasma loading Resistance can be increased 3 times in optimized selection of  $Z_c$ .



before optimization

$R_{\text{eff}}=\eta R=3.28 (\Omega)$   
 $\eta=0.955$  (power loss: 4.5%)  
 $|I_{FT}|=0.875$  (kA)  
 $|V_{FT}|=13.4$  (kV)



after optimization

$R_{\text{eff}}=\eta R=13.7 (\Omega)$   
 $\eta=0.985$  (power loss: 1.5%)  
 $|I_{FT}|=0.426$  (kA)  
 $|V_{FT}|=6.73$  (kV)



# Sudden Change in Plasma Loading Resistance at H-L mode Transition

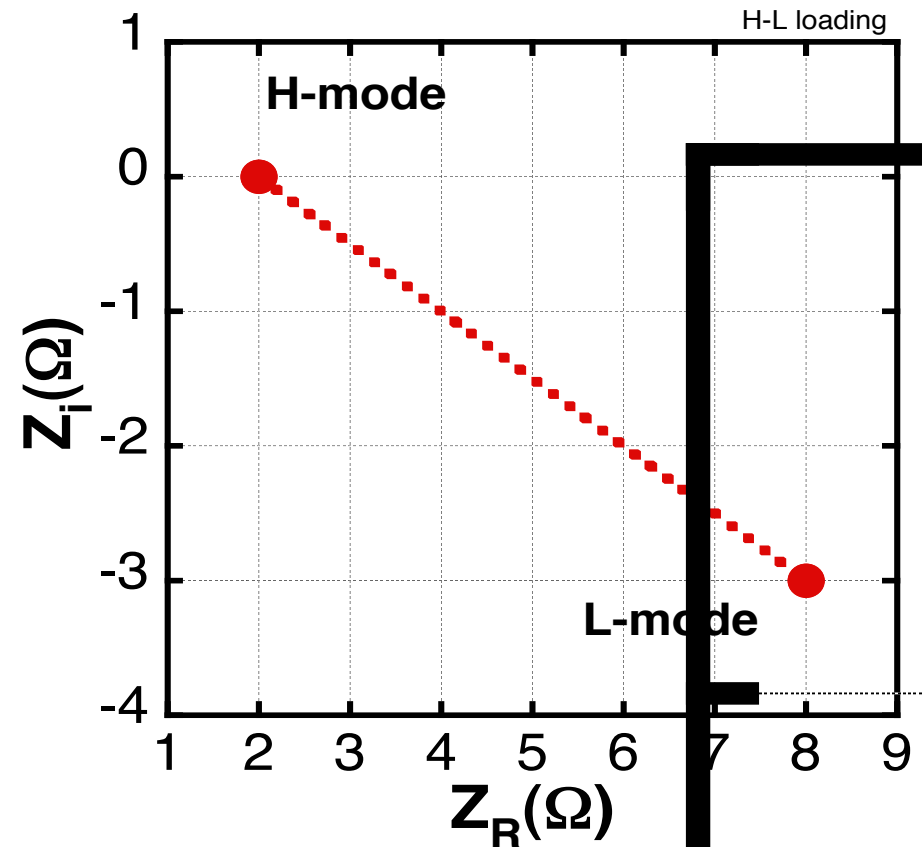
Sudden change in plasma loading resistance at H-L mode transition was found:

Example of  $Z_p$  on JET:

$Z_{RH} \sim 2\Omega$  at H-mode,

$Z_{RL} \sim 8\Omega$  at L-mode

increase in reflected power fraction,  $P_{ref}/P_{fw} \sim 5$  to 10%  
=>stopping RF generators

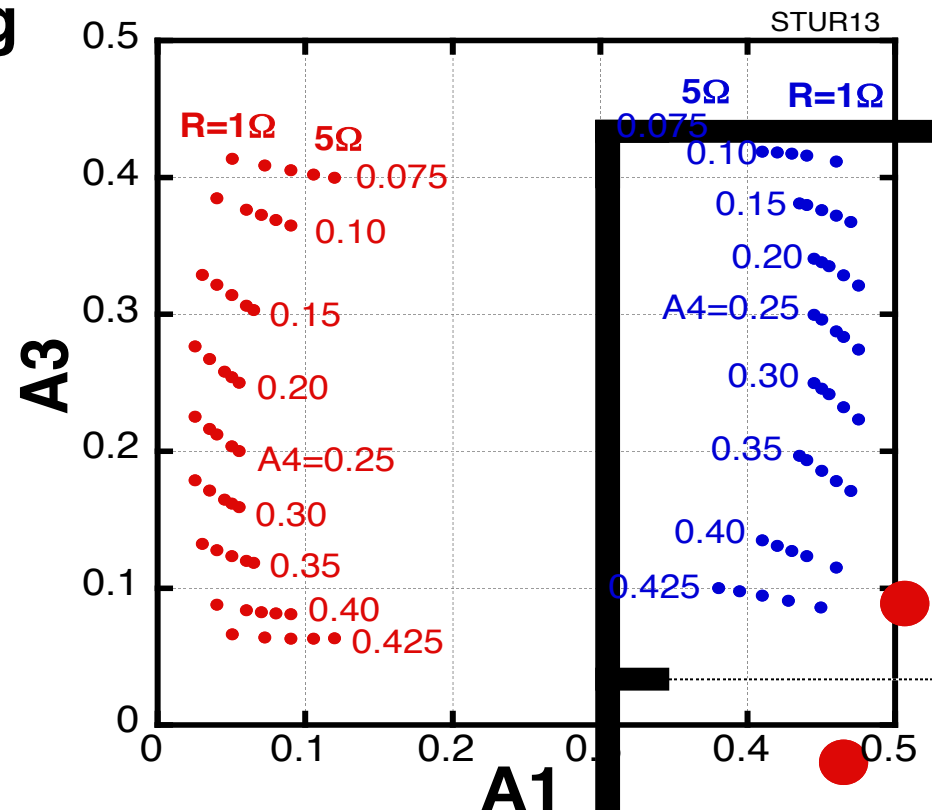
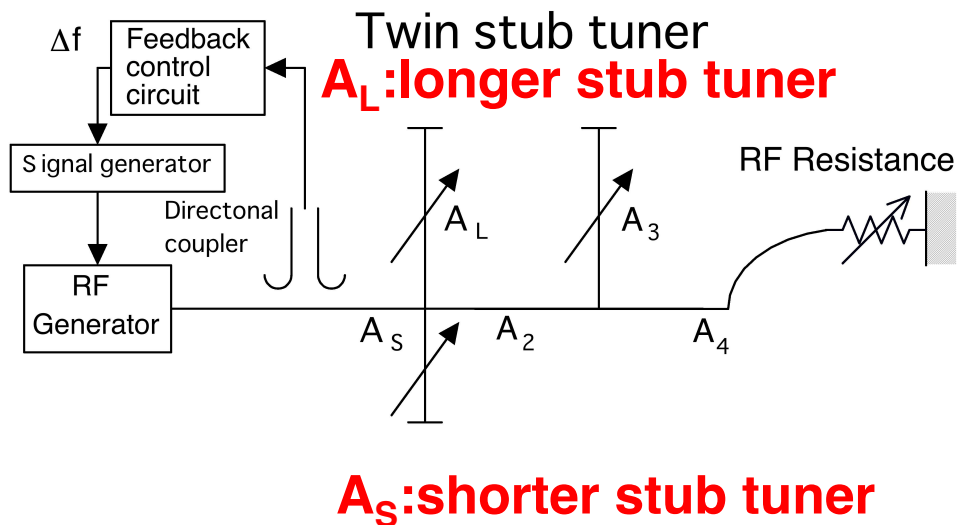


# Special Condition among Various Impedance Matching Points

-in double stub tuner-

In right figure the impedance matching is obtained for  $1\Omega < R < 5\Omega$  at various  $A_4$ . Among them even in fixed  $A_3$  the impedance matching is almost obtained in the range of  $1\Omega < R < 5\Omega$  at  $A_4 = 0.425$ .

Then easily we think of using a long stub tuner at  $A_1$  with frequency Feedback control.





# Frequency Feedback Control using Twin Stub Tuner

## -for Sudden Change in Plasma Loading Resistance-

Twin stub tuner consisting of shorter ( $A_S$ ) and longer ( $A_L$ ) stub tuners works as long stub tuner with shortening  $A_S$ .

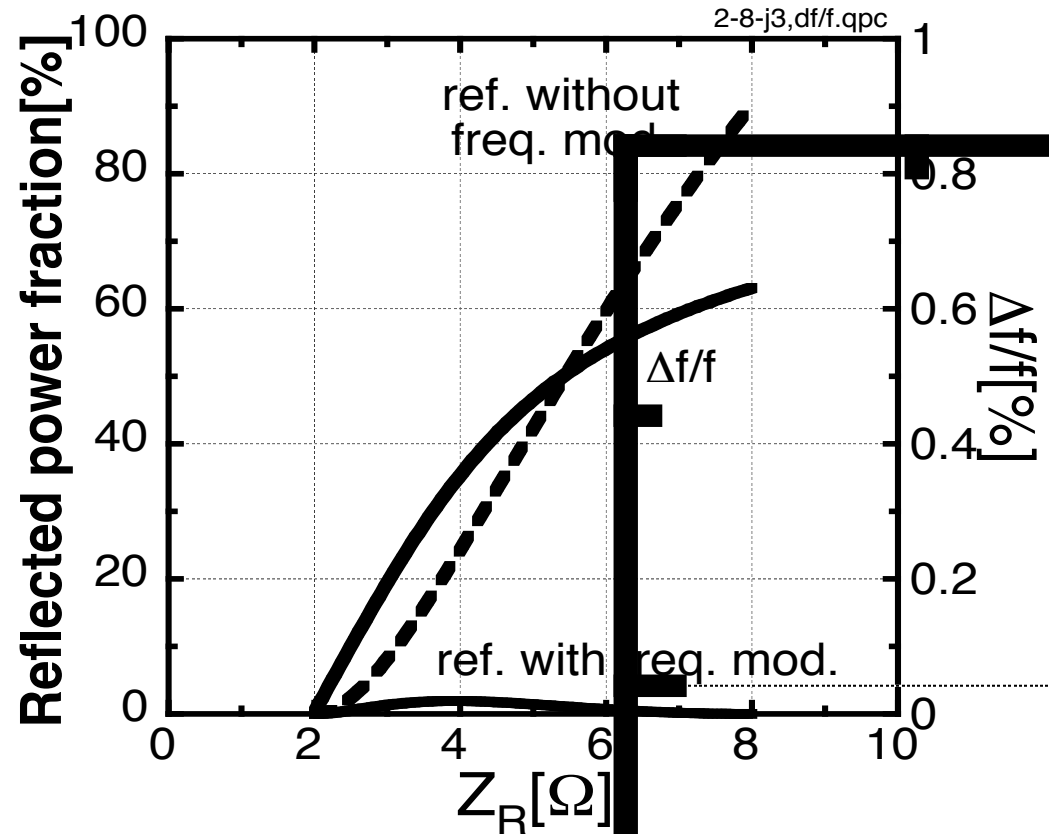
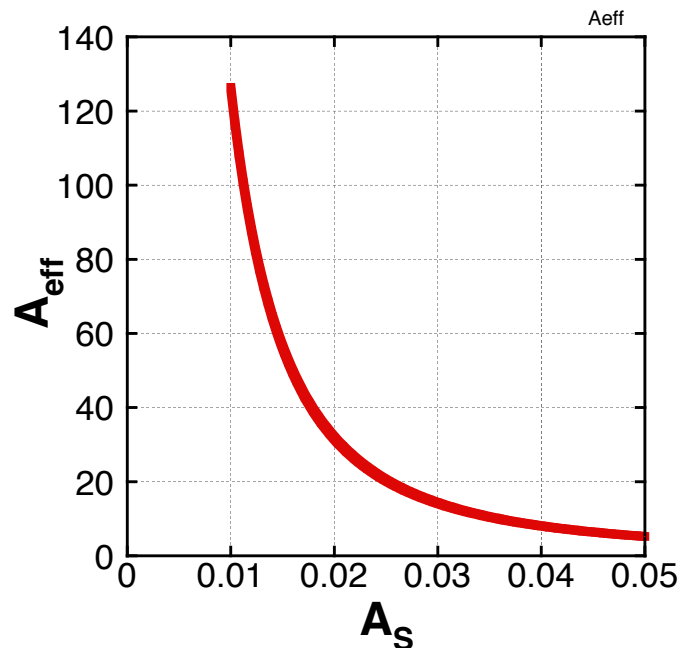
Innovative impedance matching system with twin stub tuner:

$P_{ref}/P_{fw}$  is reduced to 1% with 0.6% of  $\Delta f/f$ .  
 $P_{ref}/P_{fw}$  should have increased to 90%.

$$\frac{1}{\tan 2\pi A_R} = \frac{1}{\tan 2\pi A_S} + \frac{1}{\tan 2\pi A_L} \leftarrow A_S + A_L = 0.5$$

$$\frac{dA_R}{df} = \frac{\tan^2(2\pi A_S) \cdot \tan^2(2\pi A_L)}{\{\tan(2\pi A_S) + \tan(2\pi A_L)\}^2 + \tan^2(2\pi A_S) \cdot \tan^2(2\pi A_L)}$$

$$\times \left\{ \frac{1}{\sin^2(2\pi A_S)} \frac{dA_S}{df} + \frac{1}{\sin^2(2\pi A_L)} \frac{dA_L}{df} \right\} = \frac{dA_{eff}}{df}$$



RF power is splitted at T-junction and supplied to two identical antennas.

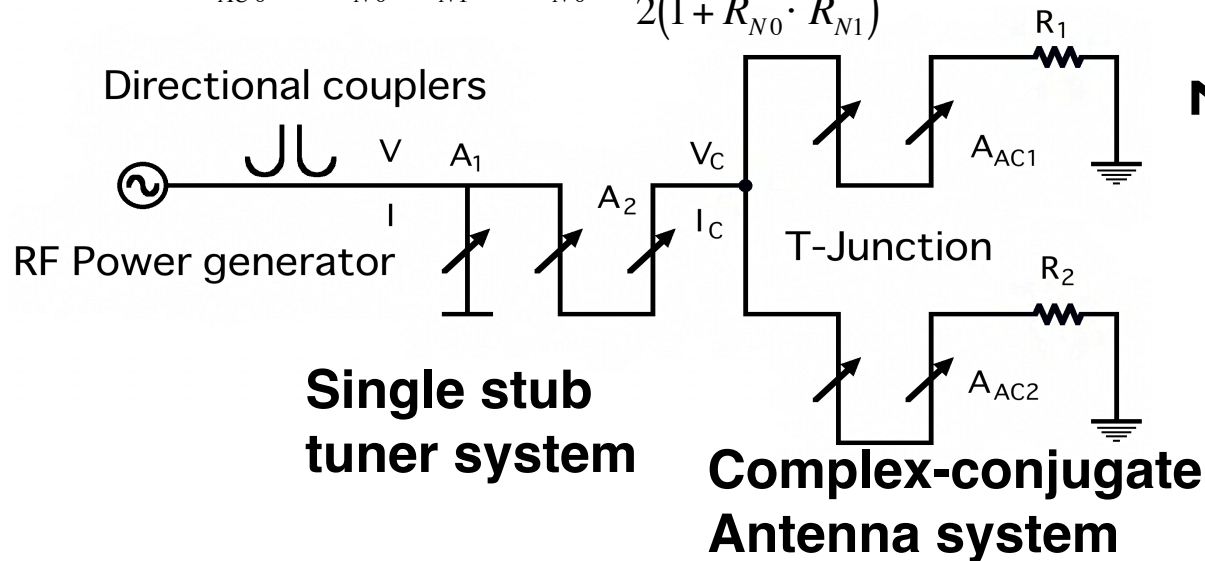
Normalized impedance at T – junction

when  $A_{AC1} + A_{AC2} = 0.5n$

$$Z_{N0} = \frac{Z}{Z_0} = \frac{R_{N0}^2 + \tan^2(2\pi A_{AC0})}{2R_{N0} \{1 + \tan^2(2\pi A_{AC0})\}} : \text{no imaginary part}$$

when  $R_{N0}$  (as H – mode) and  $R_{N1}$  (as H – mode) are known, then

$$\tan^2(2\pi A_{AC0}) = R_{N0} \cdot R_{N1} \rightarrow Z_{N0} = \frac{R_{N0} + R_{N1}}{2(1 + R_{N0} \cdot R_{N1})}$$

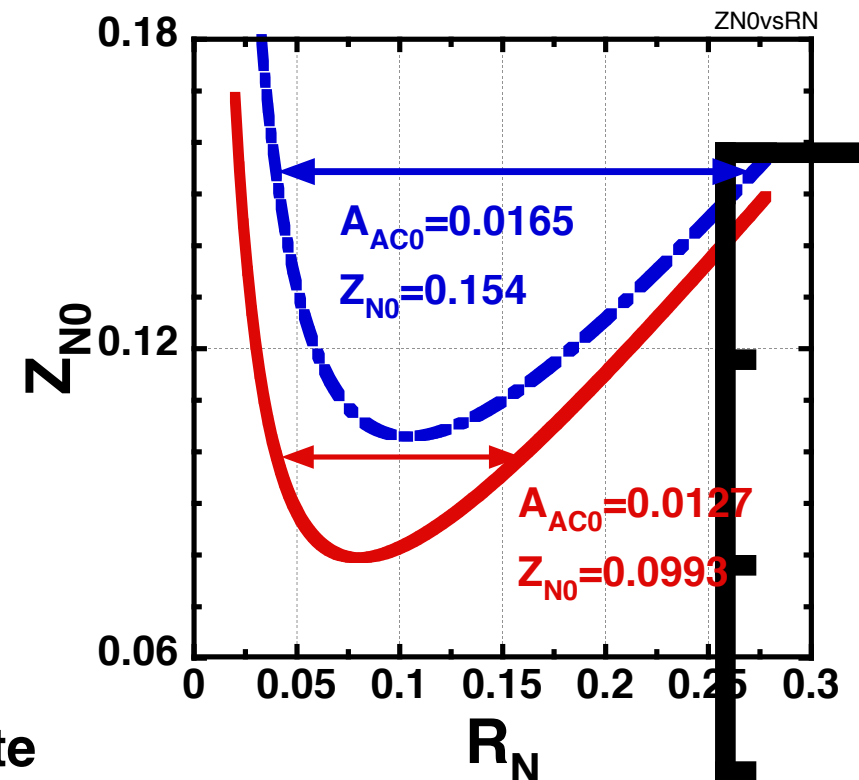


Normalized impedance at T-junction,  $Z_N$  varies with  $R_N$ .

$R_H=2\Omega \Rightarrow R_N=0.04$  and  $R_L=8\Omega \Rightarrow R_N=0.16$

Therefore  $Z_{N0}$  becomes the same at

$R_N=0.16$  in  $A_{AC0}=0.0127$ .



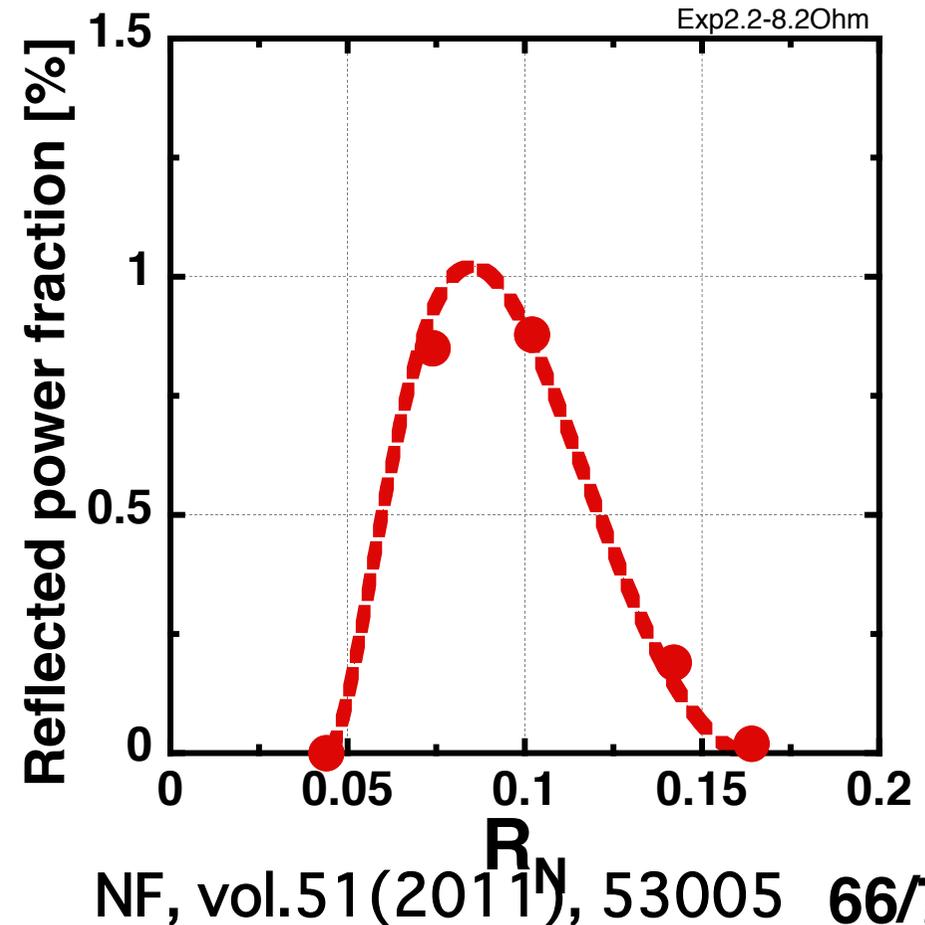
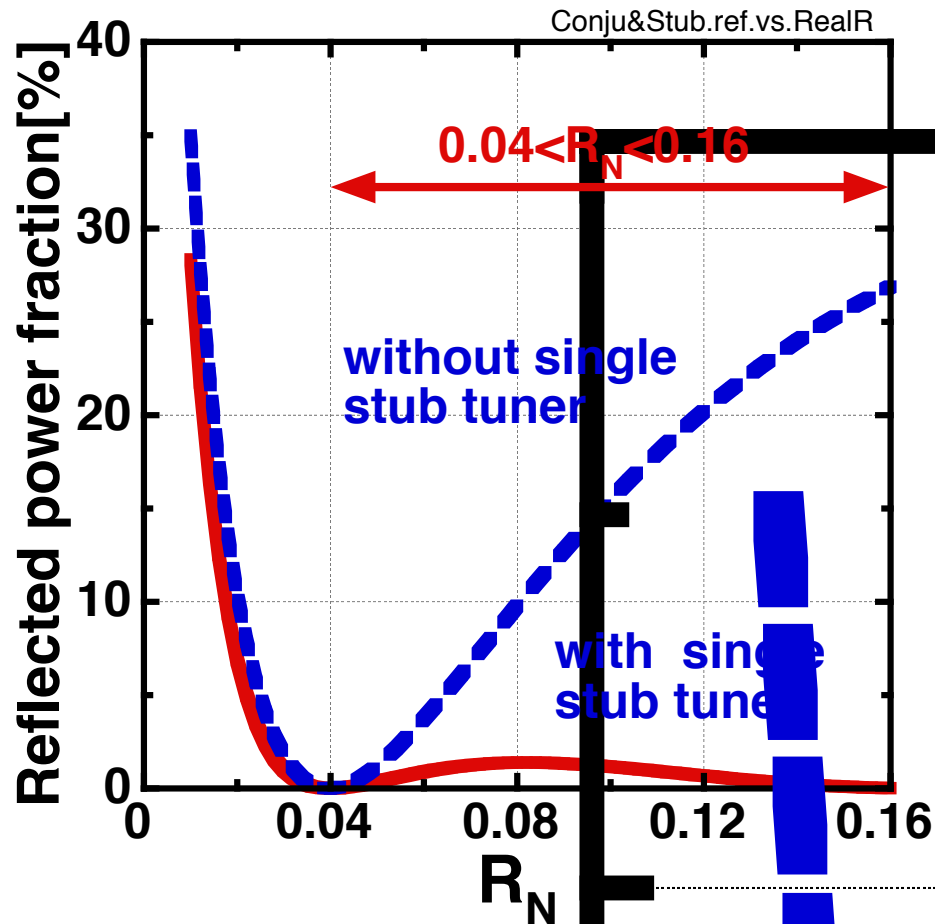


# Complex-conjugate Antenna System

## -with optimized $A_{AC}$ -

When the impedance matching is obtained at  $R_N=0.04$  (as H-mode) with tuning a single stub tuner, the reflected power fraction becomes zero again at  $R_N=0.16$  (as H-mode). The maximum reflected power fraction is **1%** between  $R_N=0.04$  and 0.16.

Experiment was done using low RF power system with resistors. Experiment data agrees with calculated value.





# Outlines

---

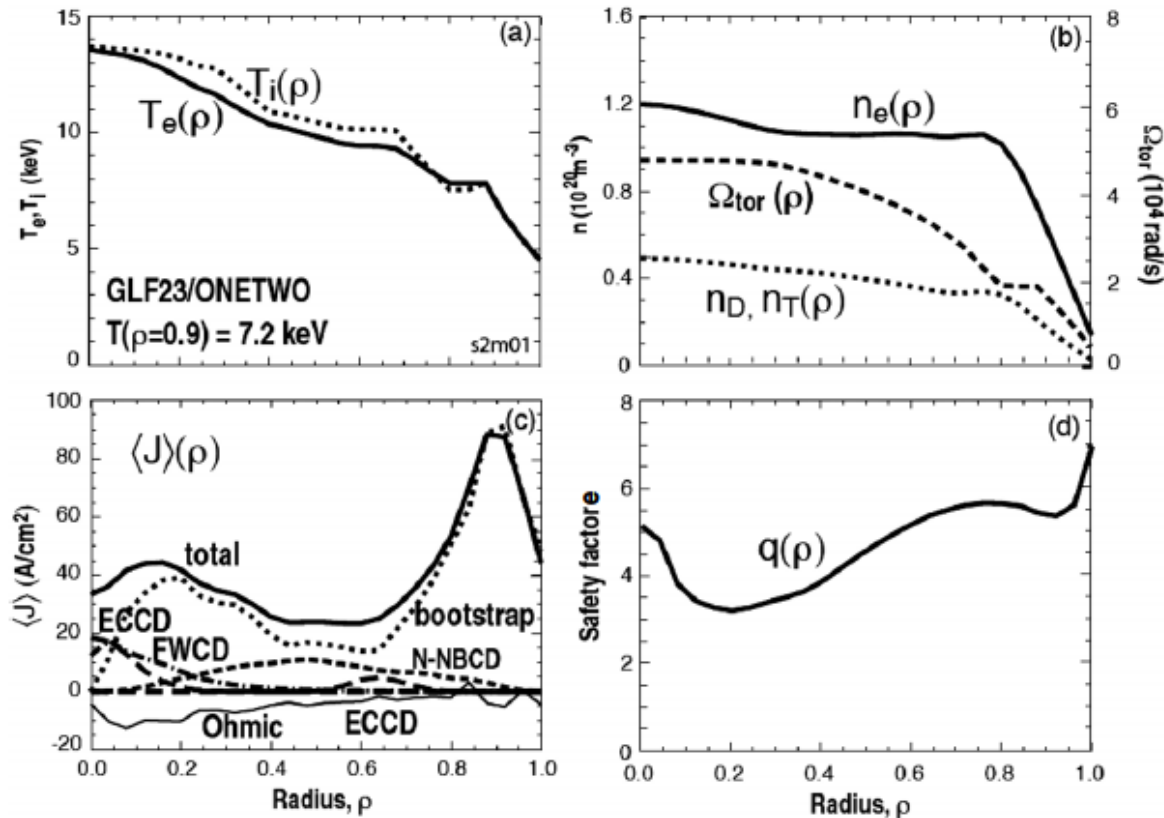
1. Waves in plasma
2. Physics of ICRF heating
3. Experiments of ICRF heating
4. ICRF heating technologies
5. **Discussion of RFH and RFCD on ITER**
6. Summary



# Review of Steady-state Scenarios on ITER

Gormezano et al., NF (2007) S285-S326: Chapter 6: Steady state operation  
This paper is the best review to know the steady-state operation on ITER, including plasma parameters of ITER, N-NBCD, ECH, ECCD, LHCD, ICRF heating and FWCD, technologies for them and many simulation codes.

Example:



Predictive modeling of ITER Steady-state scenario using GLF23 transport model:



# Steady-state Scenarios with Heating and Current Drive on ITER

## -simulation using codes-

---

One of the primary goal of the ITER project is to demonstrate reactor scale steady-state (SS) operation. ITPA (international Tokamak Physics Activity) –IOS (Integrated operation Scenario) group reports the ITER SS scenario modeling H & CD using many simulation codes.

A fully non-inductive SS scenario is achieved with  $Q=4.3$ ,  $f_{NI}$  (non-inductive fraction)=100%,  $f_{BS}$  (Bootstrap current fraction)=63% and  $\beta_N$  (normalized beta)=2.7,  $I_p=8\text{MA}$  at  $B_T=5.3\text{T}$ .



# Recent Simulation of Steady-state Scenarios on ITER

Run ID	Scenarios		
	Sc-1	Sc-2	Sc-3
Run ID	29000Z1	29000Z4h	29000Z4e
$P_{NB}$ (MW)	33	33	33
NBI	2 × off	2 × off	on + off
$P_{EC}$ (MW)	20	20	20
$P_{IC}$ (MW)	20	10	5
$B_T$ (T)	5.3	5.3	5.3
$I_p$ (MA)	8.00	8.00	8.00
$q_{95}$	5.73	5.75	5.62
$q_{min}$	1.95	2.12	1.50
$\rho_{qmin}$	0.32	0.33	0.09
$N_{GW}$	0.85	0.85	0.85
$I_{BS}$ (MA)	5.08	4.96	4.99
$I_{NB}$ (MA)	2.18	2.10	2.14
$I_{EC}$ (MA)	0.60	0.72	0.74
$I_{FW}$ (MA)	0.32	0.31	0.16
$I_{OH}$ (MA)	-0.18	-0.09	-0.08
$f_{NI}$ (%)	102.3	101.2	100.8
$Q$	3.36	3.83	4.25
$P_{DT}$ (MW)	245.0	274.4	244.7
$H_{98y2}$	1.49	1.50	1.53
$H_{89p}$	2.76	3.12	3.22
$\beta_N$	2.76	2.69	2.73
V1 (mV)	-0.38	0.13	-0.11

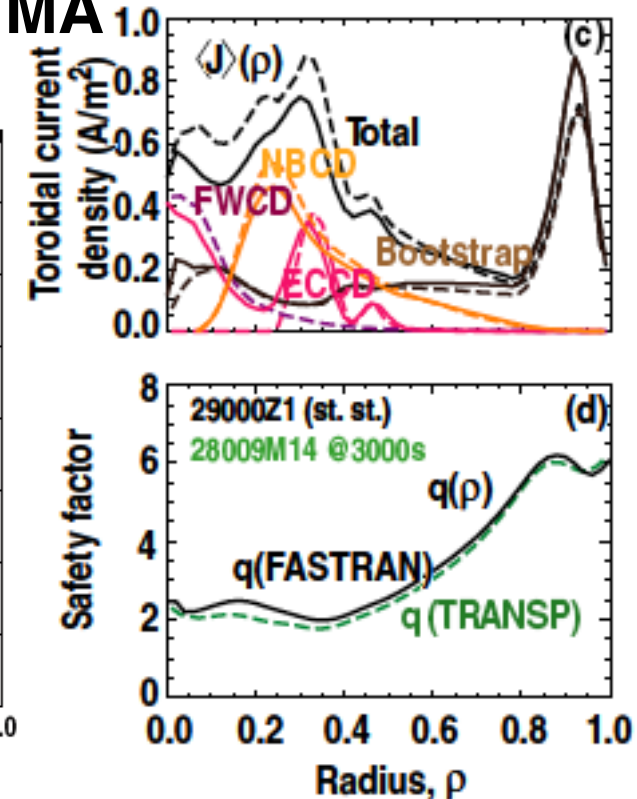
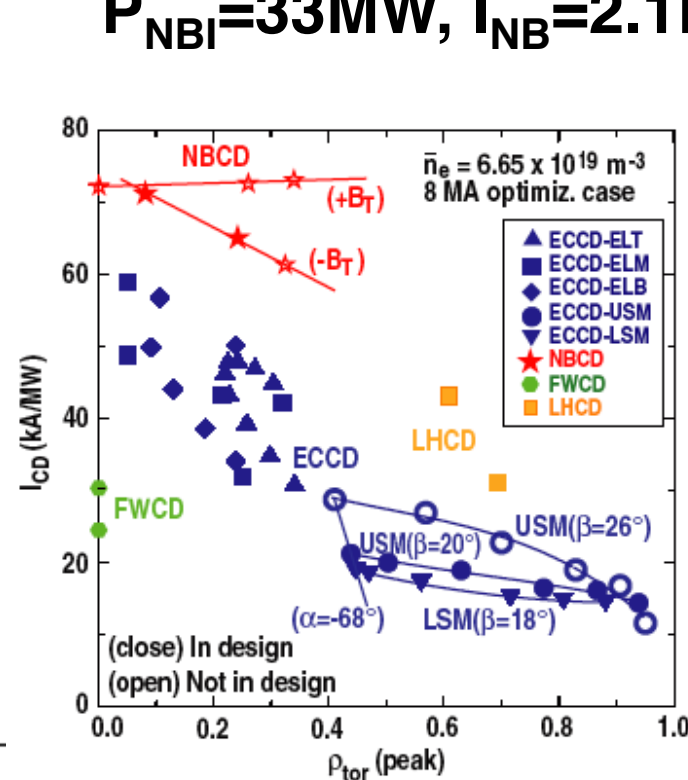
From M.Murakami et al., NF (2011) p.103006

$I_p=8MA, I_{BS}=5MA (f_{BS}=62.5\%)$

$P_{EC}=20MW, I_{EC}=0.7MA,$

$P_{IC}=20MW, I_{IC}=0.32MA$

$P_{NBI}=33MW, I_{NB}=2.1MA$





# Summary

---

- It is important to understand a basic wave physics in plasmas, e.g., CMA diagram. A newly innovative idea will come into you with deeply understanding basic wave physics in plasmas.
- RF heating experiments on LHD and its technologies are introduced. Hardware, i.e., RF generators of high power output with steady-state and impedance matching system with feedback control capability corresponding to gradual change in ICRF heating system and to sudden change in plasma loading resistance..
- It is recommended to read the review of Gormezano et al., NF (2007) S285-S326: Chapter 6: Steady state operation in order to understand the steady-state operation on ITER.

## Sources

- High Voltage Supplies (EU)
- 8 transmitters; 35-60 MHz (IN)

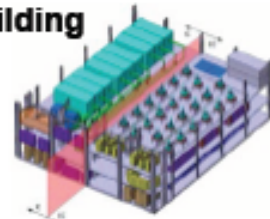
## Transmission line (US)

- 16 coaxial lines to 2 antennas
- Matching components – broadband prematch, tuning, power balancing and load resilience
- Power loads for commissioning and conditioning

## Antenna (EU)

- 2 antennas
- 24 current strap phased arrays

RF Building

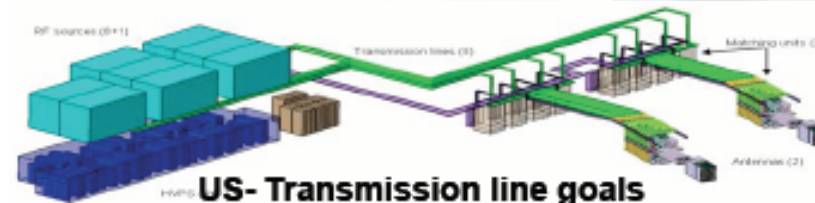


2.5 MW amplifiers

Tetrode



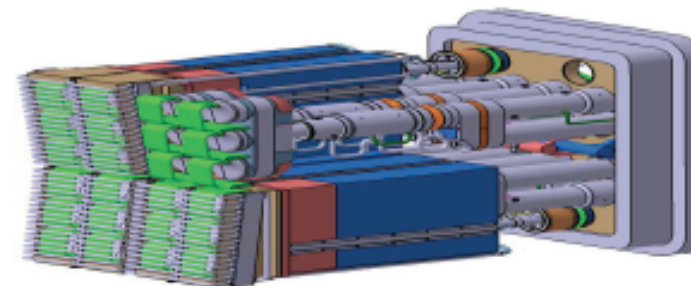
Diacrode



US- Transmission line goals  
6 MW/line 90% eff.

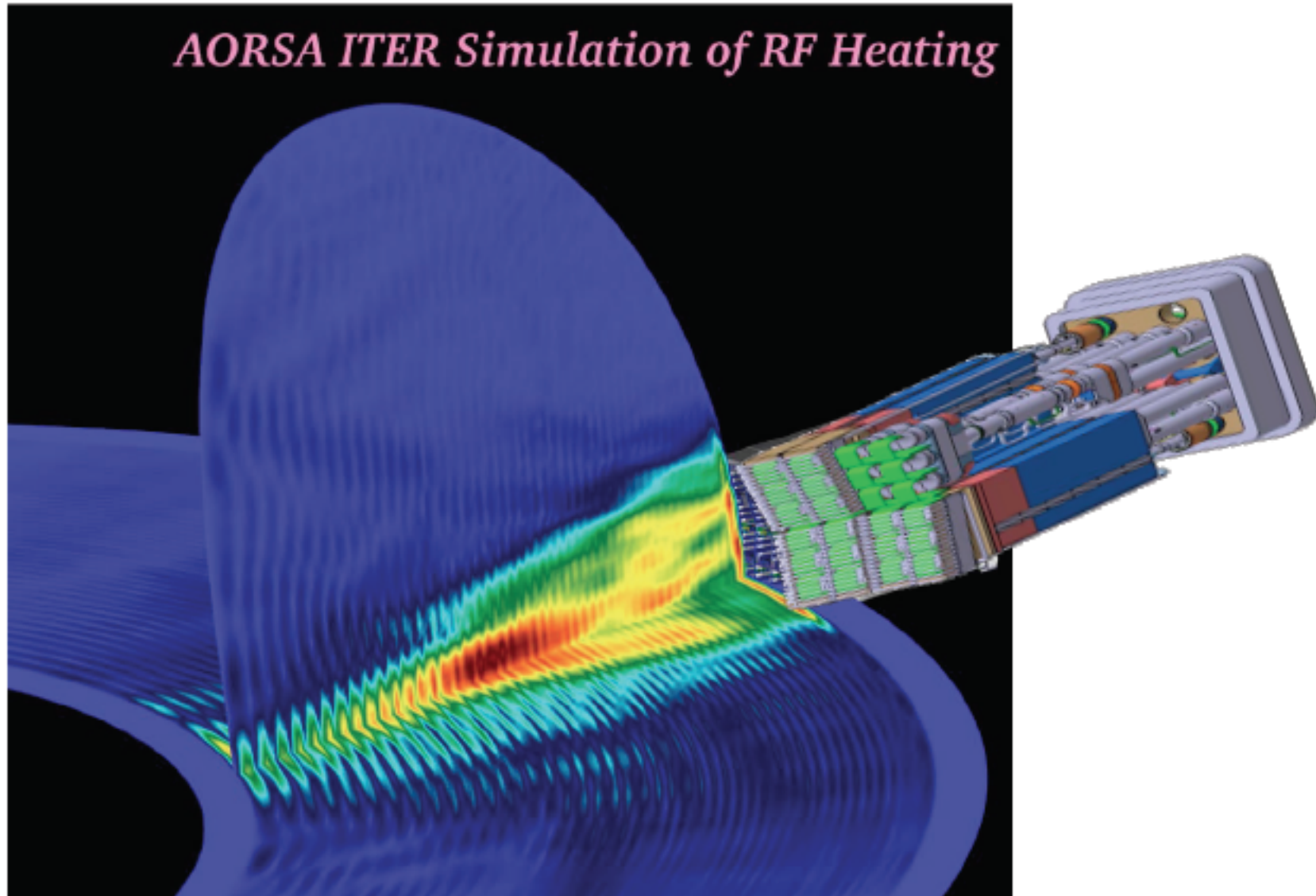
Prematch

Tuning power balancing and load resilience



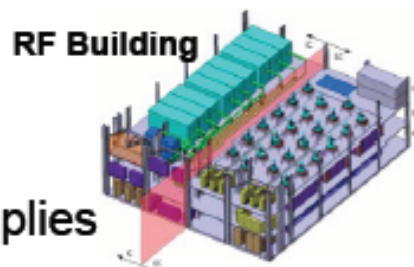


# ICRF Heating on ITER



## Sources

- High Voltage Supplies
- 24 Gyrotrons (JA, RF, EU, IN)



**JA- JAEA**  
 1.0 MW (800 s)  
 0.8 MW (3600 s),  
 >55% efficiency  
 RF gyrotron has  
 similar  
 performance



**EU- F4E**  
 2.0 MW short  
 pulse

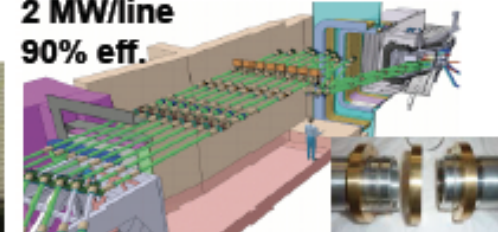
## Transmission line (US)

- Overmoded waveguide from 24 gyrotrons to 56 outputs
- Power loads for commission and test

**US- Corrugated waveguide**



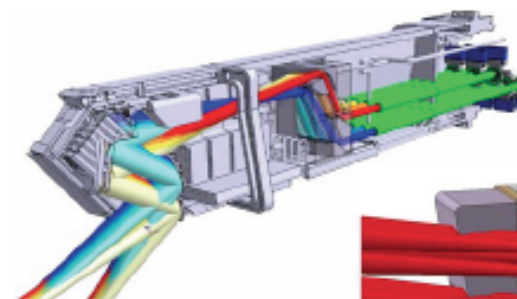
**US- Transmission line goals**  
 2 MW/line  
 90% eff.



## Launchers

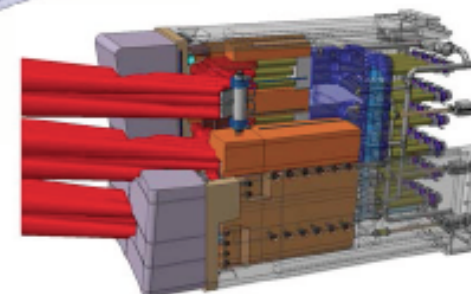
- Upper Launchers (EU)
- Equatorial Launcher (JA)
- Steerable mirrors

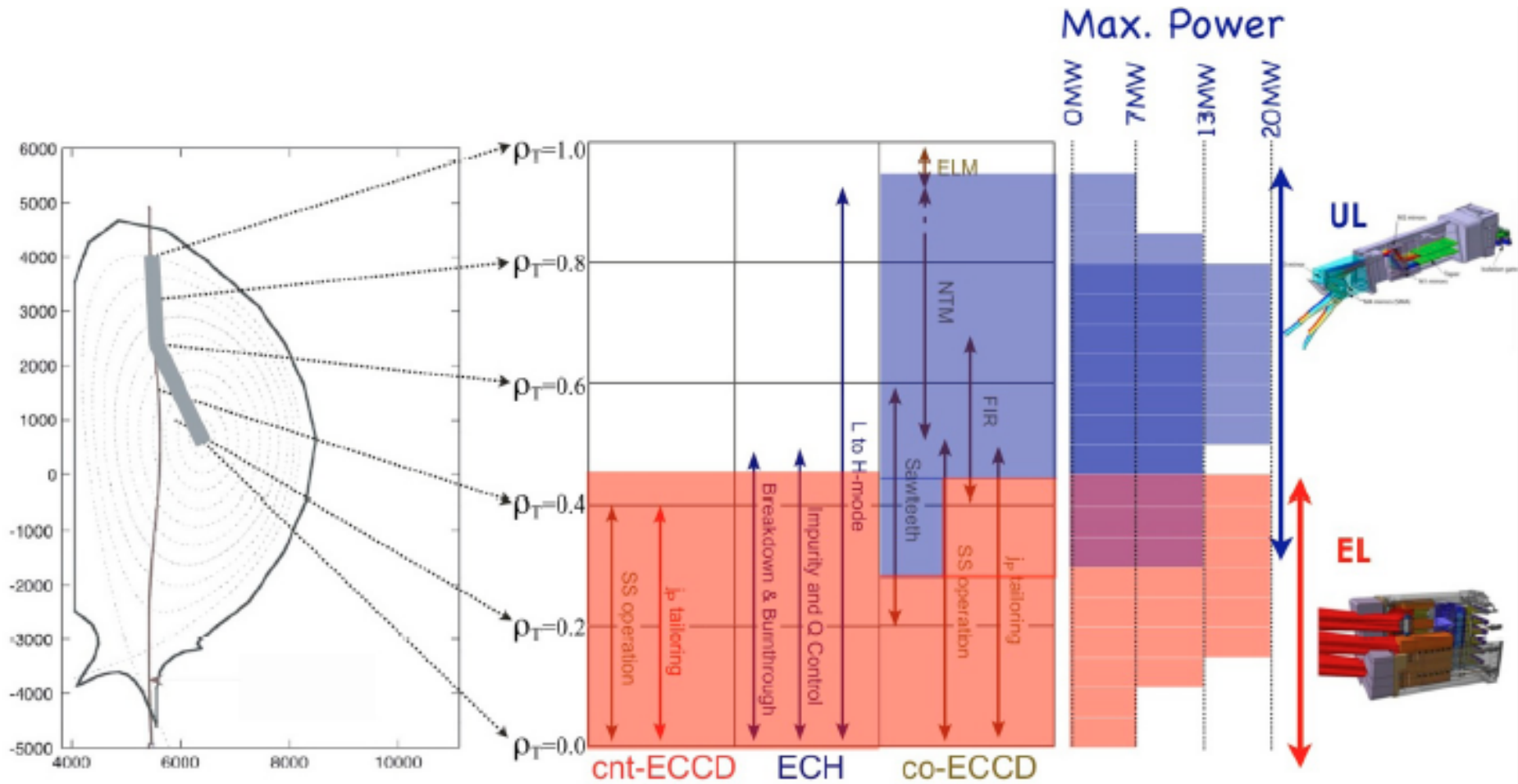
**EU- IPP/CRPP Mirror and Drive Mechanism**



**EU- IPP/CRPP  
 Upper Launcher**

**JA- JAEA  
 Equatorial  
 Launcher**



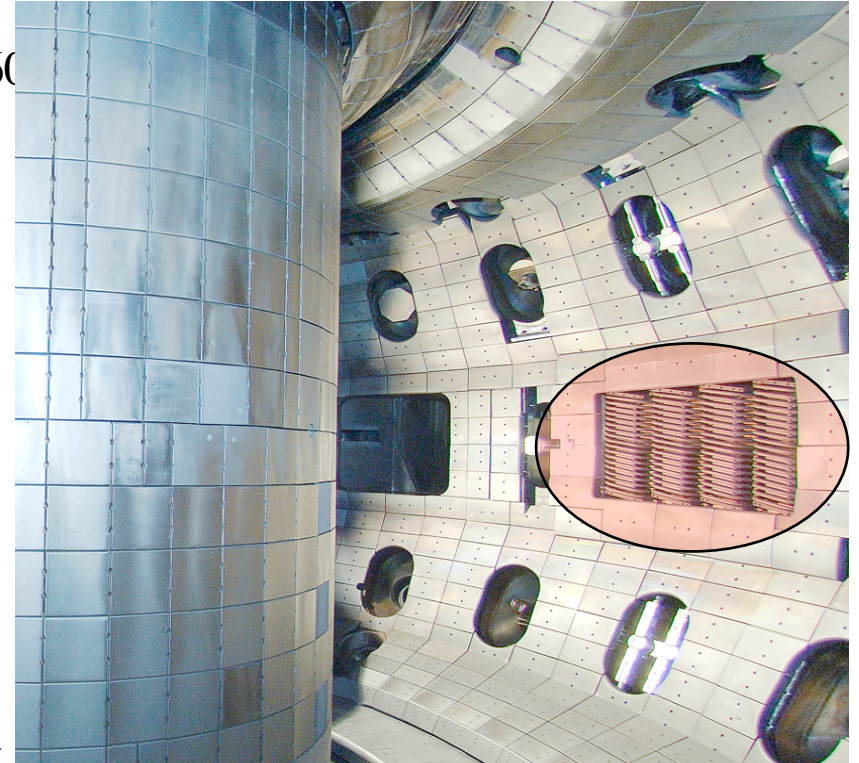


UL: applications requiring narrow/peaked  $j_{CD}$  profile

EL: applications requiring increased driven current ( $I_{CD}$ )

# DIII-D Fast Wave hardware

- 3 antenna arrays of two designs, located in the 285/300 (60 MHz) and 0 deg and 180 deg (both 90 MHz in these experiments) midplane ports
- 285/300 ~ 1 m wide, 0.5 m high
- 0 deg, 180 deg ~ 0.8 m wide, 0.4 m high
- All three 4-element arrays operated in 90 degree toroidal phasing, using decoupler
- 0, 180 deg use conventional tuning network, while 285/300 uses tunerless arrangement; both load-resilient at 90 deg phasing
- **All three antennas operate up to ~20-25 kV peak system voltage – this sets the limit of the total power that can be coupled for a given loading**



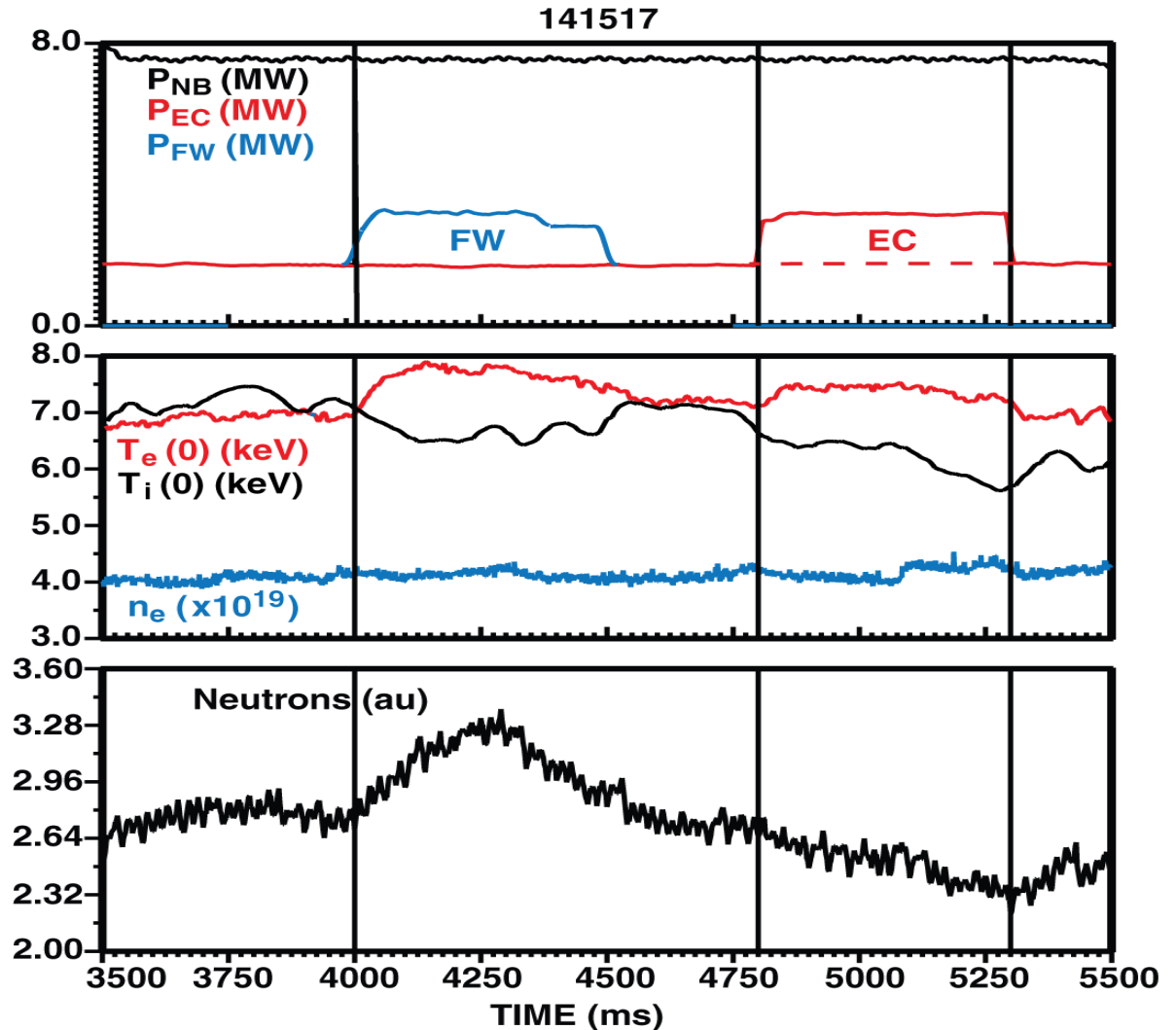
# FW core absorption efficiency similar to EC at 1.5 MW level in Advanced Inductive discharge: $\eta_{\text{abs}} \sim 100\%$

Comparison is on top of 8 MW beams, 1.5 MW EC – predicted increment in total stored energy <6% - within noise (ELMing, etc.)

- Either form of electron heating comparably raises  $T_e(0)/T_i(0)$ , FW more
  - EC is at  $\rho = 0.25$
  - FW deposition is more central

FW increases beam-target neutron rate through damping on beam ions

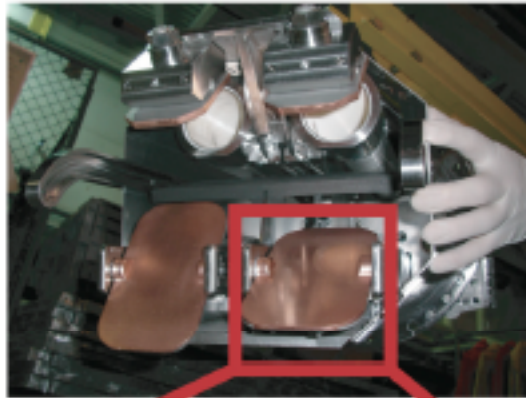
$$\beta_N \sim 2.6$$



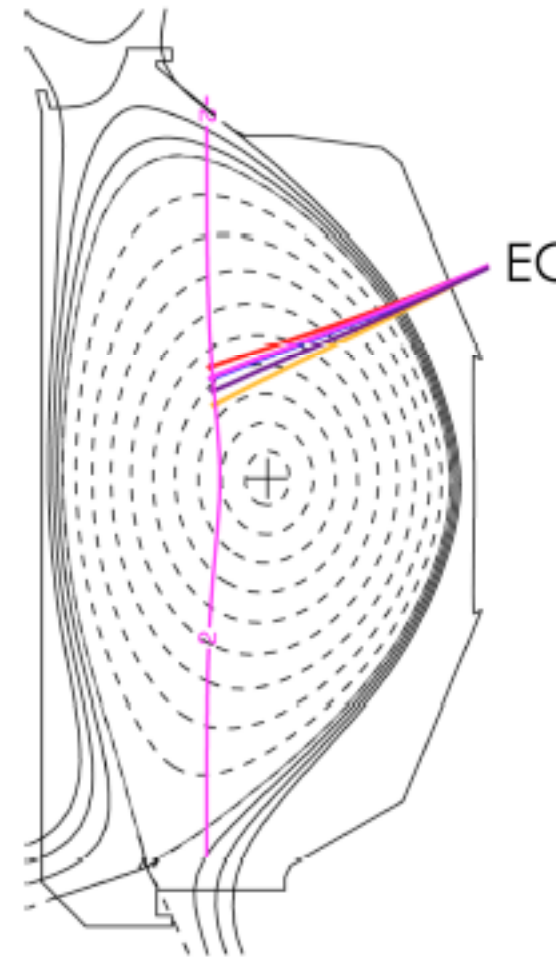
Peak injected power of 3.5 MW, pulse length up to 5 s



- Six steerable launchers

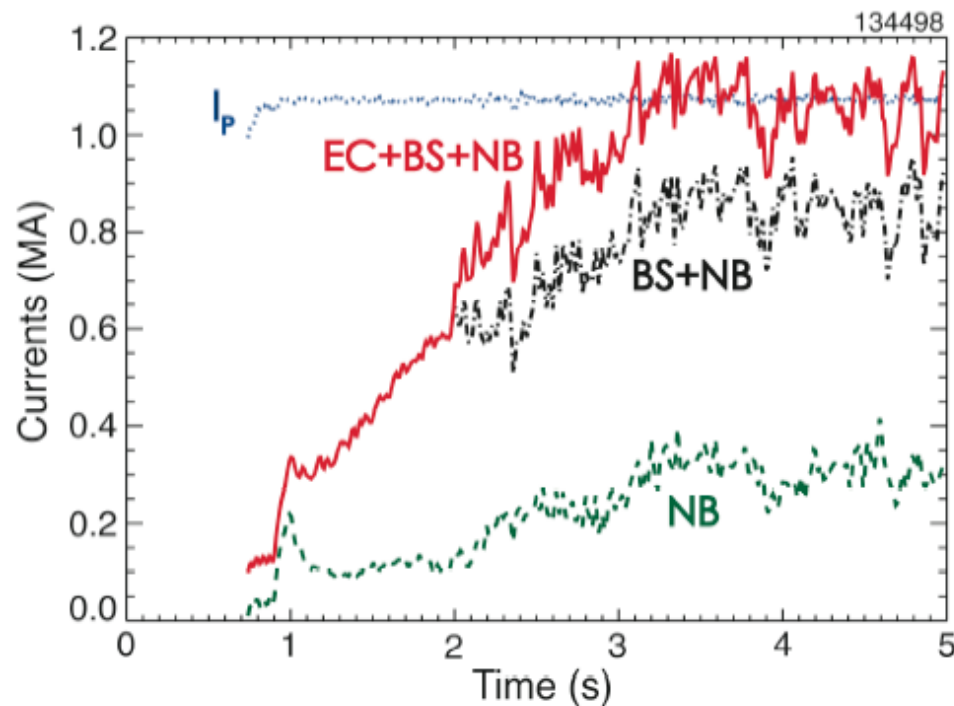


- 2<sup>nd</sup> harmonic X-mode at 110 GHz



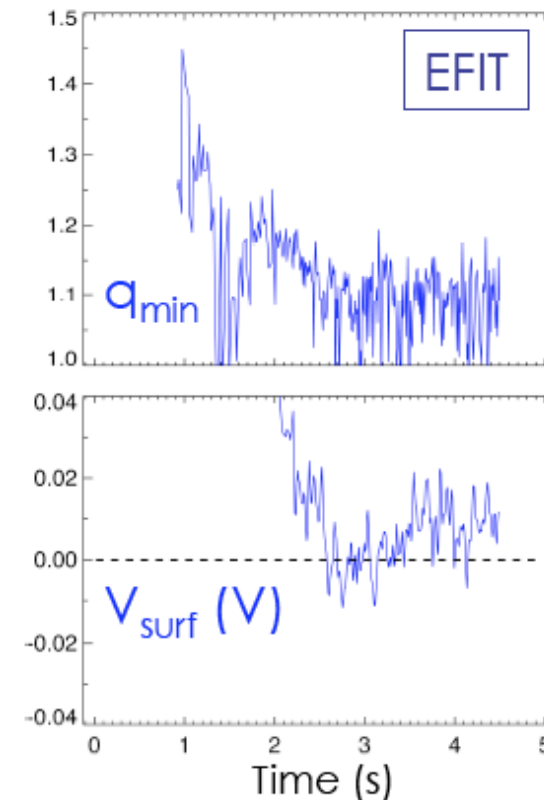
# Calculated Current Drive is Consistent With Achieving $\approx 100\%$ Non-Inductive Hybrid

- TRANSP modeling of high-beta hybrid (ECCD from CQL3D)  $\rightarrow$  50% bootstrap



Efficiencies: ECCD=0.07 A/W  
NBCD=0.03 A/W

- Despite strong central current drive,  $q_{\min} > 1$  and sawteeth are suppressed





# Relativistic Effect

**Relativistic effect must be taken account specially in high energy electrons with electron cyclotron heating :**

$$\omega - k_{\parallel} v_{\parallel} - n \frac{\Omega}{\gamma} = 0, \gamma = \left(1 - \frac{v_{\parallel}^2 + v_{\perp}^2}{c^2}\right)^{-1/2}$$

**Here velocities are transformed to their momentums;**

$$p_{\parallel} = \gamma m_e v_{\parallel}, p_{\perp} = \gamma m_e v_{\perp}$$

$$\frac{\omega^2}{\Omega^2} \left( (1 - n_{\parallel}^2) \frac{p_{\parallel}^2}{c^2 m_e^2} + \frac{p_{\perp}^2}{m_e^2 c^2} \right) - 2n \frac{n_{\parallel} \omega}{\Omega} \frac{p_{\parallel}}{c m_e} + \frac{\omega^2}{\Omega^2} - n^2 = 0$$

**To simplify,  $p_{\perp}=0$  and resonance solutions are,**

$$\left( \frac{p_{\parallel}}{c m_e} \right)_{res} = \frac{1}{1 - n_{\parallel}^2} \left\{ \frac{n \Omega}{\omega} n_{\parallel} \pm \left[ \frac{n^2 \Omega^2}{\omega^2} - (1 - n_{\parallel}^2) \right]^{1/2} \right\}$$

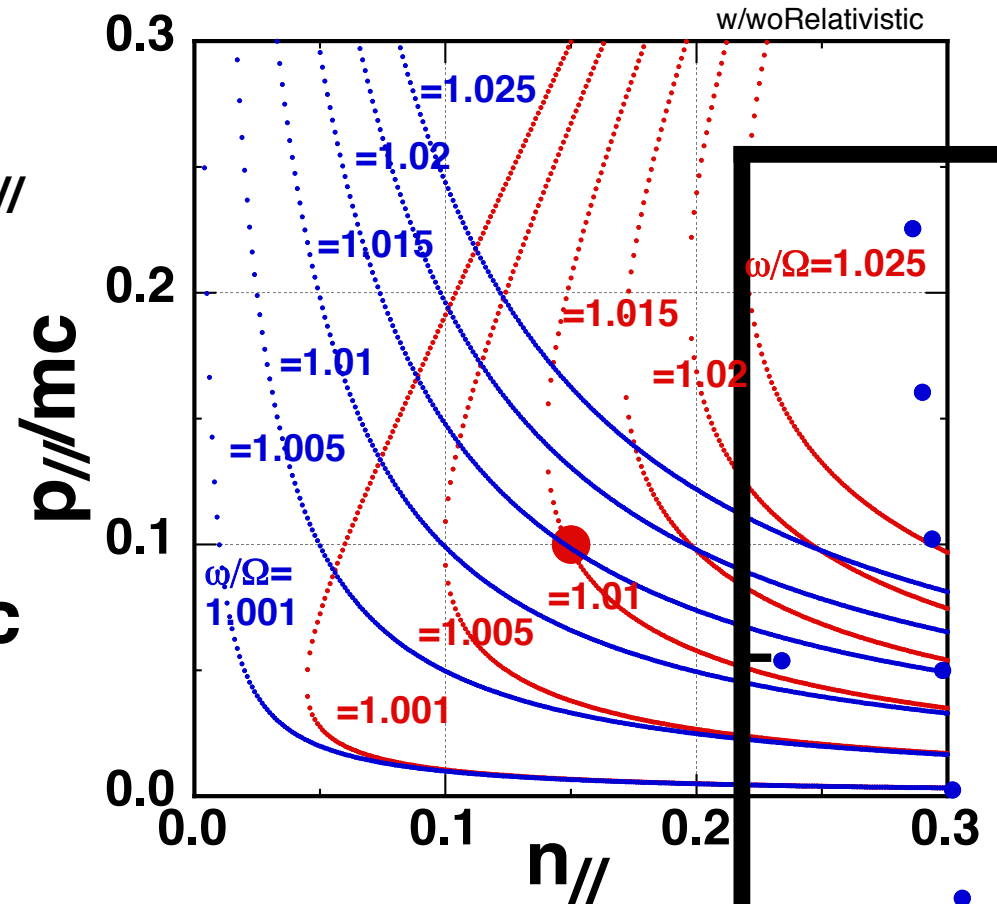
$$\left( \frac{p_{\parallel}}{c m_e} \right)_{res,cl} = \frac{1}{n_{\parallel}} \left( 1 - \frac{n \Omega}{\omega} \right)$$

**With the solution in non-relativistic resonance.**



# Relativistic Effect

Relativistic resonant parallel momentum for  $p_{\perp}=0$  versus  $n_{\parallel}$  with several  $\omega/\Omega$ ;  
When EC waves access from the low B, i.e.,  $\omega/\Omega > 1$ , electron cyclotron damping occurs at the higher magnetic field than that with non-relativistic effect as pointed with red solid circle, i.e.,  $\omega/\Omega = 1.015$  to  $=1.01$ .



Blue and red dots show parallel momentum without and with relativistic effect.



# Current Drive

## Current drive via. Landau damping, e.g., LHCD

$$\frac{I}{P} = \frac{0.122 \cdot T_e [\text{keV}]}{R [\text{m}] \cdot n_e [\text{m}^{-3} / 10^{20}] \ln \Lambda} \frac{j^*}{p^*} (\text{A/W})$$

When  $R=5\text{m}$ ,  $T_e=10\text{keV}$ ,  $n_e=10^{20}\text{m}^{-3}$ ,  $\ln\Lambda=20$  and  $j^*/p^*=20$ , then  $I/P=0.244[\text{A/W}]$ , i.e., 12MA with  $P=50\text{MW}$ . Here  $j^*/p^*$  is a normalized current drive efficiency.

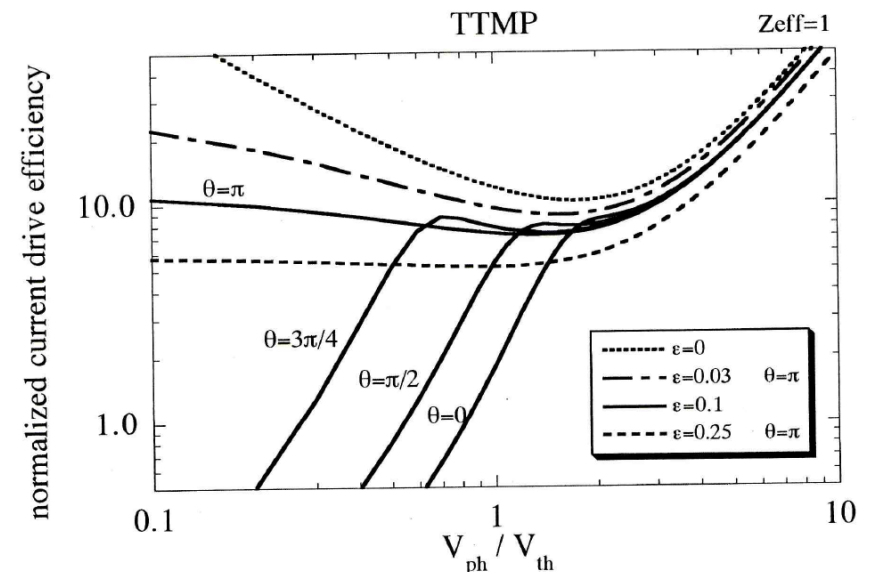
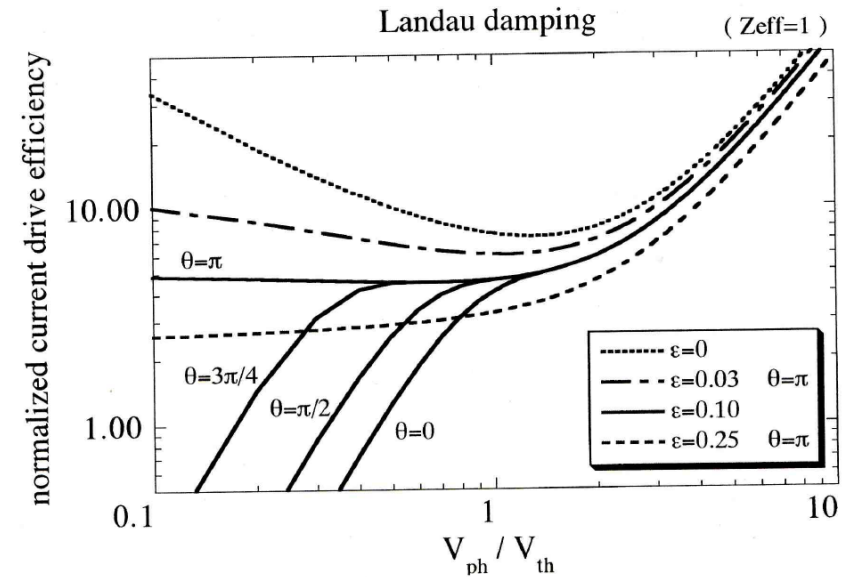
$$\text{When } \frac{\omega}{k} \ll v_e, \frac{j^*}{p^*} \approx \frac{kv_e}{\omega} \text{ and When } \frac{\omega}{k} \gg v_e, \frac{j^*}{p^*} \approx \left(\frac{\omega}{kv_e}\right)^2$$

**Current drive via. cyclotron damping, e.g., ECCD**  
energy of RF wave launched with uni-direction is absorbed with resonant electrons. It results in asymmetry in electron velocity space. Then this asymmetry produces the current. This method has a capability to control the current profile.

# Current Drive

## -effect of trapped particles-

With the presence of trapped electrons, current drive efficiency is decreased specially at low phase velocity wave. Here  $\varepsilon$  is an inverse ratio of aspect ratio, i.e.,  $\varepsilon=a/R$ .  $\theta=0$  and  $\theta=\pi$  is launched outside and inside, respectively.





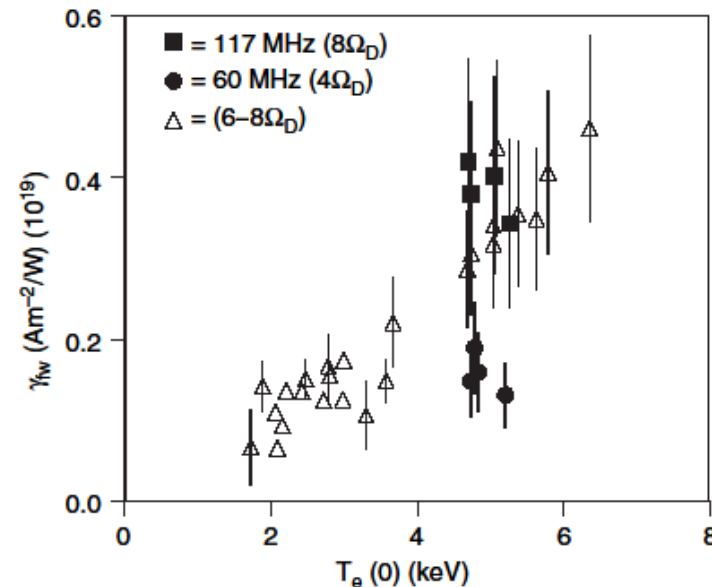
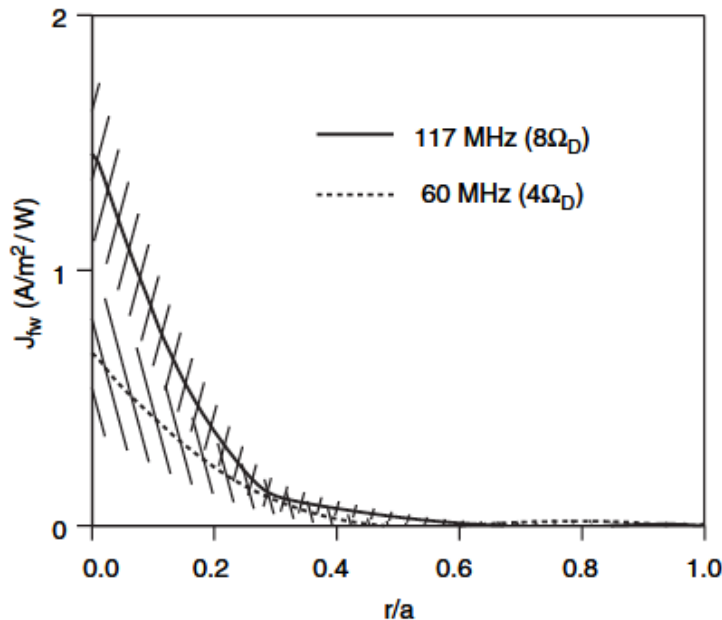
# FWCD Experiments on Tokamaks

## -higher harmonic frequency-

On DIII-D higher harmonics FWCD: acceleration of electrons

$$I_{fw} = \frac{\gamma_{fw} \cdot P_{fw}}{\bar{n}_e R}, \quad \gamma_{fw} [A/m^2/W] 10^{19} = 0.08 \cdot T_{e0} (keV) \rightarrow I_{fw} \sim 120 kA$$

$\gamma_{fw}$  is twice larger in  $8 \omega_{cD}$  than that in  $4 \omega_{cD}$ , because higher harmonic ion heating becomes smaller.



Unfortunately RF generator with 320MHz ( $8\Omega_{cD}$ ) is not prepared on ITER.



# Fast Wave Current Drive

-minority ions-

---

## Minority ion CD: MICD

High energy minority ions becomes a carrier of current drive with  $k_{\parallel}$  of uni-direction as the same as minority heating.

$$\frac{I_{CD}}{P_{abs}} \approx Z_m (Z_m - 1) \frac{3ev_{\parallel}v}{n_m v^{m/i} v_{thi}^3}$$

Physics is almost the same as ECCD.

$Z_m$ : charge number of minority ions

If  $Z_m = Z_i$  (charge number of bulk ions), no current drive.

In addition  $Z_m/A_m \neq Z_i/A_i \neq 2 Z_i/A_i$  are required to avoid bulk ion acceleration. Therefore  ${}^3\text{He}$  is the best minority ion.

The lower minority ratio ( $n_{3\text{He}}/n_e$ ) is, the lower  $v_{\parallel}$  of the resonant  ${}^3\text{He}$  ion is, but the smaller  $n_m$  is. Therefore  $I_{CD}/P_{abs}$  is constant.

In addition the small  $k_{\parallel}$  is, the wave like LHW may propagate at scrape-off region found in NSTX, i.e., difficulty of high RF power absorption.



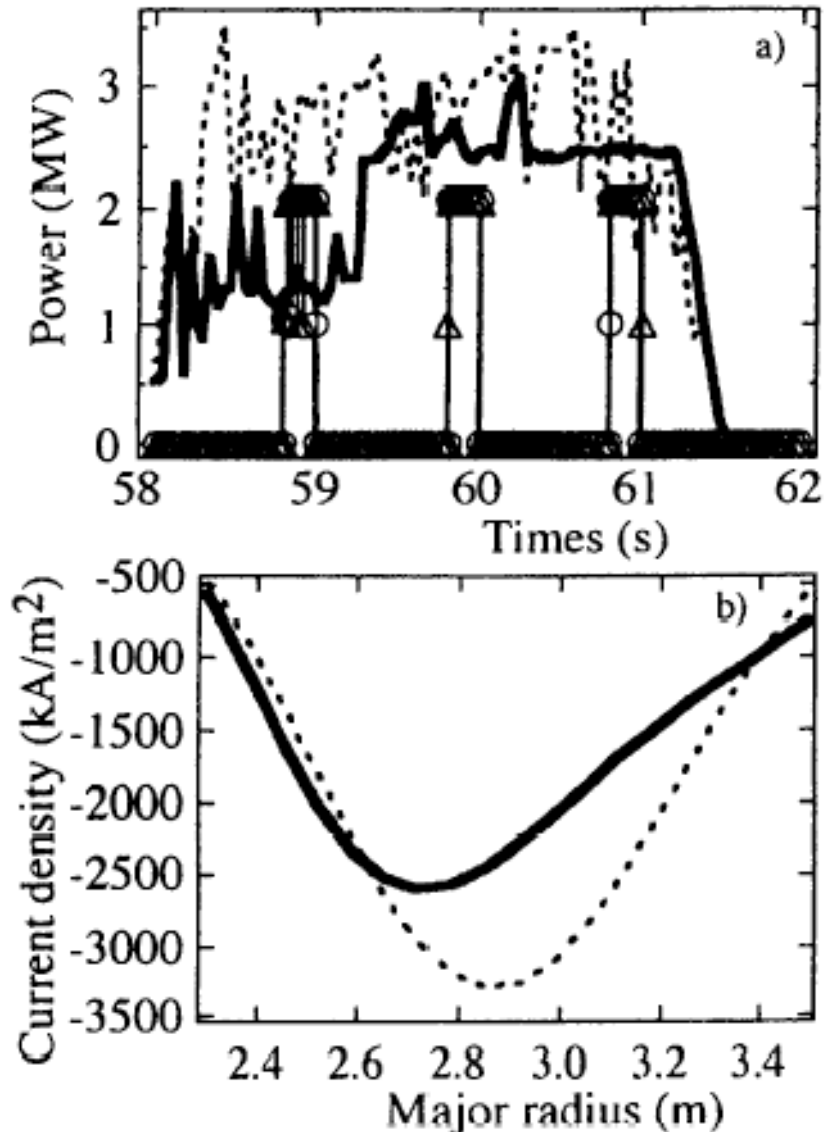
# FWCD Experiments on Tokamaks

-minority ions-

## On JET: Minority CD

$B=3.35\text{T}$ ,  $f=37\text{MHz}$  with  $^3\text{He}$   
(0.5%)

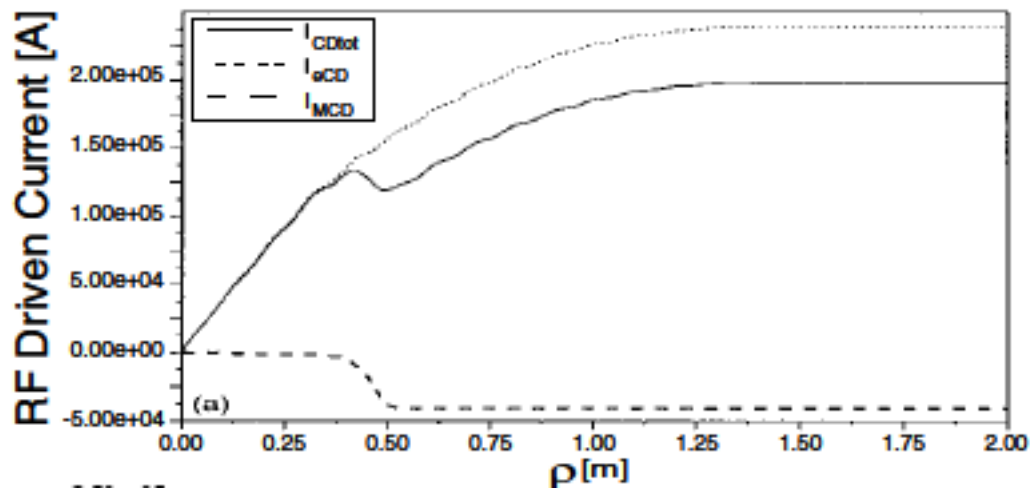
Phase difference between  
adjacent antennas:  
 $+90^\circ$  and  $-90^\circ$  with  $P_{\text{RF}}\sim 2.5\text{MW}$   
 $\Delta I_{\text{CD}}\sim 300\text{kA}$  from MSE  
(motional Stark Effect) data



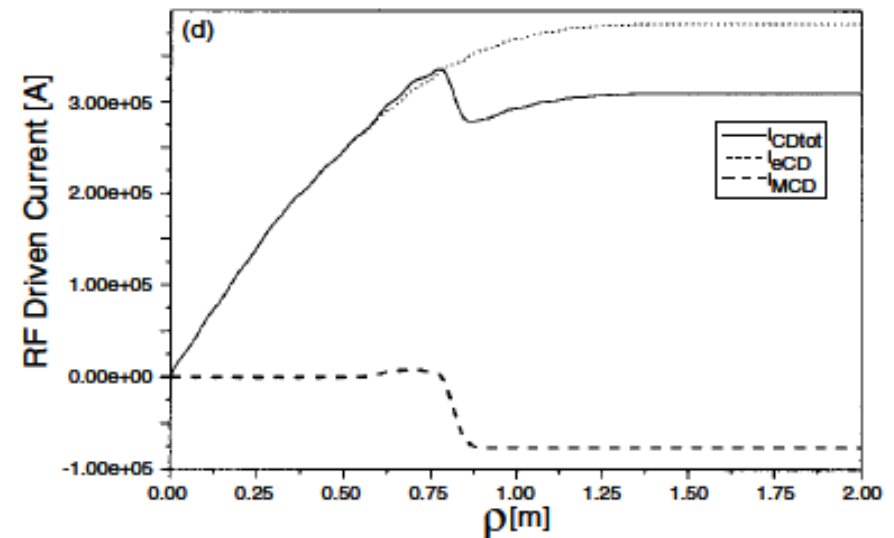
# Numerical Simulation of FWCD

FWCD simulation on ITER plasma using TOMCAT code with minority CD,  $^3\text{He}$  minority

$$I_{\text{CD}}/P_{\text{FW}}=0.02\text{MA/MW}$$



Radial profile of  $I_{\text{MCD}}$ ,  $I_{\text{eCD}}$  and  $I_{\text{CDtot}}$  at 17keV in temperature of high energy  $^3\text{He}$ .



Radial profile of  $I_{\text{MCD}}$ ,  $I_{\text{eCD}}$  and  $I_{\text{CDtot}}$  at  $f=58\text{MHz}$



# Lower Hybrid Wave

Frequency range of Lower hybrid wave (LHW) is  $|\Omega_i| \ll \omega \ll \Omega_e$ .

Dispersion relation of plasma wave:

$$SN_{\perp}^4 + \{P(N_{\parallel}^2 - S) + D^2\}N_{\perp}^2 + P\{(N_{\parallel}^2 - S)^2 - D^2\} = 0$$

$$N_{\perp}^2 = -\frac{P(N_{\parallel}^2 - S) + D^2}{2S} \pm \left\{ \left( \frac{P(N_{\parallel}^2 - S) + D^2}{2S} \right)^2 - \frac{P\{(N_{\parallel}^2 - S)^2 - D^2\}}{S} \right\}^{1/2}$$

Here,

$$S = 1 - \frac{\Pi_i^2}{\omega^2} + \frac{\Pi_e^2}{\Omega_e^2} = 1 - \frac{\Pi_i^2}{\omega^2} \left(1 - \frac{\omega^2}{|\Omega_i|\Omega_e}\right)$$

$$D = \frac{\Pi_e^2 \Omega_e}{\Omega_e^2 \omega} = \frac{\Pi_i^2}{\omega^2} \left(\frac{\omega^2}{|\Omega_i|\Omega_e}\right)^{1/2} \left(\frac{\Omega_e}{|\Omega_i|}\right)^{1/2}$$

$$P = 1 - \frac{\Pi_e^2}{\omega^2} = 1 - \frac{\Pi_i^2 \Omega_e}{\omega^2 |\Omega_i|}$$

In the plasma of  $n_e = 10^{19} \text{m}^{-3}$ ,  $B = 3 \text{T}$  and  $\omega^2 \sim |\Omega_i|\Omega_e$ ,

$$\omega \sim 1 \times 10^{10} \text{ rad/s}, \Pi_i \sim 4 \times 10^9 \text{ rad/s} \text{ and } \Pi_e \sim 2 \times 10^{11} \text{ rad/s}$$

$$S \sim 1$$

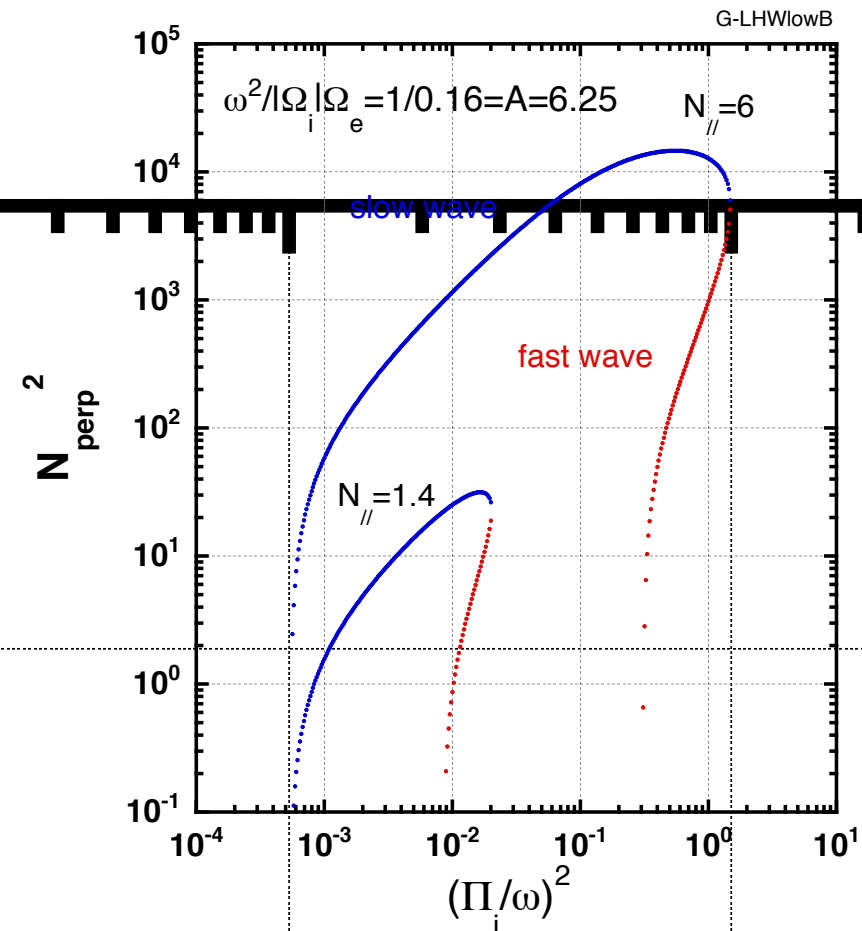
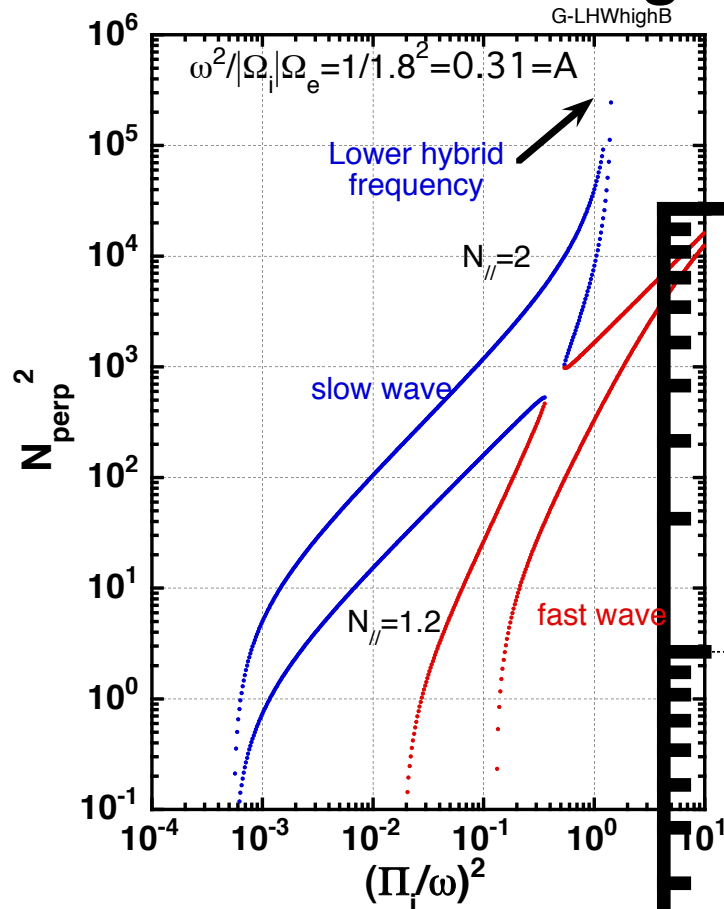
$$D \sim 10$$

$$P \sim -400$$



# Lower Hybrid Wave

$\omega^2/|\Omega_i|\Omega_e$  is determines the propagation characteristics of LHW. When  $\omega^2/|\Omega_i|\Omega_e < 1$  (in the left figure), the LHW can reach at higher density region, i.e., lower hybrid resonance. On the other hand, when  $\omega^2/|\Omega_i|\Omega_e > 1$  (in the right figure), a launched slow wave merges to a fast wave.





# Lower Hybrid Wave

$N_{\perp}^2$  ( $\gg 1$ ) for lower hybrid wave is formulated as follows;

$$\text{slow wave : } N_{\perp}^2 \approx -\frac{b}{a}$$

$$\text{fast wave : } N_{\perp}^2 \approx -\frac{c}{b}$$

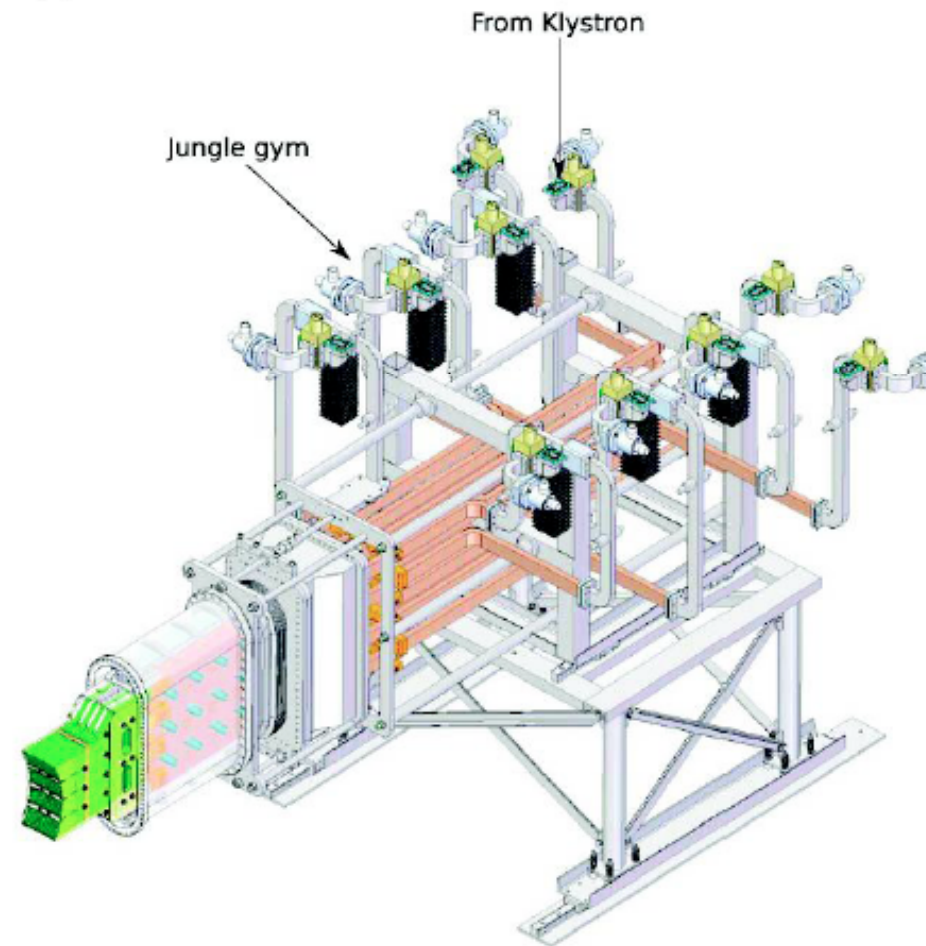
**Resonance frequency of the slow wave of lower hybrid Wave is**

$$a = S = K_{\perp} = 1 - \frac{\Pi_i^2}{\omega^2} + \frac{\Pi_e^2}{\Omega_e^2} = 0$$

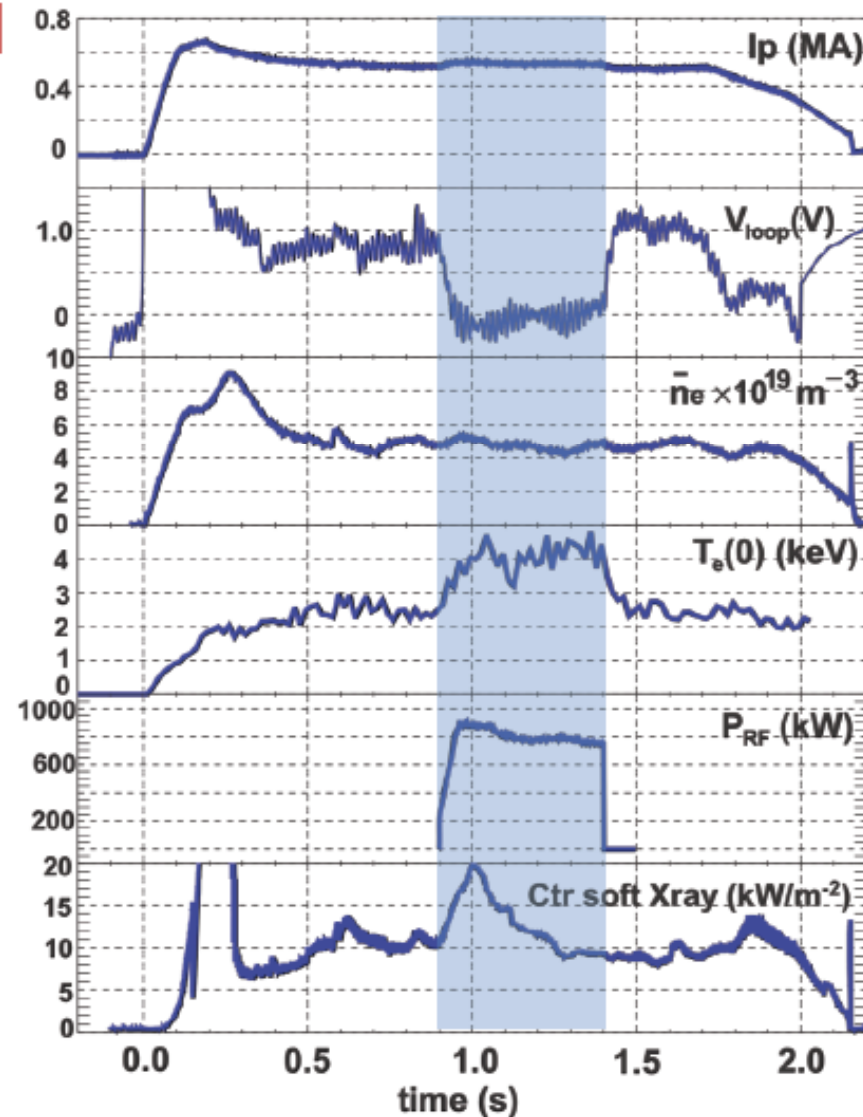
$$\frac{\Pi_i^2}{\omega^2} = 1 + \frac{\Pi_e^2}{\Omega_e^2} \rightarrow \omega^2 = \omega_{LH}^2 = \frac{\Pi_i^2}{1 + \Pi_e^2 / \Omega_e^2}$$

# C-Mod offers opportunity to investigate LH physics with ITER-like parameters

- $n_e = 0.5-5 \times 10^{20} \text{ m}^{-3}$
- $B_T = 4 - 8 \text{ T}$
- Diverted plasma configuration
- $f = 4.6 \text{ GHz}$
- 7x60 mm waveguides
- 16x4 active array
- $n_{||} = 1.5 - 3$  co- or counter-current



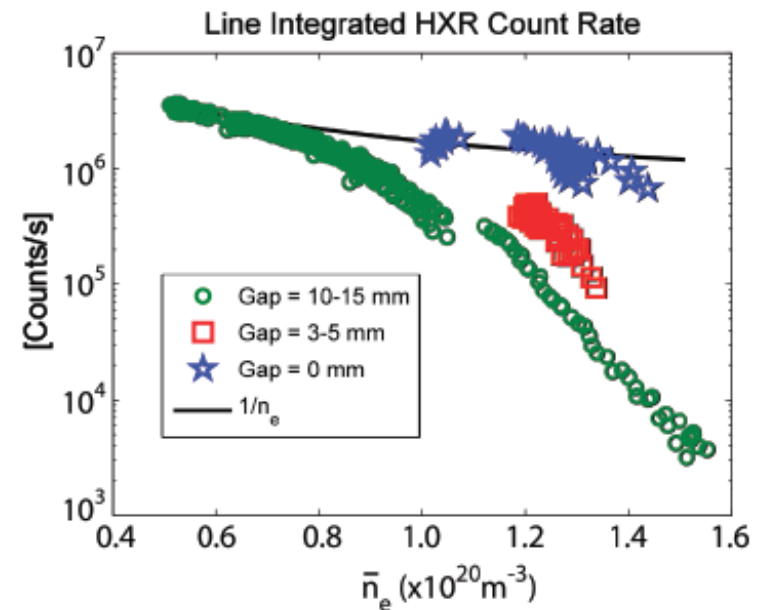
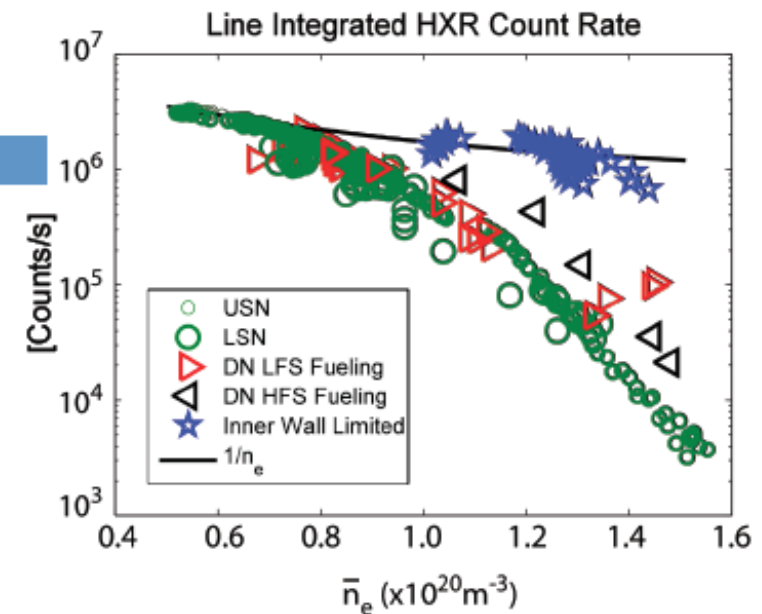
# Zero loop voltage sustained for 0.5 s LH pulses



- ❑ Zero loop voltage sustained for full length of LH pulse (0.5 s) at  $n_e \sim 0.5 \times 10^{20} \text{ m}^{-3}$ ,  $I_p \sim 500 \text{ kA}$ ,  $B = 5.4 \text{ T}$
- ❑ Current relaxation time  $\sim 0.2 \text{ s}$
- ❑ Some transformer recharge
- ❑ Current drive efficiency  $\eta \equiv n_e I_p R_0 / P_{LH} = 2.0 - 2.5 \times 10^{19} \text{ A}/(\text{Wm}^2)$
- ❑ Sawtooth suppression increases core electron temperature to over 4 keV

# LHCD at high density is sensitive to plasma topology and position

- Fast electron bremsstrahlung (FEB) emission increased in double null as compared to single null
- FEB significantly increased in limited discharges
  - Other high density ( $>10^{20} \text{ m}^{-3}$ ) LHCD experiments all on limited tokamaks (Alcator C, FTU)
- FEB increased by operating with small ( $<5 \text{ mm}$ ) inner gaps in single null
- Increase in core plasma temperature with ICRF heating does not improve LHCD performance above density limit
- Increase in edge temperature with I-mode improved performance slightly at high  $n_e$
- Results support conjecture that SOL physics plays a critical role in the LHCD density limit





# Density Limit on LHCD

**Lower hybrid waves mode-transfer to the electrostatic Waves at the higher density as seen in the following equation, and ions are heated with this wave.**

$$\left(\frac{\omega_{pi}}{\omega}\right)^2 = \left\{1 - \hat{\omega}^2 + 1.5^{3/2} N_z^2 \hat{\omega}^2 \frac{v_{te}}{c} \left(1 + \frac{4}{\hat{\omega}^4} \frac{T_i}{T_e}\right)^{1/2}\right\}^{-1}$$

when  $\hat{\omega} = 1, \frac{T_i}{T_e} = 1,$

$$\left(\frac{\omega_{pi}}{\omega}\right)^2 = (4.11 N_z^2 \frac{v_{te}}{c})^{-1} \leftarrow N_z = 2$$

$$\left(\frac{\omega_{pi}}{\omega}\right)^2 = (T_e (keV)^{1/2})^{-1} \leftarrow \frac{v_{te}}{c} = 0.06 T_e (keV)^{1/2}$$

$$\left(\frac{\omega_{pi}}{\omega}\right)^2 = \frac{1}{T_e (keV)^{1/2}} \rightarrow \left(\frac{\omega_{pi}}{\omega}\right)^2 = 0.45 \leftarrow T_e = 5 keV$$

$$\frac{\omega_{LH}}{\omega} = \frac{\omega_{pi}/\omega}{\{1 + (\omega_{pe}/\omega_{ce})^2\}^{1/2}} \leftarrow \frac{\omega_{pe}}{\omega_{ce}} = \frac{5.56 \cdot 10^{11} (n_e/10^{20})^{1/2}}{1.76 \cdot 10^{11} B} = \frac{3.16 (10^{20}/10^{20})^{1/2}}{B(5T)} = 0.63$$

$$\rightarrow \frac{\omega_{LH}}{\omega} = \frac{0.45^{1/2}}{(1 + 0.63^2)^{1/2}} = 0.37$$

**Therefore the critical density should have been higher than the Observed one.**

In higher frequency as  $|\Omega_i| \ll \omega \sim \Omega_e$

$$K_{\perp} = 1 - \sum_k \frac{\Pi_k^2}{\omega^2 - \Omega_k^2} \approx 1 - \frac{\Pi_e^2}{\omega^2 - \Omega_e^2}$$

$$K_{\times} = -\sum_k \frac{\Pi_k^2}{\omega^2 - \Omega_k^2} \frac{\Omega_k}{\omega} \approx -\frac{\Pi_e^2}{\omega^2 - \Omega_e^2} \frac{\Omega_e}{\omega}$$

$$K_{\parallel} = 1 - \sum_k \frac{\Pi_k^2}{\omega^2} = 1 - \frac{\Pi_i^2 + \Pi_e^2}{\omega^2} \approx 1 - \frac{\Pi_e^2}{\omega^2}$$

Wave propagating perpendicularly to B, i.e.,  $\theta = \pi/2$   
and  $N_{\parallel} = 0$ ,

$$K_{\perp} N_{\perp}^4 - (RL + K_{\parallel} K_{\perp}) N_{\perp}^2 + K_{\parallel} RL = 0$$

$$(K_{\perp} N_{\perp}^2 - RL)(N_{\perp}^2 - K_{\parallel}) = 0$$

Ordinary wave:

$$N_{\perp}^2 = K_{\parallel} = 1 - x$$

Extra-ordinary wave:

$$N_{\perp}^2 = \frac{RL}{K_{\perp}} = \frac{(1 - y - x)^2 - x^2 y}{(1 - y)(1 - y - x)}$$



# Electron Cyclotron Wave

As seen in the left-bottom of CMA, characteristics of EC waves are plotted in the linear scale:

$\omega_R$  :

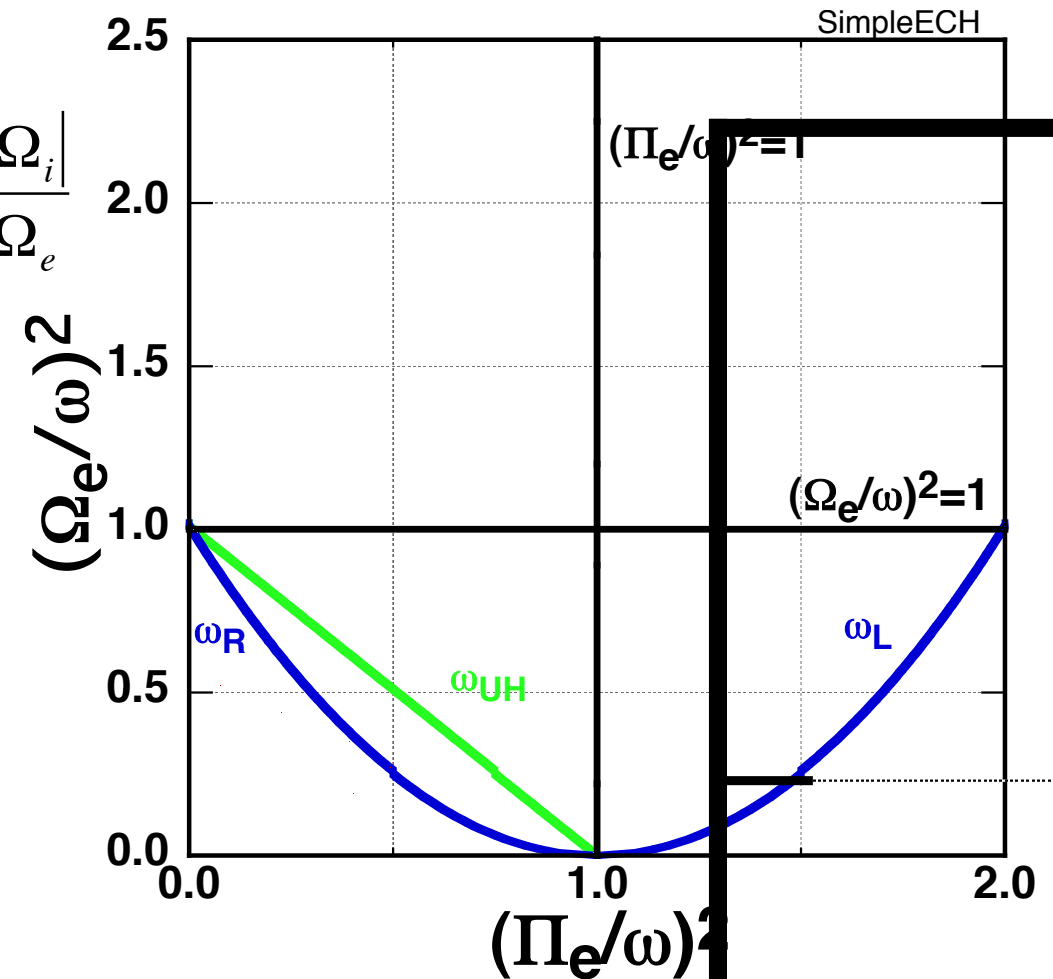
$$x = \frac{\Pi_e^2 + \Pi_i^2}{\omega^2} = 1 - Ay - (1 - A)y^{1/2} \leftarrow A = \frac{|\Omega_i|}{\Omega_e}$$

$\omega_L$  :

$$x = 1 + (1 - A)y^{1/2} - Ay$$

$\omega_{UH}$  :

$$\frac{x}{1 + A} + y = 1$$

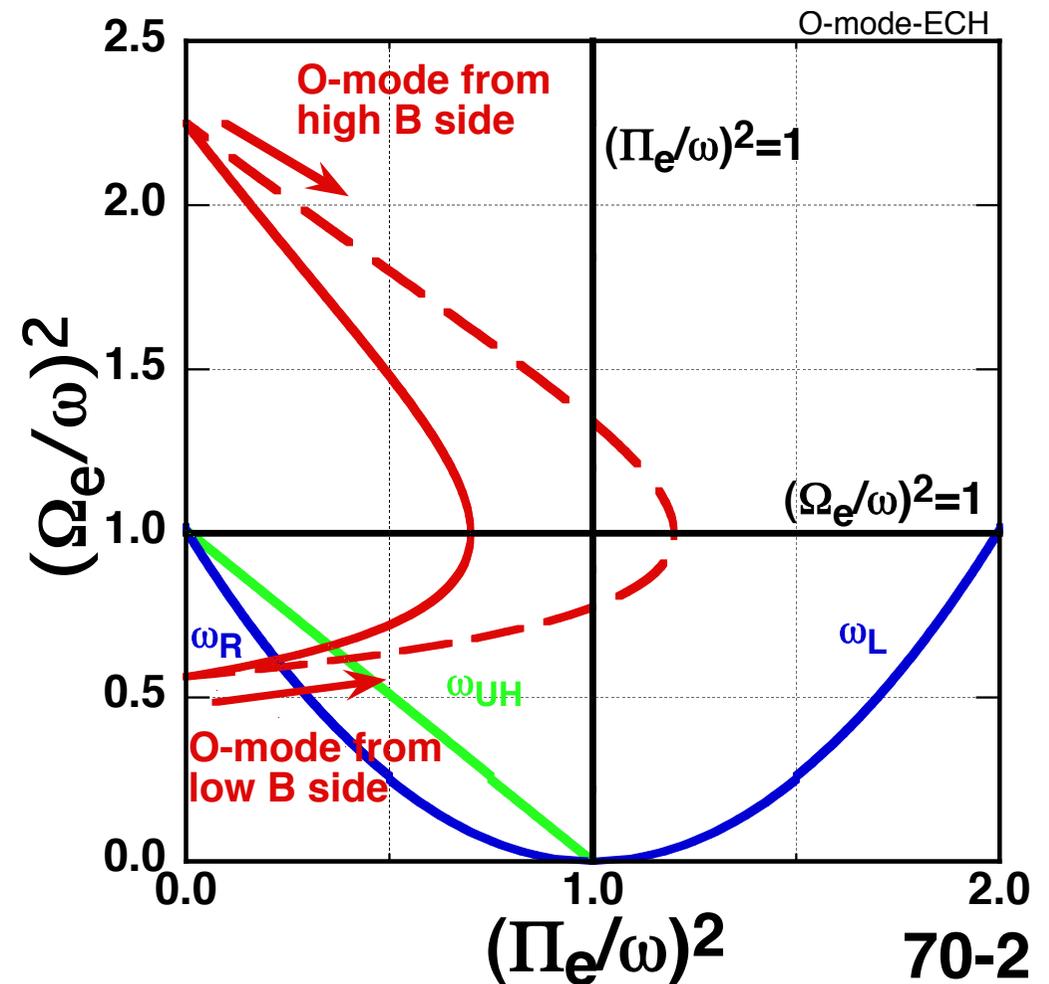
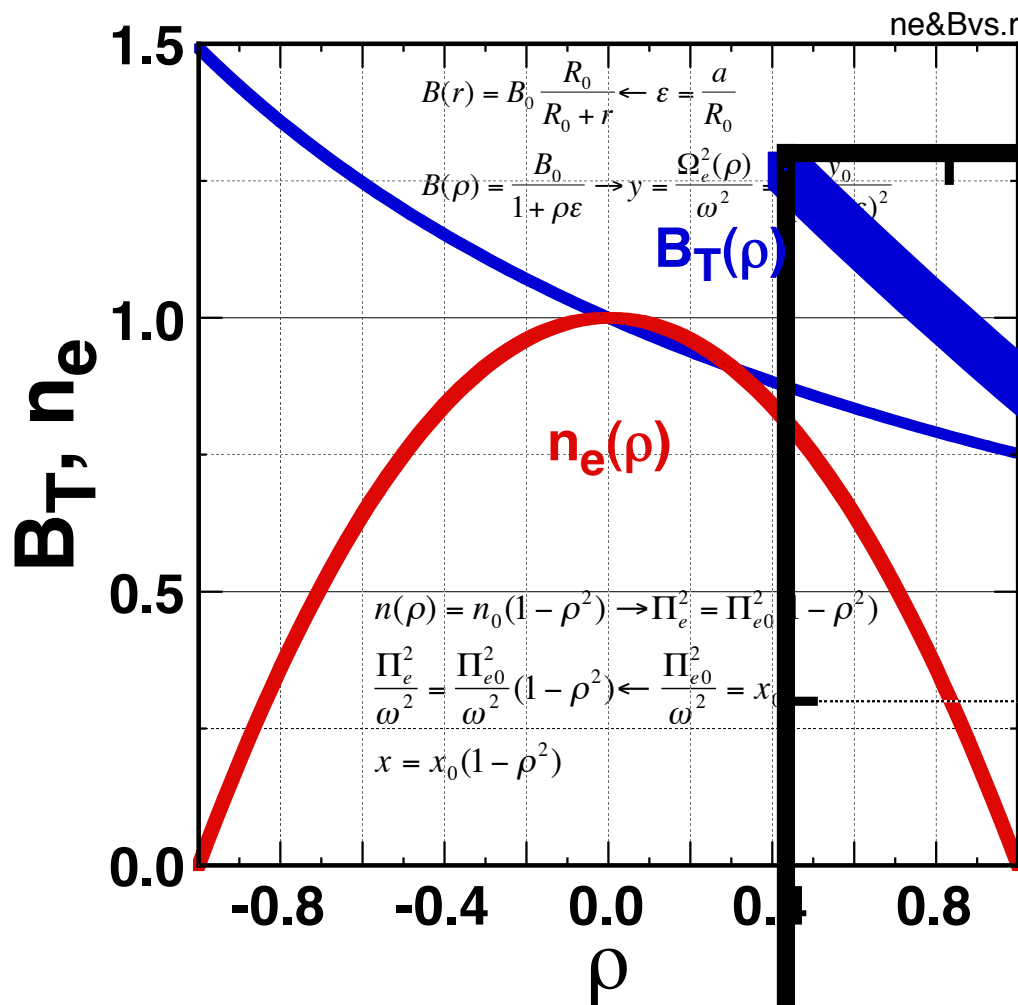




# Electron Cyclotron Wave

## -O mode-

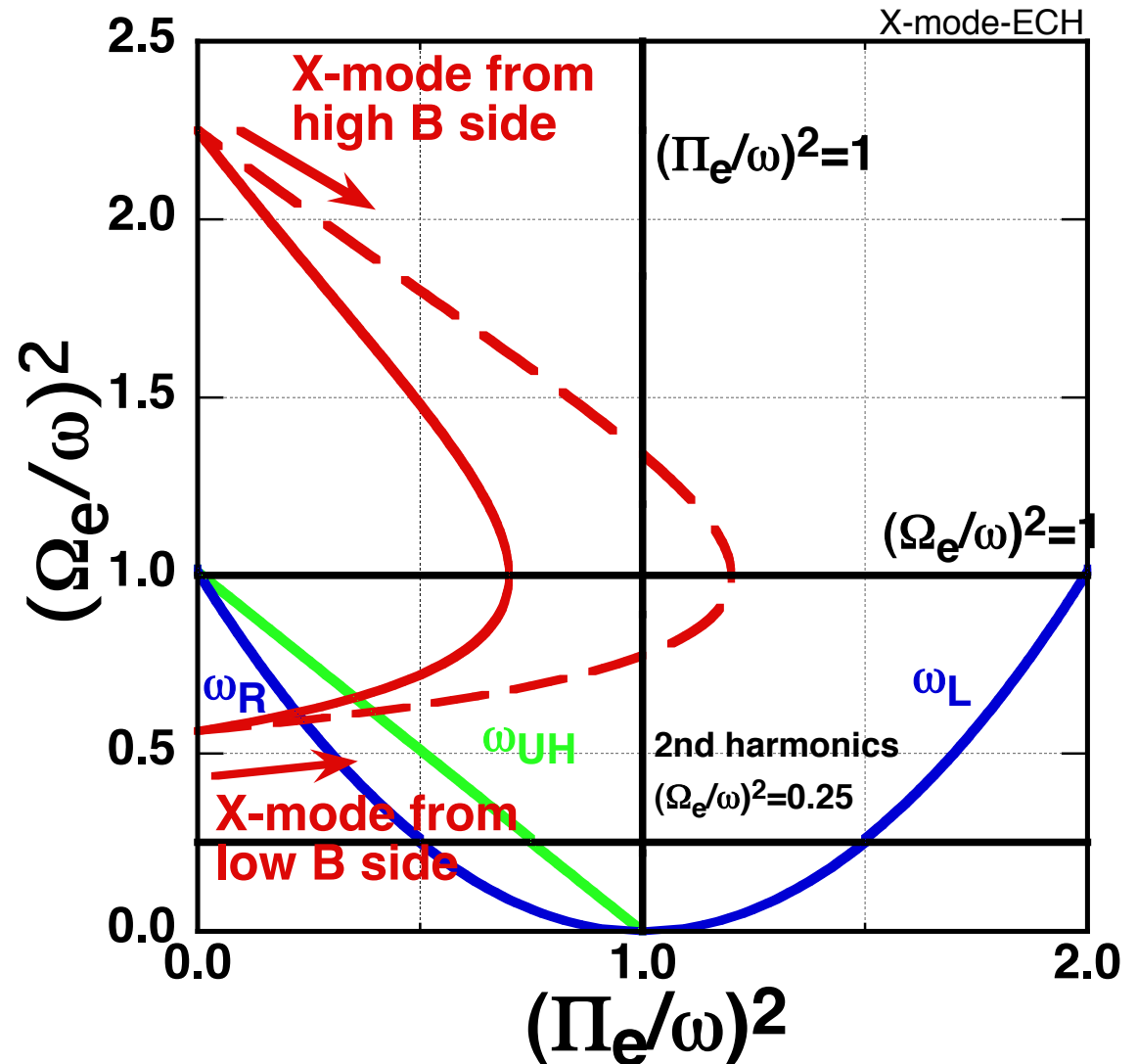
When EC waves access to the plasma from the out-side place with lower magnetic field, Taking into account of  $n_e(r)$ ,



# Electron Cyclotron Wave

## -X- mode-

When EC waves with X-mode access to the plasma from the inside place with higher magnetic field, it can access to electron cyclotron resonance layer even in  $\Pi_e/\omega > 1$ . On the other hand, EC waves with X-mode from the outside place with lower magnetic field suffers from cutoff in lower density.





# Higher Harmonic Electron Cyclotron Wave

Higher harmonic EC wave with X-mode has also a cut-off density as follows;

$$y_0 = (x_0 - 1)^2 \leftarrow y_0 = \frac{1}{n^2}$$

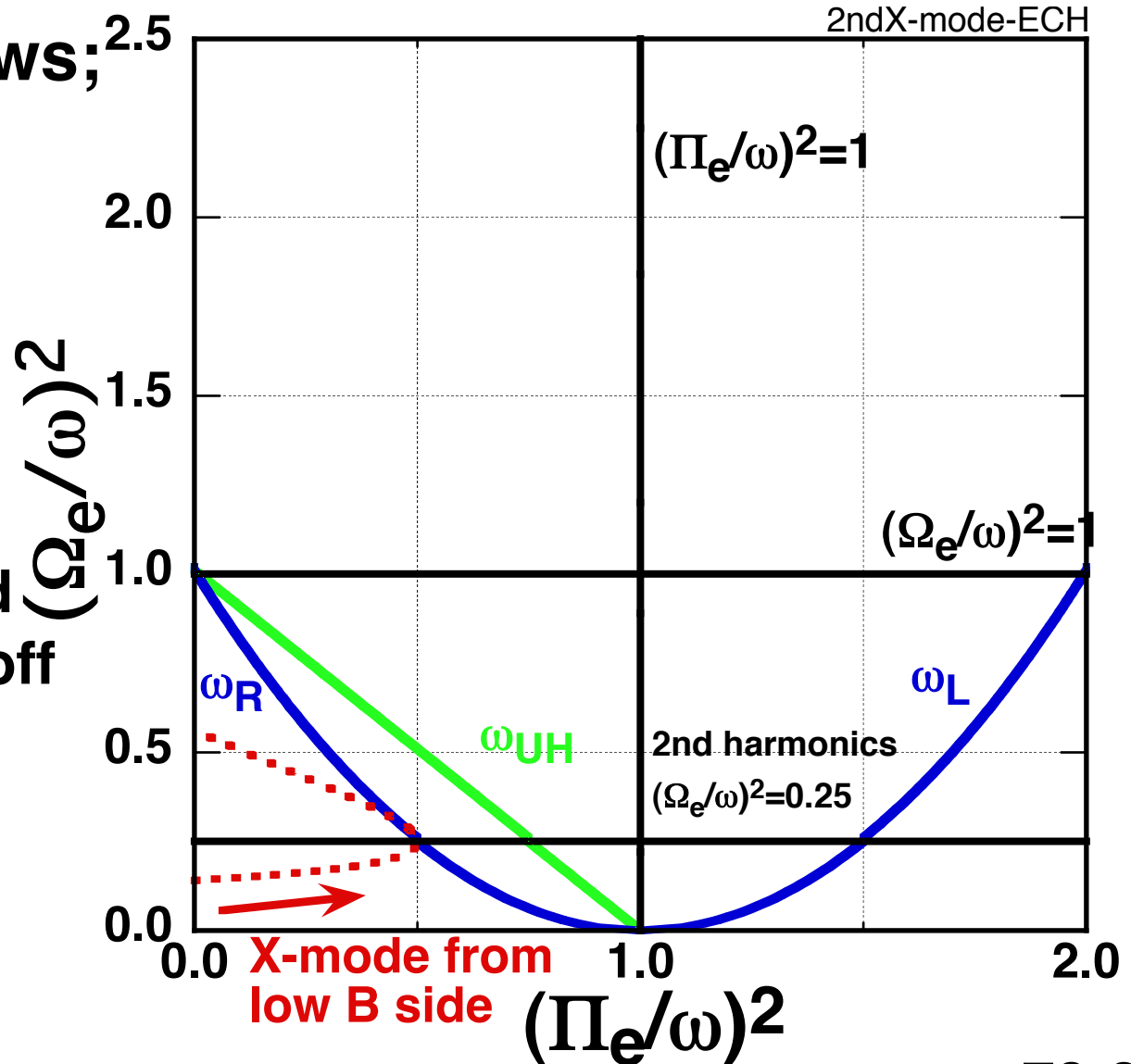
$$x_0 - 1 = \pm \frac{1}{n} \rightarrow x_0 = 1 \pm \frac{1}{n}$$

smaller  $x_0 : x_0 = 1 - \frac{1}{n}$

For example, in the second Harmonic heating the cut-off density is

$$x_0 = 1 - \frac{1}{n} = \frac{1}{2}$$

$$\Pi_e^2 = \frac{1}{2} \omega^2$$



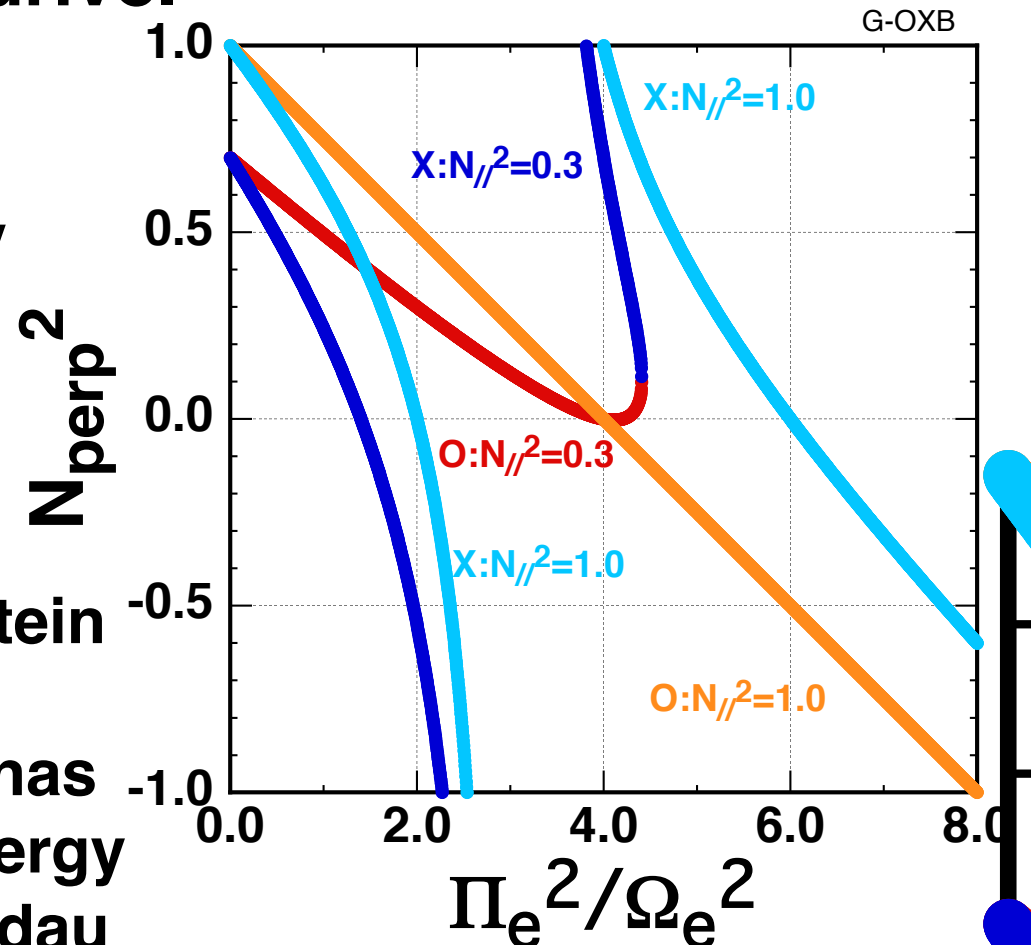


# OXB Heating

EC waves have a cut-off density depending on applied frequency, i.e.,  $\omega = \Omega_e$ . It means the density limit for heating and current drive.

When the launched O mode with a finite  $N_{//}$ , i.e., oblique injection to B,  $N_{\text{perp}}^2=0$  at the higher density than the cut-off density as seen in the right graph. Then this O wave mode-transforms to X mode.

This X mode is mode-converted to the electrostatic Electron Bernstein wave (EBW) at the upper hybrid resonance, i.e.,  $\omega = \omega_{UH}$ . The EBW has no cut-off density, so this wave energy is transferred to electrons via Landau damping.





# O- and X-modes Heating

Using hot dispersion eq.  $E_x$ ,  $E_y$  and  $E_z$  are calculated, then

$$\text{Right hand polarization: } \frac{E_x - iE_y}{E_z \text{ or } E_y}$$

Absorption coefficient  $a$  is deduced.

O-mode heating rate is expressed as follows:

$$\alpha_1^{(0)} \approx \left( \frac{\Pi_e}{\Omega_e} \right)^2 \frac{\Omega_e}{c}, \quad \alpha_2^{(0)} \approx \left( \frac{\Pi_e}{\Omega_e} \right)^2 \left( \frac{v_e}{c} \right)^2 \frac{\Omega_e}{c}$$

On the other hand X-mode heating rate is as follows:

$$\alpha_1^{(X)} \approx \left( \frac{\Pi_e}{\Omega_e} \right)^{-2} \left( \frac{v_e}{c} \right)^2 \frac{\Omega_e}{c}, \quad \alpha_2^{(X)} \approx \left( \frac{\Pi_e}{\Omega_e} \right)^2 \frac{\Omega_e}{c}$$

Heating efficiency for O-mode is better with plasma with higher Density. On the other hand the optimized condition for heating efficiency in X-mode is opposite to that in O-mode.



# OXB Heating

$N_{//0}$  is the particular wave index with that minimum  $N_{\text{perp}}^2=0$ . In other  $N_{//}$ ,  $N_{\text{perp}}^2$  becomes negative and this EC wave has a cut-off. Then this wave becomes evanescent in the density region of  $N_{\text{perp}}^2 < 0$ , but in the higher density again it can propagate as the X-mode. Then the tunneling efficiency  $\eta$  can be calculated via Budden's formula. Generally the higher frequency is, i.e., the larger  $k_0$ , the lower  $\eta$  becomes.

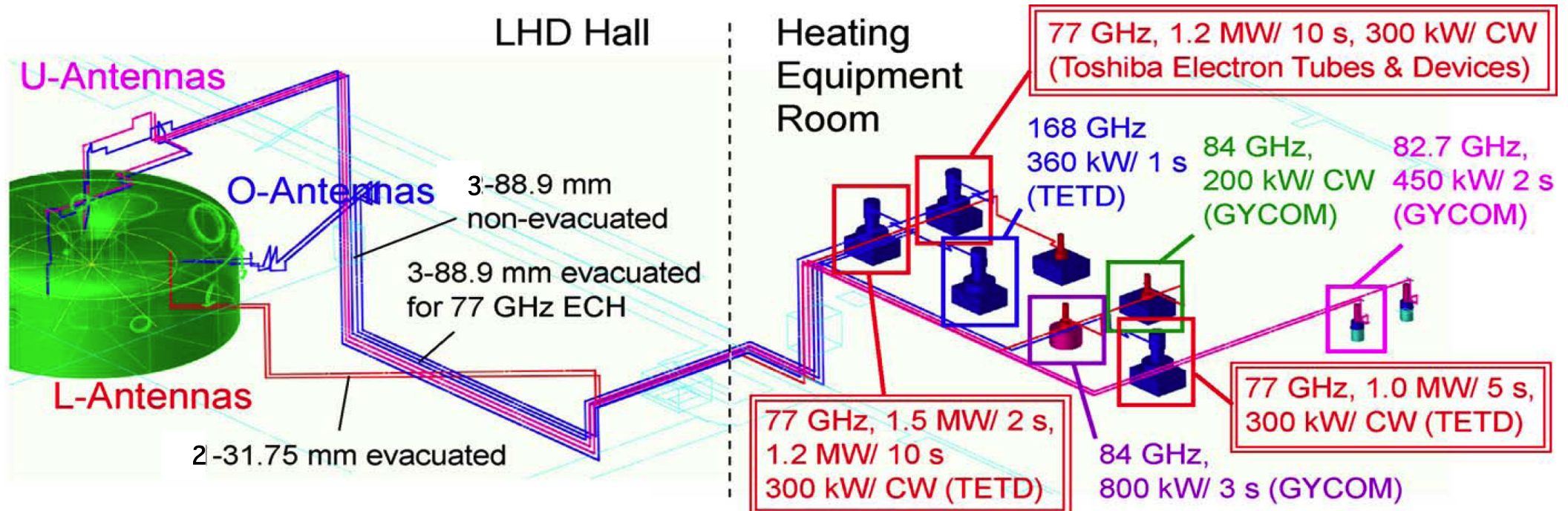
$$\eta = \exp\left[-\frac{1}{4} \pi k_0 \frac{2^{1/2}}{Y^{1/2}} L\{2YN_y^2 + (1+Y)^2(N_{//0}^2 - N_{//}^2)^2\}\right]$$

$$L = 1 - \frac{\omega_{pe}^2}{\omega^2} + \frac{\omega_{pe}^2}{\omega^2} \frac{\omega_{ce}/\omega}{1 + \omega_{ce}/\omega}, Y = \frac{\omega_{ce}}{\omega}$$

# High Power ECRH Experiments on LHD

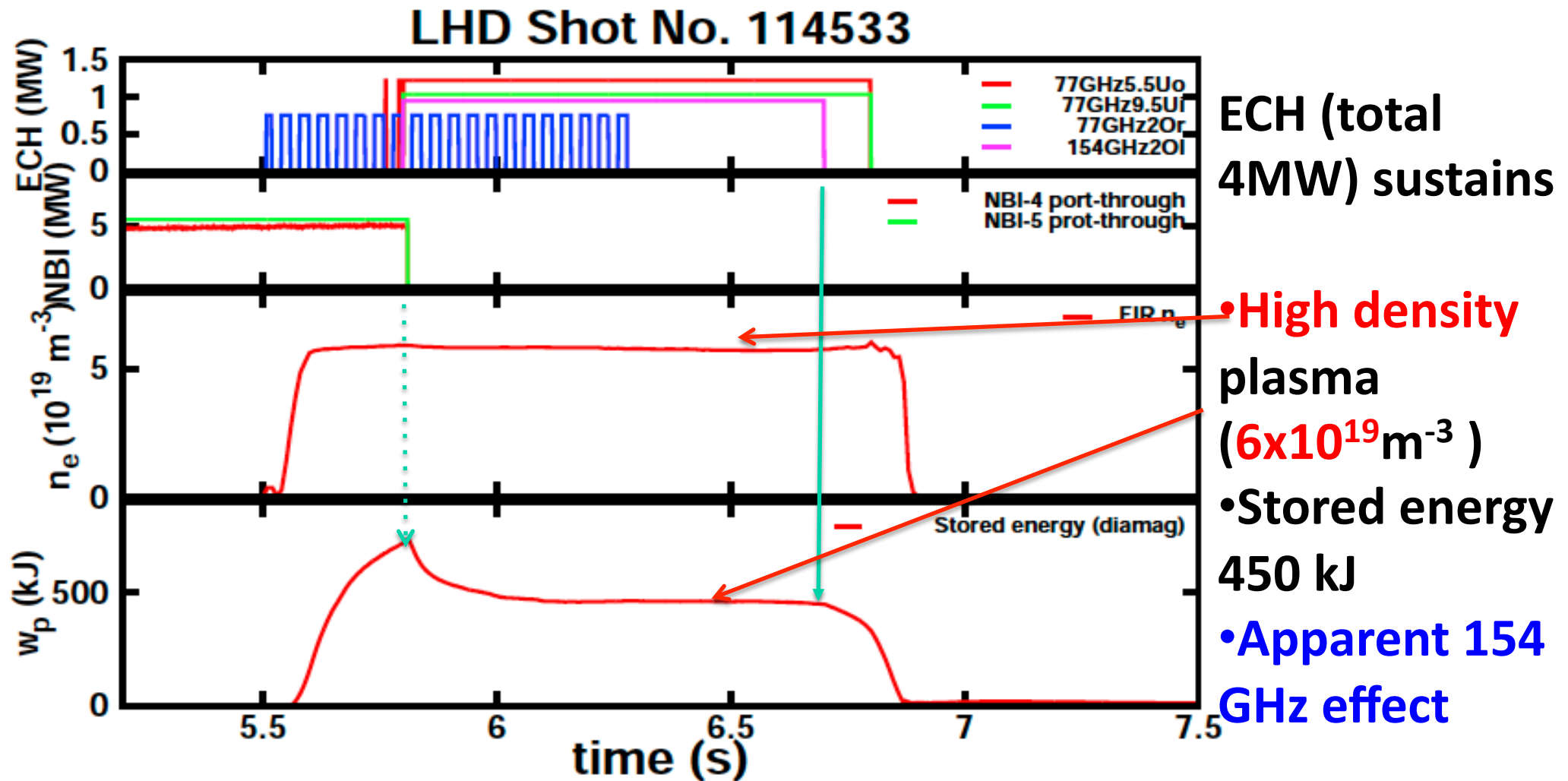
- **Extension of high  $T_e$  regime**
- **ITB study**
  - Transport study in low collisional regime
- **OXB heating experiments**
- **Higher harmonic ECH experiments**
- **ECCD experiments**

# State of ECH System on LHD

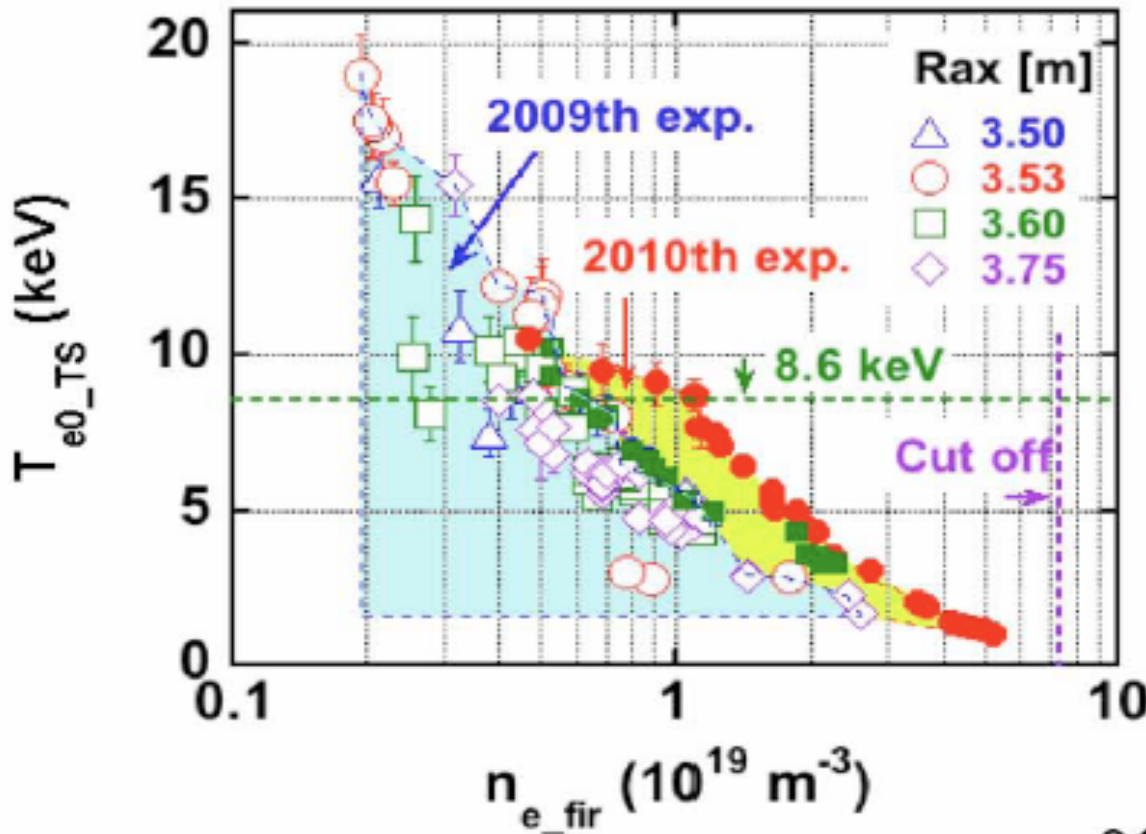


- > New high-power, long-pulse 77GHz gyrotrons (#1 started working on 2007, #2: on 2008 and #3: on 2009)
- > 5 working gyrotrons (77G x3, 82.7G x1, 84G x1)
- > 8 transmission lines (evacuated x5, non-evacuated x3)
- > Max. total injection power to LHD simultaneously was 3.7MW last experimental campaign

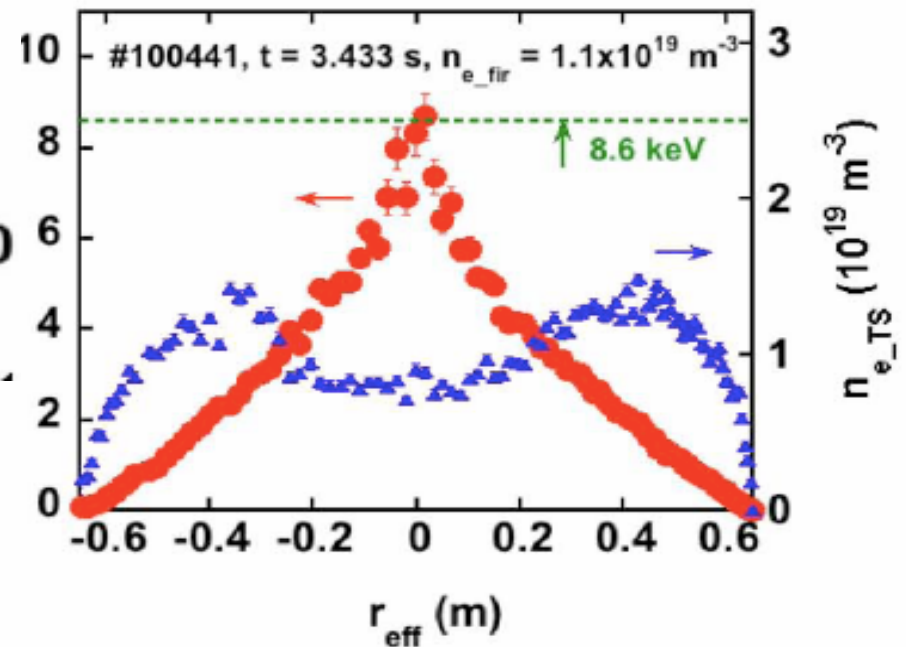
# High Stored Energy with ECRH



# High Te region extended by 77 GHz high power injection ( $P_{in} > 3\text{MW}$ )



At  $n_e 1 \times 10^{19} \text{ m}^{-3}$   
 $T_{e0}$  reached 100 million  $^{\circ}\text{C}$



Attainable plasma parameter region extended as the power increased

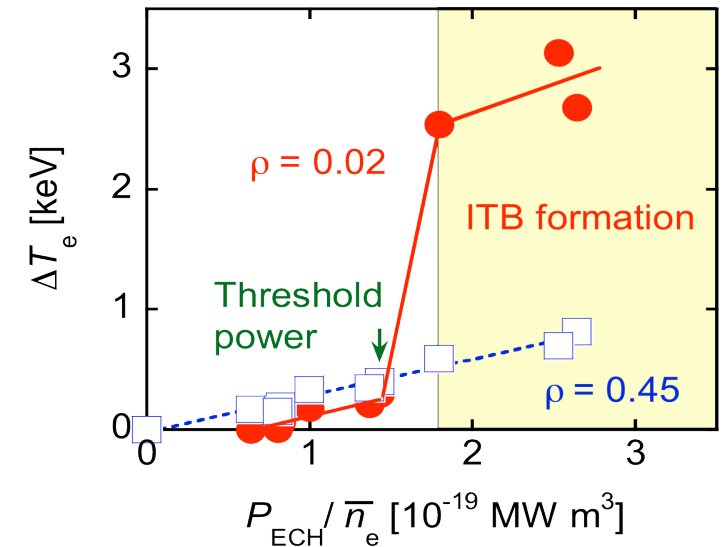
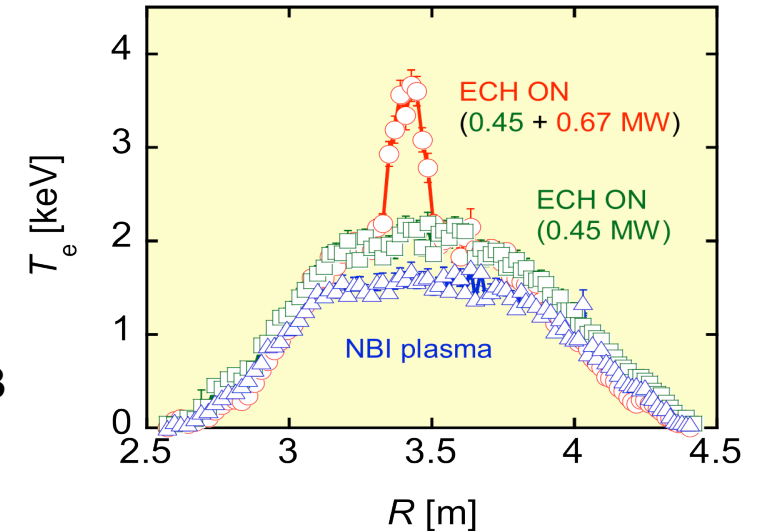
# Internal Transport Barrier (ITB) formation

## e-ITB formation was attained by centrally focused ECH.

- The foot point locates near the rational surface of  $\nu/2\pi = 1/2$ .
  - > **Lower-order rational surface** may trigger ITB.
- There is the threshold in ECH power.
  - > **Local parameter control** plays a key role for ITB formation.

## Prospective effect by 77 GHz gyrotron

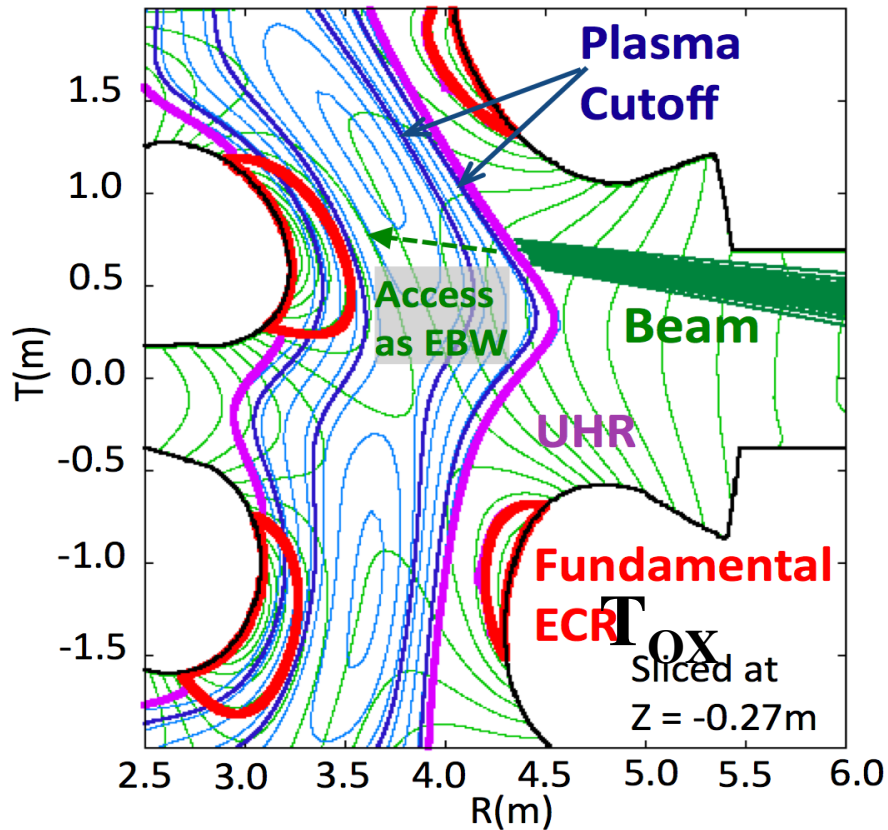
- Expansion of central heating source.
  - > **Improvement of core temperature/ pressure.**
- Different frequency from those of existing gyrotrons.
  - > simultaneous-multi-point heating of plasma
  - > **Local control of radial electric field/ radial transport** by local collisionality control.
  - > Influence of **deposition power/ position** on the ITB formation.



# Experimental Setup for EBWH with O-X-B method in LHD

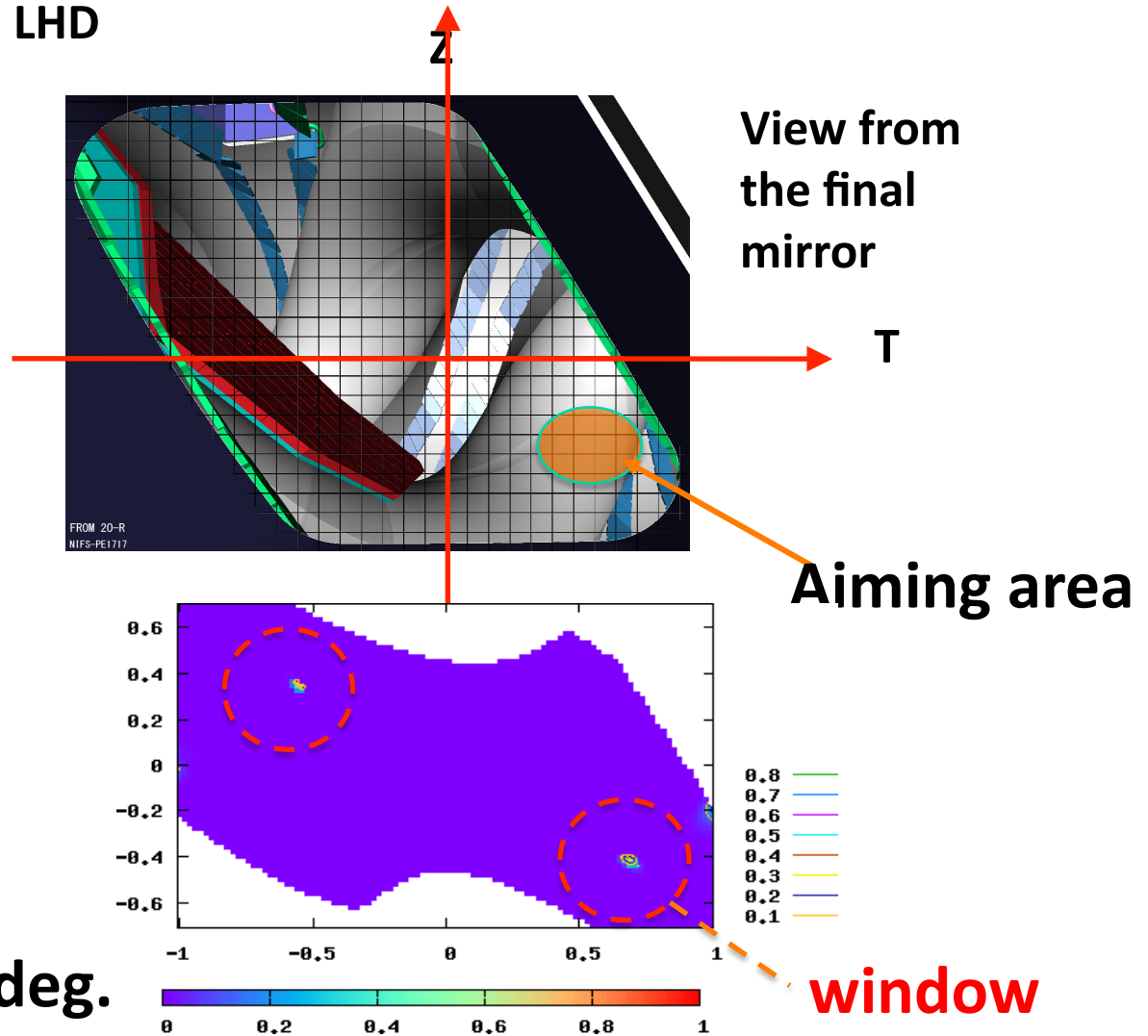
77GHz millimeter wave is launched from a steerable quasi-optical mirror antenna in the horizontal port in LHD

Top slice at  $z=0.27\text{m}$



$(R_{ax}, B_t) = (3.75\text{m}, 2.4\text{T})$

$\phi_{\text{horiz}}$  (deg.)

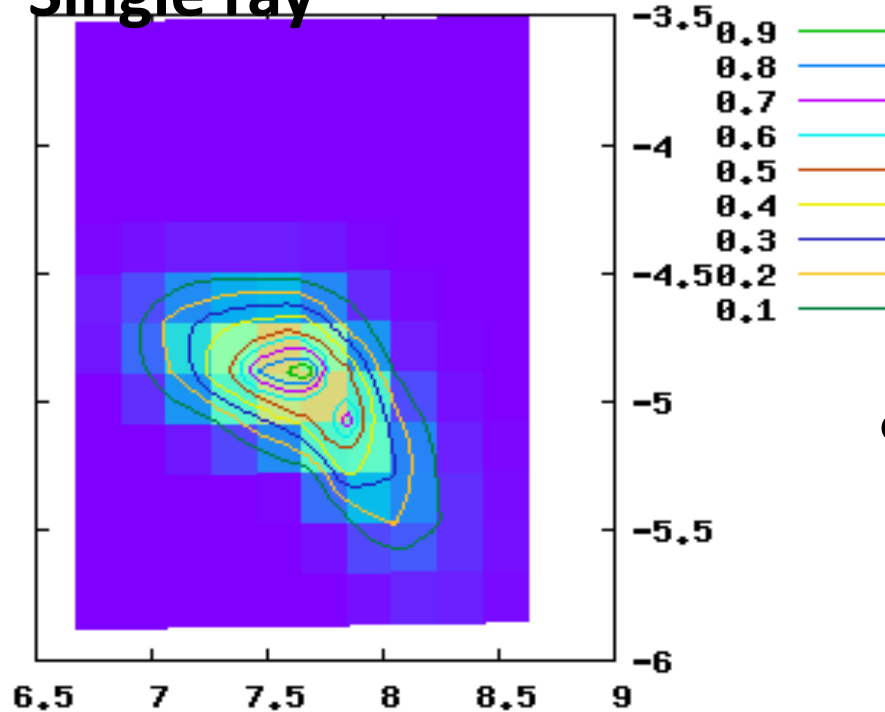


window

**Width of the window of  $T_{ox} \sim 20\%$  (1deg.) is comparable to the controllable minimum of the steering mirror antenna**

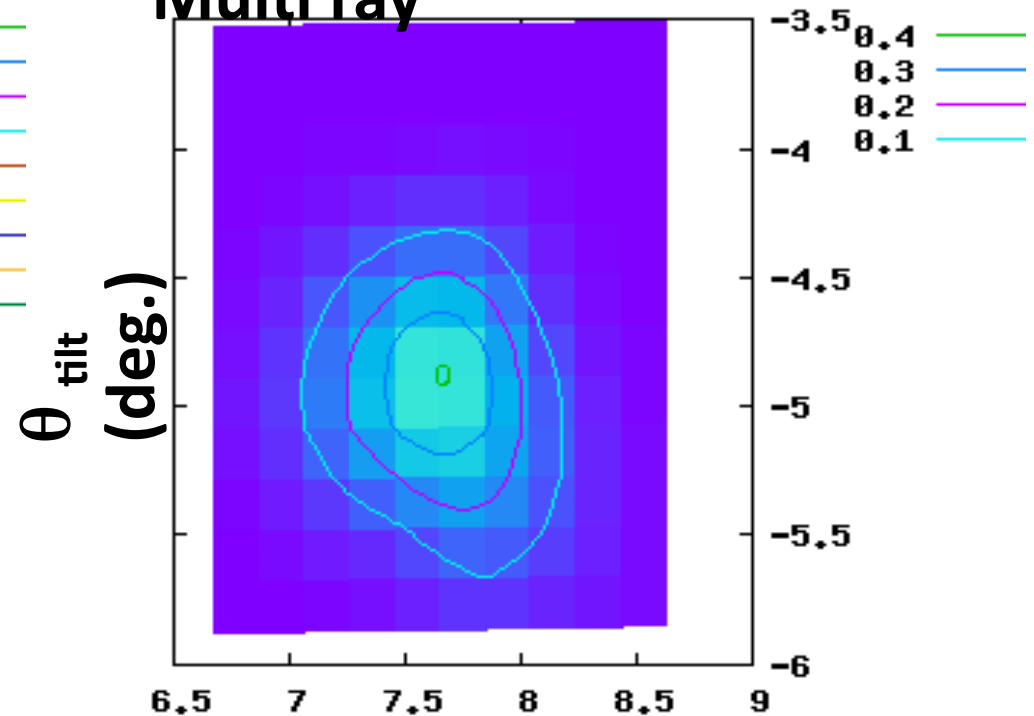
**$\sim 0.4$  deg. is the controllable minimum**

**Single ray**



$\phi_{horiz}$  (deg.)

**Multi ray**

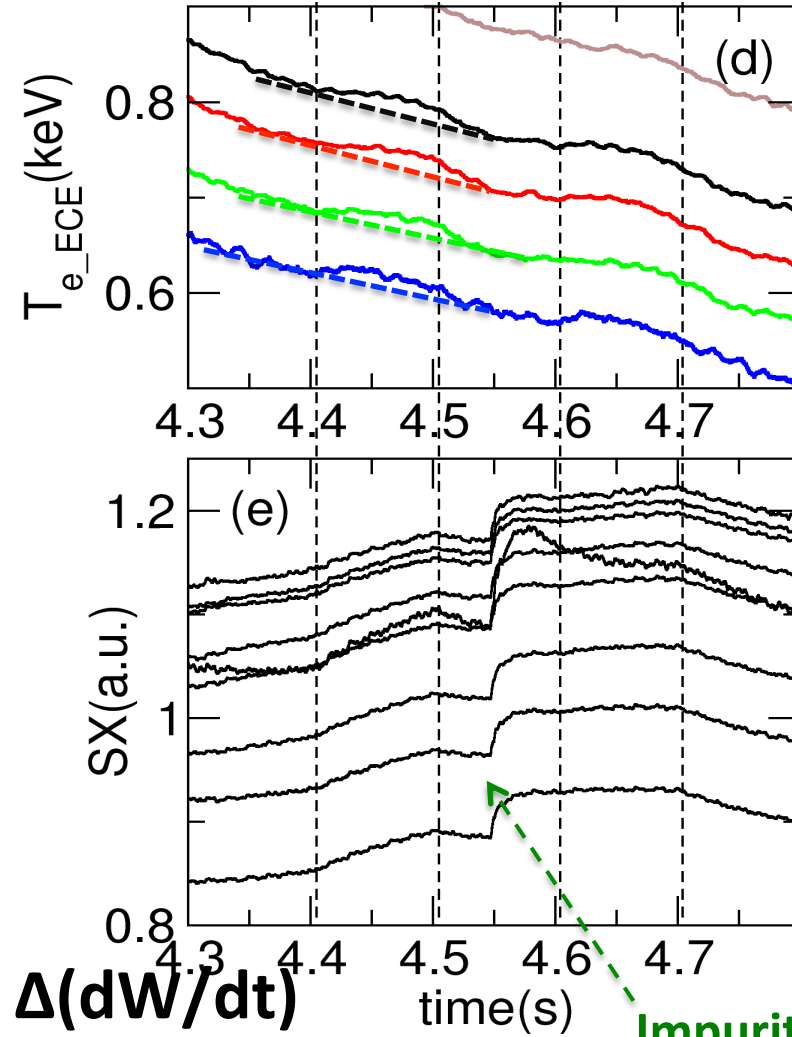
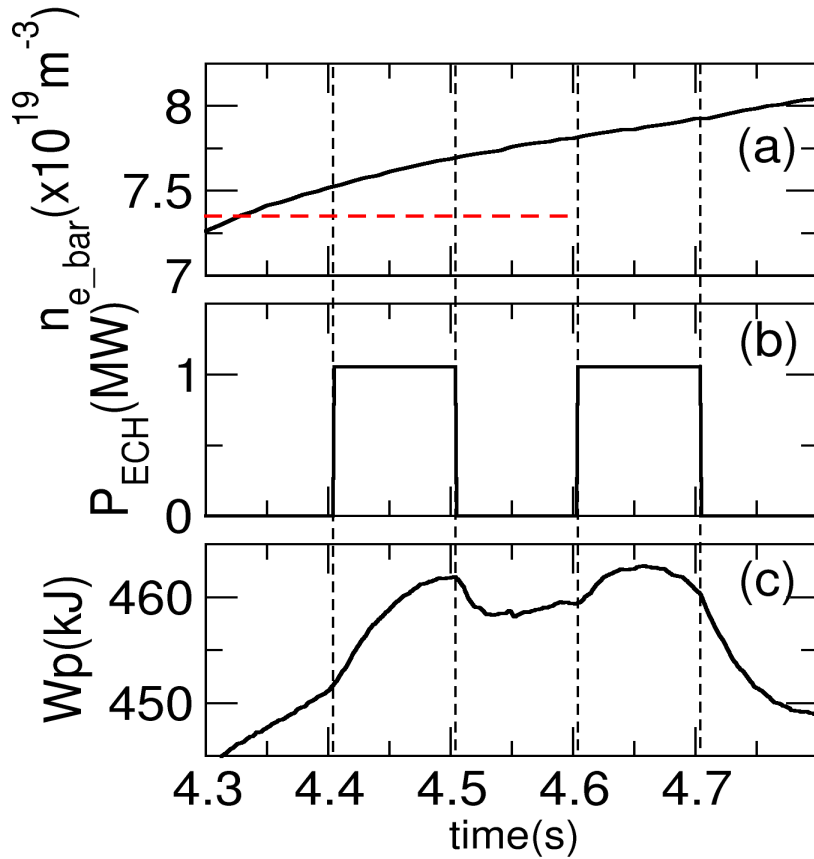


$\phi_{horiz}$  (deg.)

#106297 t=4.66s (Rax, Bt) = (3.75m, 2.4T)

# Stored energy and 2<sup>nd</sup> ECE increase during ECH

(Rax, Bt) = (3.75m, 2.4T)

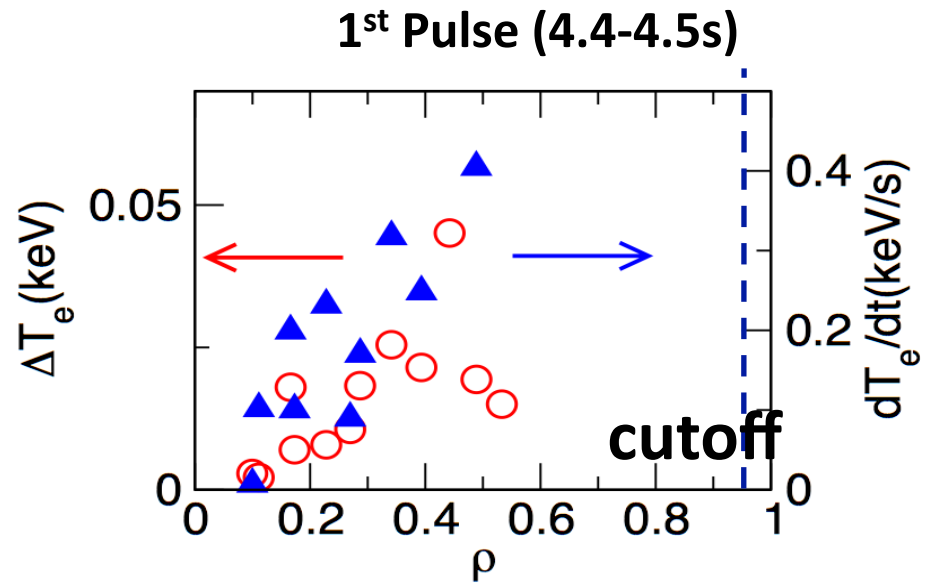
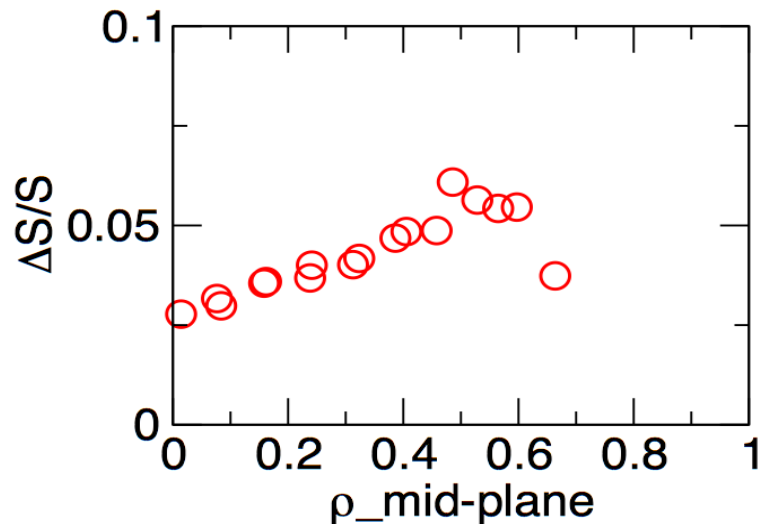


Absorbed Power :  $P_{abs} = \Delta(dW/dt)$

$(P_{abs}/P_{in})_{on} = 8.7\%$

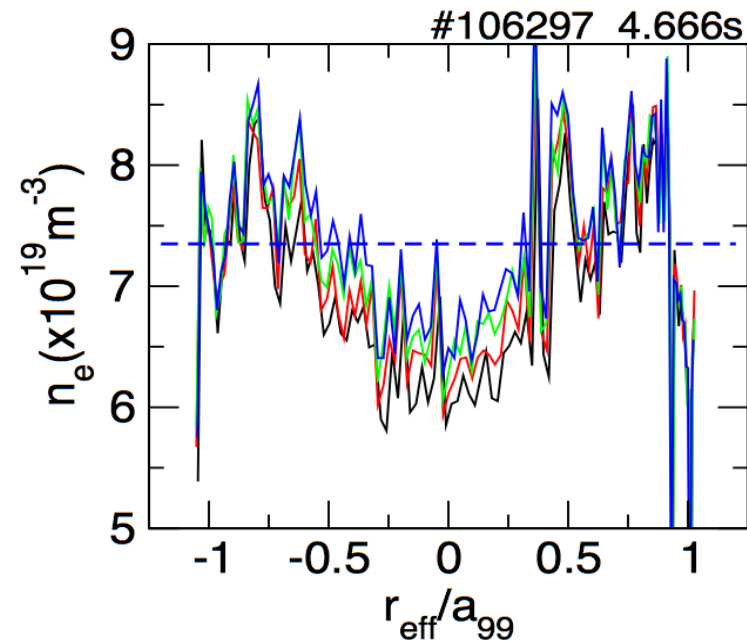
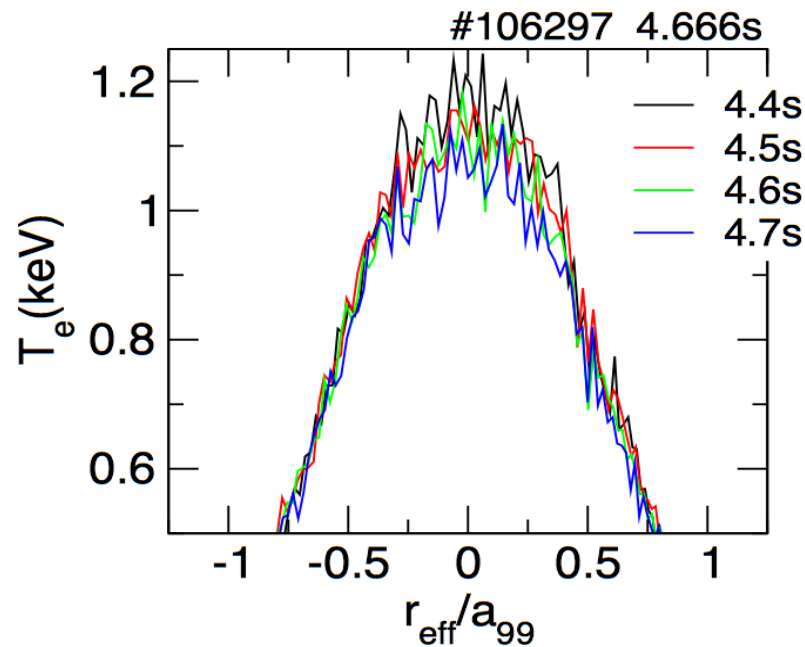
$(P_{abs}/P_{in})_{off} = 17.1\%$

**$0.3 < \rho < 0.4$  , increase of  $T_e$  and  $dT_e/dt$  was observed inside the plasma cutoff**

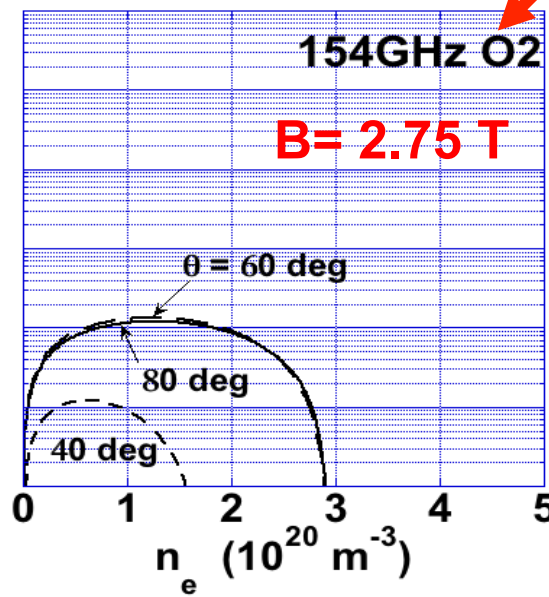
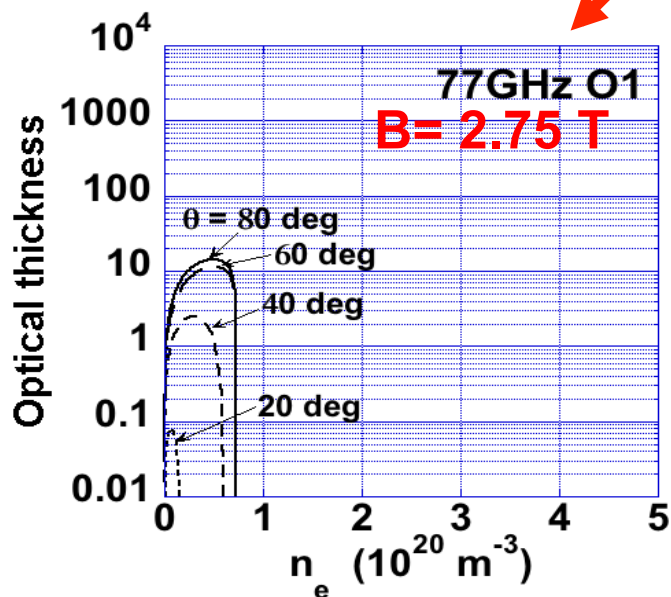
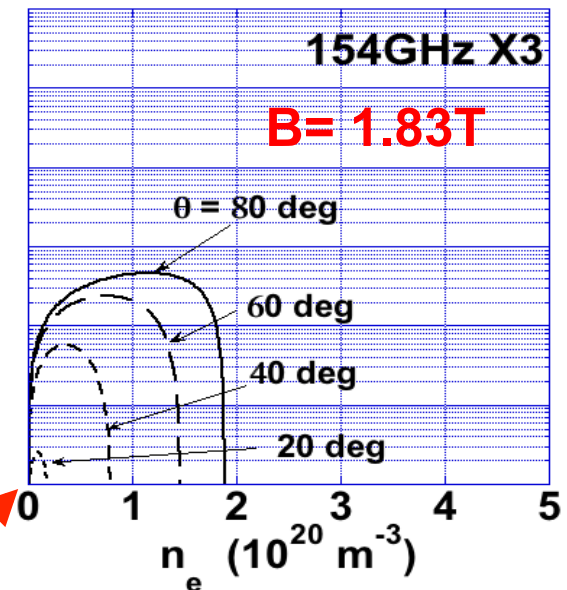
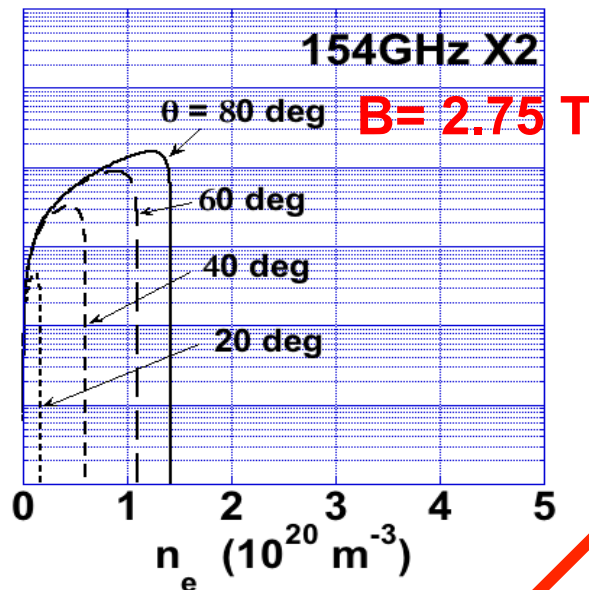
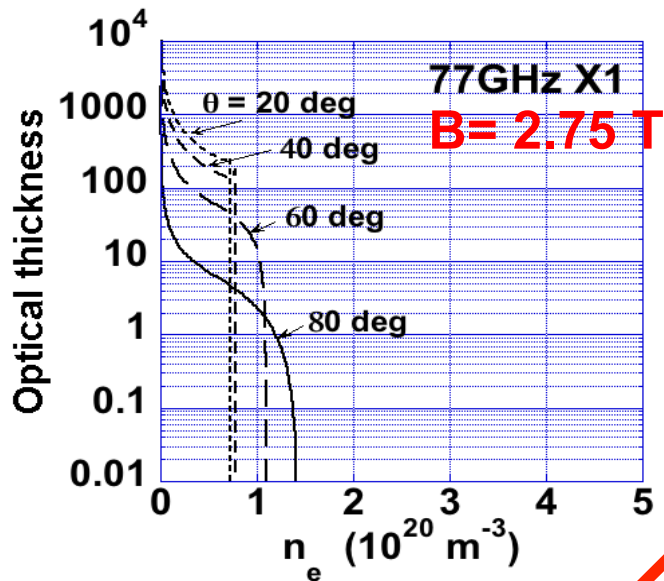


# Near the plasma cutoff ( $r_{\text{eff}}/a_{99} \sim 0.93$ ), profiles of $T_e$ and $n_e$ did not change significantly

Condition of the O-X-B mode conversion might not change very much  
Near the magnetic axis,  $T_e$  decreased and  $n_e$  increased.



# ECH Power Absorption Characteristics with Injection modes



With  $T_e = 5 \text{ keV}$

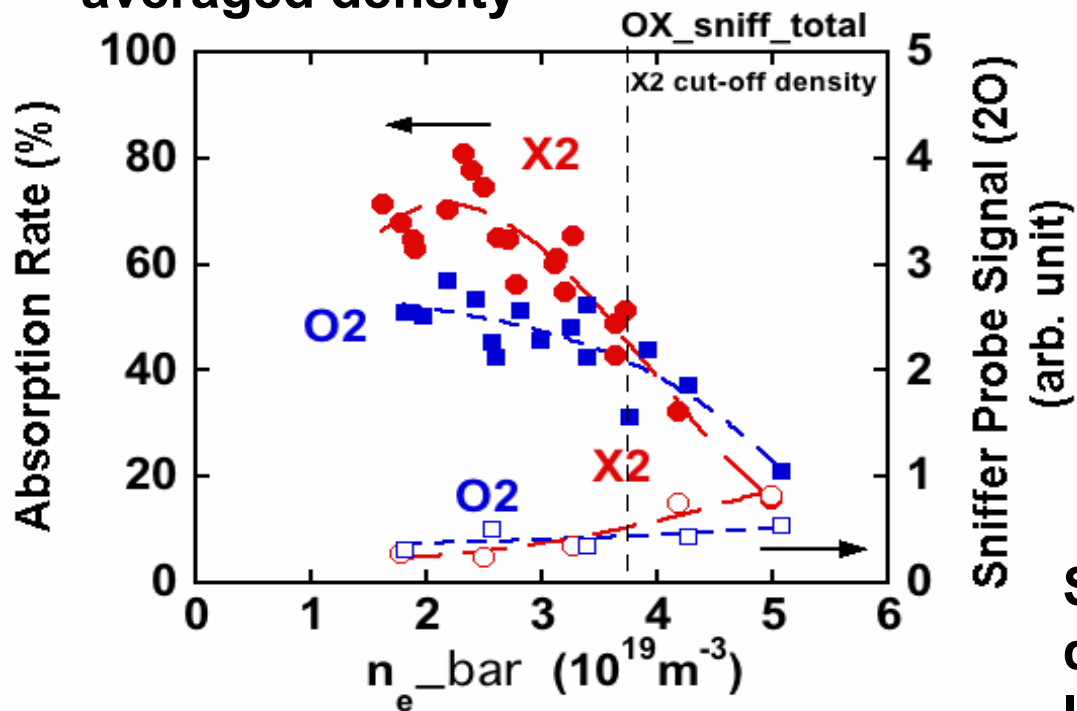
X-mode :  $\tau \sim (T_e/mc^2)^{n-1}$

O-Mode :  $\tau \sim (T_e/mc^2)^n$

Better power absorption in high density plasma with perpendicular injection.

# Efficient heating was observed for O2 mode heating above X2 cut-off density

Dependence of absorption rate and scattered power on line-averaged density



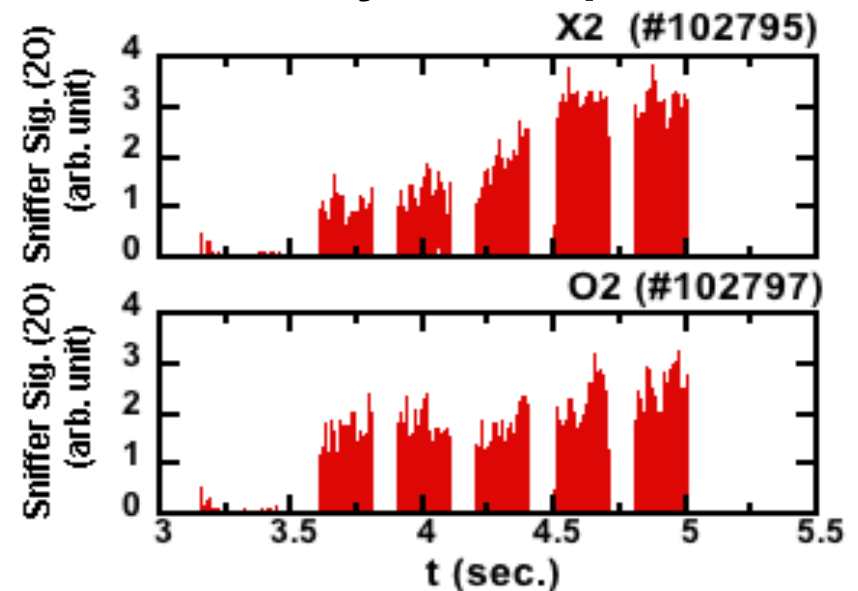
Below X2 cut-off density:

X2  $\rightarrow$  80% O2  $\rightarrow$  50%

Above X2 cut-off density:

X2  $\rightarrow$  20% O2  $\rightarrow$  ~40%

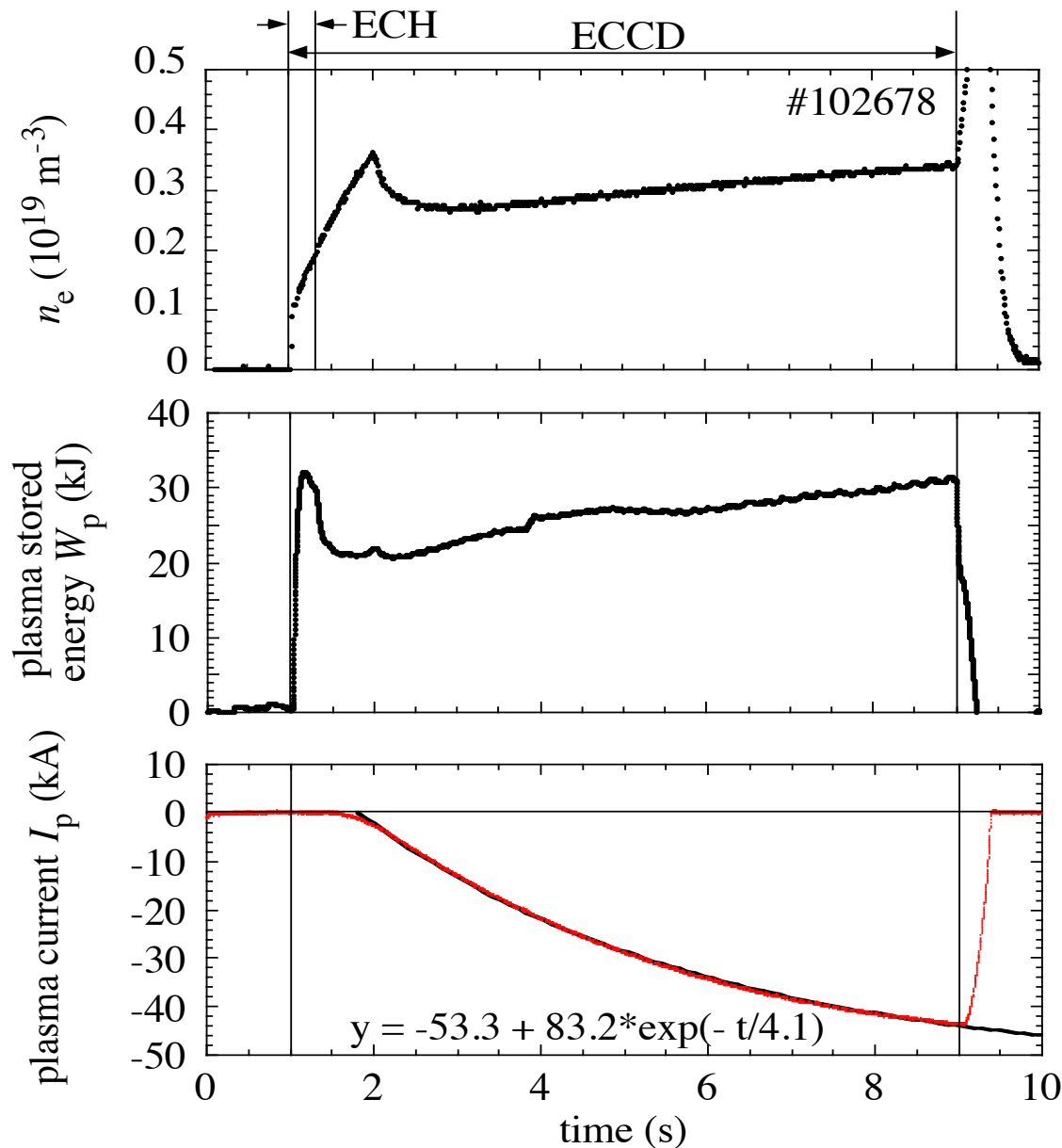
Non-absorbed RF signal detected by sniffer-probe



Signal gradually increases with density for X2 mode injection. It keeps nearly constant for O2 mode injection.

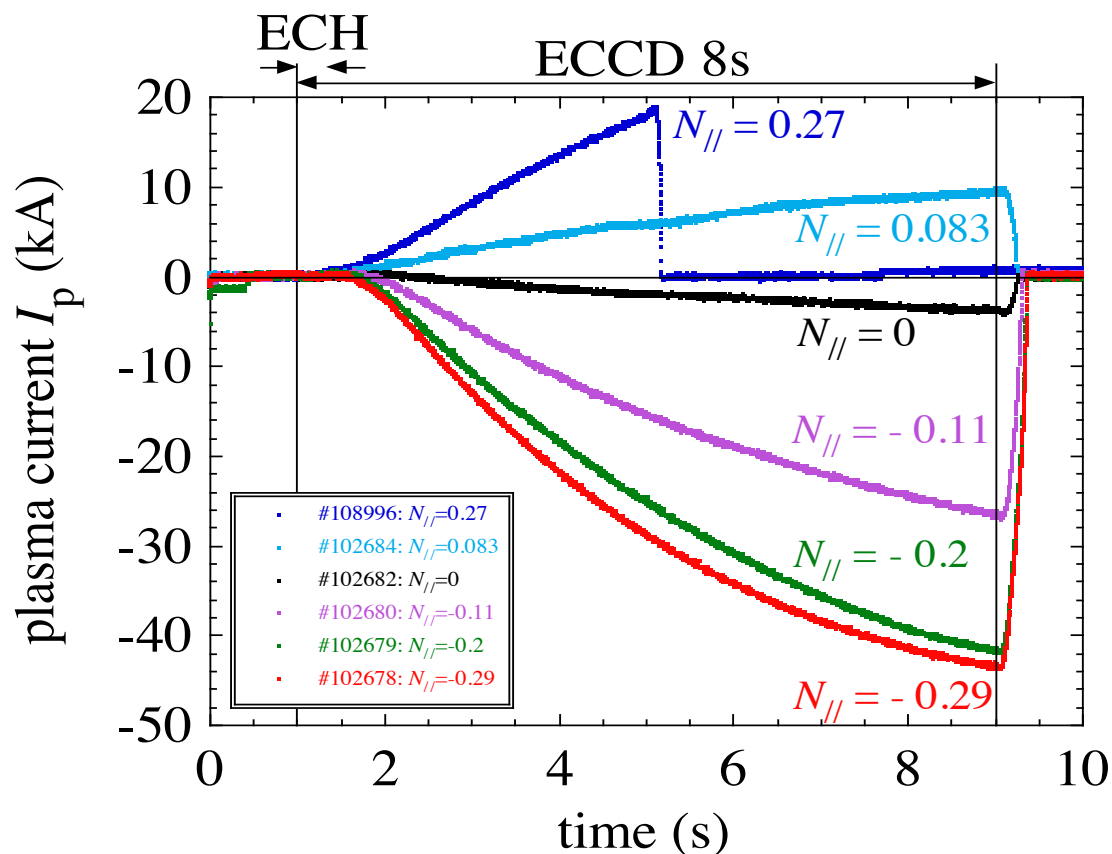
Good O2 absorption above X2 cut-off density

## Waveforms in high-power, long-pulse ECCD exp.



- > Heating source is 775kW, 8s, 77GHz EC-wave only
- >  $R_{ax}=3.75\text{m}$ ,  $B_{ax}=1.375\text{T}$
- >  $B_{ax}$  is set for 2nd harmonic resonance for 77GHz wave
- > EC-wave beam direction was scanned in toroidal direction for ECCD
- > Plasma current over 40kA was observed
- > Plasma parameters such as  $n_e$  and  $W_p$  are kept nearly constant for  $t > 2.5\text{s}$
- >  $I_p$  increases continuously during the discharge with time-constant of 4.1 s, and is still not saturated at 9s
- > long-pulse is necessary for precise evaluation of  $\eta_{ECCD}$

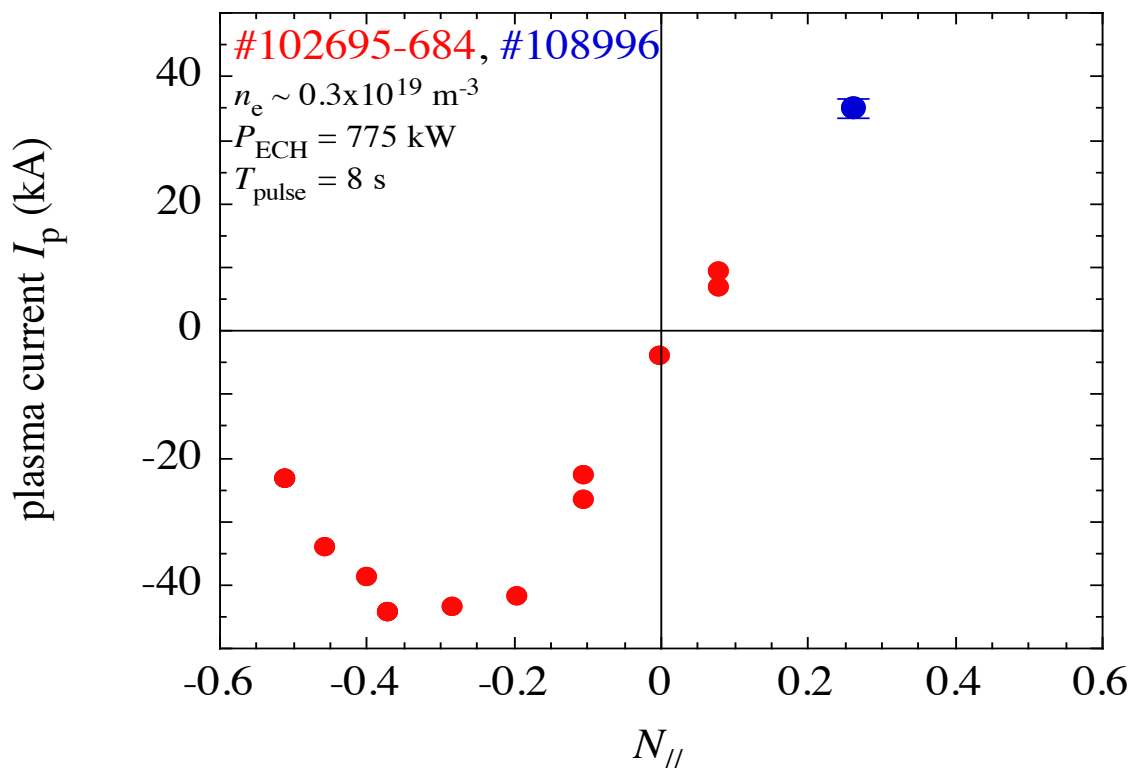
# Successful ECCD in both the positive and negative directions (1)



- > EC-wave beam direction is scanned toroidally aiming at magnetic axis
- > Pulse width was 8s except for the discharge with  $N_{\parallel}$  of 0.27 (4s)
- > Right-hand circular polarization for non-zero  $N_{\parallel}$
- >  $I_p$  reverses its direction by the reversal of EC-wave beam direction (=sign of  $N_{\parallel}$ )
- > Direction of  $I_p$  agrees with the Fisch-Boozer theory
- > Max. ECCD efficiency  

$$\eta = n_e * R_{ax} * I_{ECCD} / P_{EC} \sim 5.8 \times 10^{17} \text{ A/Wm}^2$$
- <- 1.7 times higher than previous 84GHz case

## Successful ECCD in both the positive and negative directions (2)



- > Plasma currents  $I_p$  at the end of discharges are plotted against  $N_{//}$  in the ECCD discharges with  $n_e \sim 0.3 \times 10^{19} \text{ m}^{-3}$ ,  $P_{\text{ECH}} = 775 \text{ kW}$ ,  $T_{\text{pulse}} = 8 \text{ s}$
- >  $I_p$  with  $N_{//} = 0.27$  ( $T_{\text{pulse}} = 8 \text{ s}$ ) is estimated from the experimentally obtained data with  $T_{\text{pulse}} = 4 \text{ s}$
- >  $N_{//}$  larger than 0.27 is not available due to the limitation of interference of EC-wave beam and LHD vacuum vessel
- > Negative  $I_p$  peaks at  $N_{//} \sim -0.3$ , and probably positive  $I_p$  peaks at  $N_{//} \sim +0.3$



# ICRF Heating on ITER

**It is expected that ITER will start its operation with Hydrogen and  $^4\text{He}$  plasmas at reduced B field. At half the nominal field, i.e.,  $B=2.65\text{T}$  will be discharged the plasma with  $n_{e0}\sim 3.5\times 10^{19}\text{m}^{-3}$ ,  $T_i\sim 8\text{keV}$  and  $T_e\sim 10\text{keV}$  using  $P_{\text{NBI}}\sim 15\text{MW}$ ,  $P_{\text{ECH}}\sim 15\text{MW}$  and  $P_{\text{ICH}}\sim 10\text{MW}$ .**

**In hydrogen plasma as a minority with  $^4\text{He}$  majority plasma the minority ICRF Heating will be applied with  $f\sim 40\text{MHz}$ . In addition 2<sup>nd</sup> harmonic heating will also be carried out with  $^4\text{He}$  plasma using the same frequency. As the other ICRF heating scenario 2<sup>nd</sup> harmonic heating with  $^3\text{He}$  plasma is possible with  $f=53\text{MHz}$ .**